CULVERT OUTLET ENERGY DISSIPATOR INCORPORATING RADIAL FLOW AND A TRANSVERSE SILL

by

Robert R. Wear
Walter L. Moore

Research Report Number 92-3

Performance of Circular Culverts on Steep Grades
Research Project 3-5-66-92

conducted for

The Texas Highway Department

in cooperation with the
U. S. Department of Transportation
Federal Highway Administration
Bureau of Public Roads

by the

CENTER FOR HIGHWAY RESEARCH
THE UNIVERSITY OF TEXAS AT AUSTIN

PREFACE

This is the third of a series of reports on Research Project No. 3-5-66-92, entitled "Performance of Circular Culverts on Steep Grades."

The support of this work by the Texas Highway Department and the U. S. Bureau of Public Roads is acknowledged. Particular thanks are due to Dr. Frank D. Masch, who gave pertinent advice.

In addition, the authors wish to thank Mrs. Linkous who typed this report, Mrs. Roberts who prepared the figures, and William Henderson and John U. Miller who assisted in constructing the model and made many of the experimental measurements.

The opinions, findings, and conclusions expressed in this publication are those of the authors and not necessarily those of the Bureau of Public Roads.

ABSTRACT

A study is reported herein of the performance of either an abrupt rise or a partial transverse sill as a part of a culvert energy dissipation scheme in which flow parallel to the culvert axis is transformed into supercritical radial flow. Energy dissipation is accomplished by means of a hydraulic jump which was formed as a result of the combined effect of radial flow and a transverse sill. A sill or an abrupt rise was introduced just downstream from the radial channel transition in an effort to reduce the velocity of flow and impart stability of the jump position in addition to that provided by radial flow characteristics alone. Experimentation was carried out to determine the jump stability and velocity reduction achieved by means of the geometric configuration consisting of either a sill or a rise.

TABLE OF CONTENTS

LIST OF FIGURES

GLOSSARY OF SYMBOLS

Symbol	Definition
b	Width of the entrance channel, ft
B	Width of the main channel, ft
B_v	Distance from and perpendicular to the channel centerline to a point of velocity measurement, ft
F_t	Froude number at the section where V_t occurs, $V_t/\sqrt{gy_t}$
g	Gravitational acceleration, ft/sec^2
H_D	Piezometric head on abrupt rise, ft
H_R	Height of abrupt rise, ft
H_s	Height of partial transverse sill, ft
L	Distance between the upstream and downstream end of the flared wingwalls measured parallel to the channel centerline, ft
L_s	Distance from upstream end of flared wingwalls to transverse sill
L_v	Distance, measured parallel to the channel centerline, from the downstream end of the flared wingwalls to the transverse section where velocity measurements were taken, ft
L_R	Distance from the downstream end of the flared wingwalls to the abrupt rise, measured parallel to the channel centerline, ft
Q	Discharge, ft^3/sec
r	Radius of curvature of the curved portion of the entrance channel bottom, ft
S	Length of the partial transverse sill, ft
V	Velocity in main channel, ft/sec
V_m	The mean velocity in the outlet channel
V_t	Velocity of flow at the beginning of the vertical curve of the entrance channel bottom, ft/sec

W_s	Width of the partial transverse sill, ft
x	Distance from the upstream end of the flared wingwalls to the leading edge of the jump, measured parallel to the channel centerline, ft
y_3	Tailwater depth in main channel, ft
y_t	The depth of flow measured at the section where V_t occurs
Z	Elevation of the entrance channel bottom upstream from the point of curvature, ft
θ	Horizontal deflection angle formed by the intersection of two corresponding horizontal lines of the entrance channel bottom each line connecting a point on the center template to a point of the same elevation on the outside curve of the side template, degrees
α	Vertical angle between the tangent portion of the entrance channel bottom and the horizontal stilling basin, degrees
γ	Specific weight of water, lbs/ft^3

INTRODUCTION

As a result of the high flow velocities which often exist in single pipe or box highway culverts in mountainous country, a large potential for scour is often created at culvert outlets. The flow as it enters a channel maintains a concentrated jet for some distance downstream, thus creating a separation zone between the flow and the wingwalls. Unless controlled by raising the tailwater, the flow will persist down the channel at high velocity and low depth. This presents the optimum condition for scouring to occur. The primary purpose, therefore, of various methods of energy dissipation is to achieve tranquil flow conditions as the flow enters the downstream channel and to convert as much of the kinetic energy of the flow as possible into turbulent energy and ultimately into heat.

Usually the most effective means of attaining this energy dissipation is through use of a hydraulic jump. When a jump is formed on a horizontal apron made of smooth material, the jump often is unstable and will drift upstream or downstream unless some means is employed to hold it in place. Stilling basins employing special geometric configurations are often used to accomplish this aim. For economic reasons stilling basins are designed to be as short as possible with excavation, forming, and construction held within practical limits.

This paper introduces the concept of combining the effect of an abrupt rise or sill, with the phenomena of radial spreading action as an economical means of effectively dissipating outlet flow energy with a stabilized hydraulic jump.

OBJECT AND SCOPE

The object of this study is to investigate by model simulation, the performance of a partial transverse sill or an abrupt rise in the apron of an outlet structure which incorporates radial spreading action. A schematic layout of the model with the inclusion of a sill is shown in Figure 1, while Figure 2 presents a schematic layout of the model with an abrupt rise included.

This scheme combines three features which bring about reduction of flow velocity, dissipation of energy, and jump stability within a short length of stilling basin. High pressure with some associated energy reduction is produced as the flow impinges on the basin floor and is spread rapidly. Radial flow produces in general, reduction in water depth as the flow progresses forward. For this reason, a hydraulic jump formed in a radial basin will have improved stability characteristics. The third feature which aids in energy dissipation and jump stability is a sill or an abrupt rise. Either form of this feature produces a stabilizing force due to dynamic pressure developed at the face, as well as pressure inherent in the increased elevation head.

The purpose of this study was to determine the energy dissipation and jump stability characteristics of this basin and to provide usable information for field design purposes.

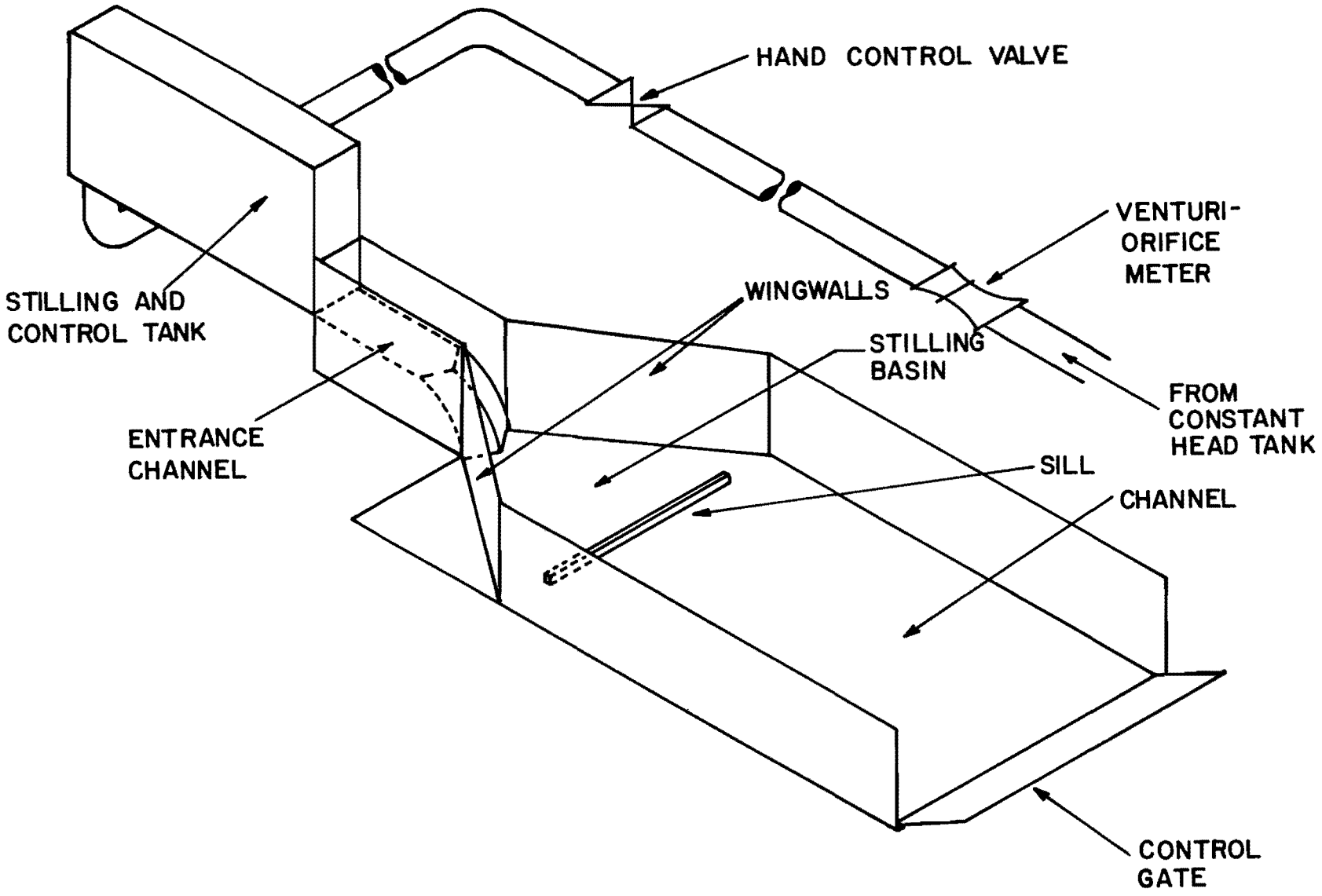

FIGURE I - SCHEMATIC LAYOUT OF MODEL WITH PARTIAL TRANSVERSE SILL

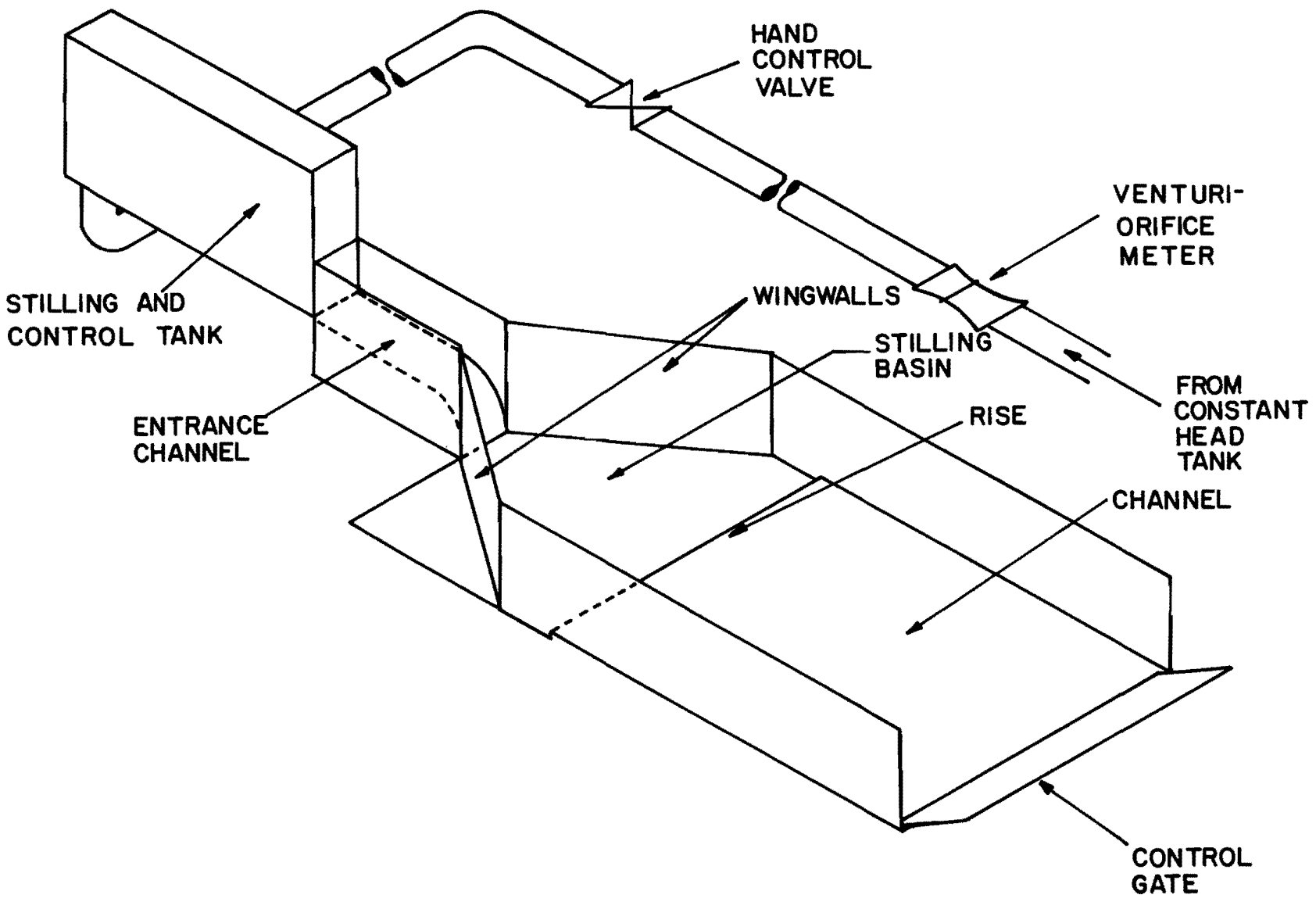

FIGURE 2-SCHEMATIC LAYOUT OF MODEL WITH RISE

PREVIOUS STUDIES

Numerous technical papers have been devoted to the study of different types of stilling basins at culvert outlets. A number of these have been summarized in a report by Aguirre[1]. Many of the basins which have been designed are of a standardized form making use of such devices as blocks, sills, and baffles to reduce culvert flow energy. Although these basins are designed generally to meet varying conditions, they often are limited by safety considerations or economic factors to a certain range of outlet flow conditions.

Two simple energy dissipation devices in existance are the straight drop spillway developed by the United States Soil Conservation Service[2], and an ungrouted rock-lined depression made in the outlet channel[4]. The former is installed in small drainage structures where the topography is steep enough so that a straight drop can be employed at the culvert outlet. The ungrouted depression has the advantage of providing complete drainage of the pool left after a flood.

For flow from pipe culvert outlets with low specific energy, a concrete stilling basin has been developed by the Public Works Department of New South Wales, Australia[5]. The basin has vertical walls which flare out from the end of the pipe at an angle of 17^{o} from the centerline. The bottom of the basin slopes downward from the end of the pipe at a slope of 1:4 (vertical to horizontal) for a distance of 2D (pipe diameter), continues horizontally for a distance of 1.5D and then slopes upward at a slope of 1:1.5 over a distance of 0.5D. The basin slope terminates at a vertical sill, 0.17D high. Flows into this basin are limited to a Froude number ≤ 1.4.

---

[1] Numbers refer to references listed at the end of the report.

Impact type energy dissipators such as the Bradley-Peterka design of the Bureau of Reclamation Basin[6] are particularly well-suited for flows with Froude numbers of 3 and greater. A transverse impact wall or baffle is placed across the flow to force it to change direction. The flow, thereby, dissipates a portion of its energy before it is discharged in the original flow direction into a concrete basin. This type of basin is most effective at higher Froude numbers when all of the flow strikes the impact wall.

The Contra Costa impact type energy dissipator[7] employs two transverse walls, which extend completely across the bottom of a trapezoidal concrete outlet channel. Satisfactory results have been obtained from laboratory testing of this device over a broad range of outlet flow depths and Froude numbers. Field data on the operation of this device is not available however.

Other types of stilling basins have been designed by the United States Bureau of Reclamation[8] making use of chute blocks, baffle piers, and end sills. In these designs, flow entering the basin is split and aerated by "triangular chute blocks" mounted at the base of the slope. To protect the bed from direct current action, part of the flow leaving the basin is directed upward and away from the unpaved riverbed by the end sill arrangement. Henderson[9] suggests that another purpose of the end sill is to set in motion a reverse roller which by directing bed material back towards the basin prevents undermining of the structure. Baffle piers are installed downstream of the chute blocks in the Type III basin. This basin is designed for low enough velocities so that the baffle piers will not be severely damaged by scouring. The piers offer added resistance which permits the use of a shorter basin with lower tailwater level.

Another well-known standard design has been developed at the St. Anthony Falls Hydraulic Laboratory, University of Minnesota, for the United States Soil Conservation Service and has been described by Blaisdell[3]. It is designed for use with low-head structures, as is the United States Bureau of Reclamation Basin III, however, it is applicable over a wider range of upstream Froude numbers. The St. Anthony Falls basin has a steep chute which runs into a horizontal apron. The sidewalls may be parallel or

diverging in plan. Chute blocks are utilized at the end of the chute, with floor blocks downstream from the end of the chute a distance of one-third the length of the basin. The basin is terminated with an end sill which extends over the full width of the basin. The St. Anthony Falls basin has another advantage over the Bureau of Reclamation Basin III, in that it is shorter in length. As pointed out previously, these basin designs are standard for generalized situations. Special circumstances of a specific project have often dictated that model studies be employed to test and develop more specific design of arrangements.

For a jump to form unaided, the floor of the stilling basin must be placed a substantial distance below tailwater level. The required excavation for this may make the basin very expensive. Henderson[9] indicates that excessive depth of excavation can be avoided by widening the stilling basin. This suggests not only that the basin should be as wide as possible, but also that if it were tapered in plan with the width increasing downstream, then the jump would remain stable in one position for given values of upstream and downstream depths. Radial free surface flow has not only been studied by Davis[10], who investigated transition phenomena in radial free surface flow, but also by Saddler and Higgins[11]. The purpose of the investigation by Saddler and Higgins was to predict quantitatively the surface curves and hydraulic jump heights with any axially symmetric bottom configuration for radial free surface flows and to provide a working computer program from which additional values might be calculated. The Chezy method for introducing roughness was utilized in devising the differential equation from which their theoretical curves were computed. Saddler and Higgins found in general, good agreement between their theory and experiments.

In radial flow, the Froude number and depth of flow vary much more than they would in the same length of a uniform channel. In addition, both Froude number and depth of flow may decrease as flow progresses downstream. These factors permit the required sequent depth y_2 to decrease rapidly within a short length of basin. This characteristic of radial flow produces a degree of hydraulic jump stability which cannot be achieved with the common parallel flow hydraulic jump on a horizontal basin

floor. With this as a basis, a model study was performed by Aguirre[1] to analyze the performance of a new type of culvert flow energy dissipator in which flow parallel to the culvert axis was transformed into supercritical radial flow. The outlet structure of the model allowed flow to drop along a steep slope into a horizontal basin with flared wingwalls, producing radial flow. The basic model geometry and parameters tested are shown in Figure 3. Experiments were performed to ascertain the jump stability, velocity reduction, and degree of angular uniformity of the radial flow attained from the various geometric schemes.

In order to analyze the jump stability, the parameters x and y were varied over a certain range while V_t and y_2 were held constant. The absolute value of the slope of each curve of x/y_2 vs y_2/y_t was analyzed as an indication of the degree of stability of the hydraulic jump. A study of these curves indicated that the hydraulic jump was highly stable within the region of the basin with flared wingwalls. As the jump moved into the zone with parallel training walls, the absolute value of the slope of the curve decreased rapidly. Another variation of the parameters which was plotted was that of y_2/y_t vs F_t for constant values of x/y_t.

From an analysis of the behavior of the various parameters for each geometric combination tested, certain observations were made. It was observed that the performance of the entrance channel bottom with $\beta = 0^o$ was comparable to that for $\beta = 60^o$. In addition, it appeared that the wingwall flare angle θ had more of an effect on the formation of the jump near the basin entrance than the entrance channel angle β. Better spreading action was observed with the larger flare angle of 45^o. In general, tailwater requirements at small values of x/y_t were lower for arrangements with $\theta = 45^o$. At values of x/y_t of 5 and larger, it was observed that the lowest y_2/y_t requirements were for arrangements with B/b of 6.

The type of structure studied in this model is only applicable when the topography permits a steep drop from the culvert outlet into the main channel. In order to alleviate the need for such a large difference in elevation between the culvert outlet and the channel and to provide additional energy dissipation, an abrupt rise has been added to the geometric

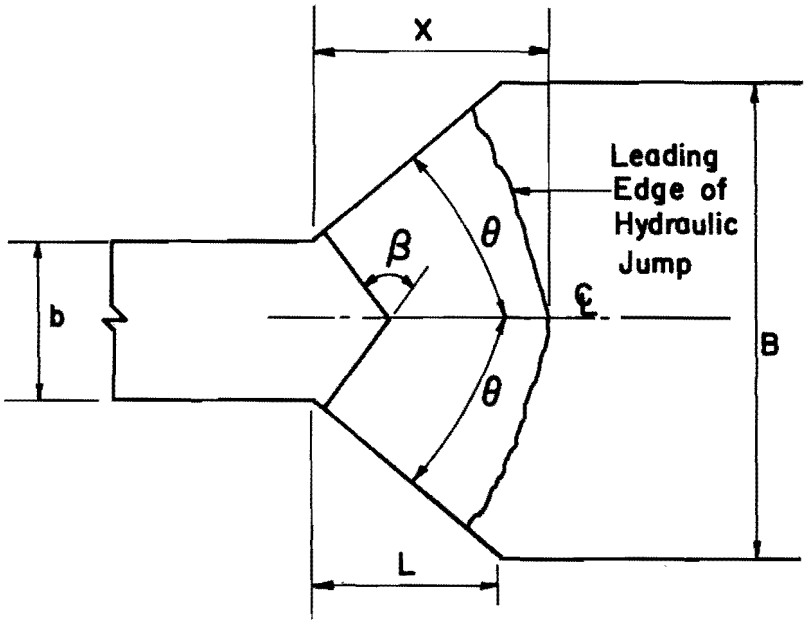

PLAN

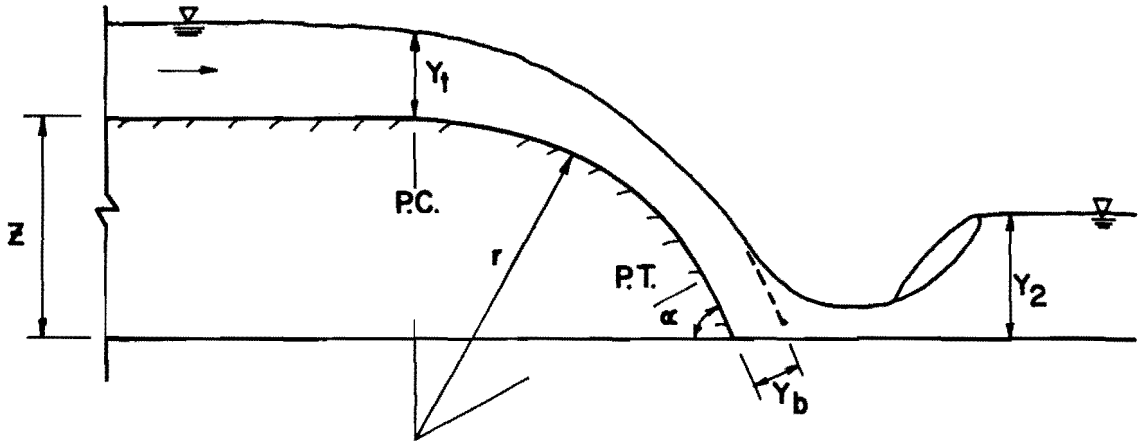

ELEVATION

FIGURE 3 - DEFINITION OF PARAMETERS FOR MODEL OF AGUIRRE

model of Aguirre[1] in the study reported herein. The abrupt rise as well as the abrupt drop, and sharp edged and broad crested weirs have been studied as means of insuring the formation of a jump and the control of its position under a broad range of probable operating conditions.

The stabilizing effects of an abrupt drop in a channel bottom was investigated by Rouse, Bhoota, and Hsu[12]. From their investigation they observed that two flow situations are possible. In the first flow case, the toe of the jump is upstream of the drop and the thrust on the drop is determined by the depth downstream from the drop. In the second flow situation, the toe of the jump is at the edge of the drop. In this case, the thrust on the drop is determined by the depth of flow upstream from the drop. An undular wave was found to characterize the transition from one type of flow to the other. The type of flow which would exist was found to depend upon whether the downstream depth was above or below the depth required for formation of the undular standing wave. It was determined that experimental measurements must be relied upon in lieu of momentum and continuity relationships in predicting the conditions which would produce the undular stage. Moore and Morgan[13] reported results of an experimental study related to the behavior of a hydraulic jump at an abrupt drop in the channel bottom. The study emphasized the characteristics of the jump, when the drop is located within the length of the jump. It was observed that the pressure on the face of the drop was hydrostatically distributed under a piezometric head, h_D, which changed with the location of the jump relative to the drop. An important characteristic of the jump observed in this experimental scheme was that it formed over a wide range of y_2/y_1 for the whole range of entering Froude numbers encompassed by the experiments.

In order to demonstrate the effectiveness of the different types of jumps in decreasing the flow velocity along the channel bottom, this velocity was plotted against distance from the drop. The jump designated type B, in which the jump forms downstream from the edge of the drop, produced relatively high velocities along the channel bottom. On the basis of the study, three conclusions were arrived at.

(1) An abrupt drop in the bottom of a rectangular channel provides an effective means of stabilizing a hydraulic jump over a large and continuous range of relative downstream depths.

(2) As the hydraulic jump passes through its three different forms while moving progressively downstream under reduced downstream depths, the corresponding pressure on the face of the drop decreases continually.

(3) An analysis based on momentum principles, including the effect of the pressure force on the vertical face of the drop, provides results which are consistent with the experimental observations.

Forster and Skrinde[14] have developed diagrams, from experimental data and theoretical analysis for the sharp crested weir, broad crested weir and the abrupt rise, showing the relations of the important flow parameters. For the abrupt rise, the diagram demonstrates the relations among F_1, y_3/y_1, and h/y_1 for an abrupt rise with $x = 5(h + y_3)$.

The parameters investigated in this study are shown in Figure 4.

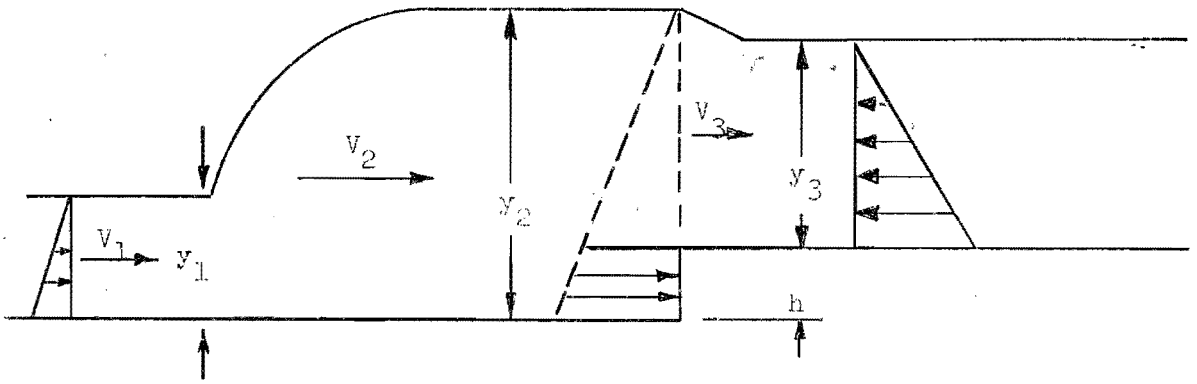

Figure 4. Definition of parameters for abrupt rise in rectangular channel [after Forster and Skrinde, (14)].

A diagram allows the prediction of the stabilizing effect of a given rise height at the end of a jump when V_1, y_1, y_2 (the sequent depth), y_3, and h are known. Experimental results indicate values of tailwater depth required to stabilize the jump, which are less than those obtained by applying the momentum equation between sections 1 and 3. The authors attributed the difference between the experimental and theoretical curves to the presence of a non-uniform velocity distribution at the ratio $x/(h + y_3) = 5$. They stated that better verification of experimental results would be obtained when $x/(h + y_3)$ approaches 10. Forster and Skrinde assumed that the thrust on the face of the rise was due to the hydrostatic head created

by the sequent depth of y_2. However, all of the discrepancy cannot be attributed to the non-uniform velocity distribution. Others[9,16] have pointed out that it is not permissible to omit the dynamic force on the face of the abrupt rise. This force, although small at times, becomes very significant when the jump is located close to the rise. Laushey[16] states that "as long as x is greater than the length of the jump, the assumption can be made that the jump is not changed by the rise that follows." Another source of error in the experimental work of Forster and Skrinde was the measurement in general of very small D_1 values. Boundary layer effects as well as depth fluctuations appear to limit the accuracy of their measurements of D_1 for these small depths. Moore and Morgan[17] have performed additional investigation of the characteristics of the hydraulic jump at an abrupt rise. Their study reports measurements of the pressure on the face of the rise for different positions of the jump. In addition, velocity distributions were determined within the jump, before, at, and after the rise. One of the dimensionless parameters investigated in their work was h_D/y_1, h_D being the pressure head on the rise and y_1 the upstream depth. It was noted in their investigation that a reduction in the relative downstream depth produces an increase in h_D/y_1 to maintain a stable jump. Their results reflected the fact that an increase in dynamic pressure takes place as the jump approaches the rise. This increased head results in a lower tailwater depth requisite for jump stability than that which is predicted from hydrostatic conditions. Experimental results of this study more closely verified theoretical analysis than the results obtained by Forster and Skrinde[13].

Some evidence has been seen in field applications that under low flow conditions, a flow obstruction such as an abrupt rise may cause accumulation of debris. This debris which accumulates immediately upstream of a rise may create a reduction in flow area and hamper the dissipation of energy in the basin until swept out by high flow conditions. Normal flow velocities, however, usually prevent any significant accumulation of debris.

Rand[18] investigated the flow over a vertical sill in an open channel. In this investigation a model was adopted that consisted of a vertical gate, of a movable apron with an adjustable sill, and of a gate for tailwater control. These components were all built into a glass-walled flume. The

sluice gate produced a nearly horizontal flow for depths to 1.2 inches and its downstream edge served as an observable reference line for the stabilization of the jump at its basic position at the gate entrance. It was assumed that the tangent to the flow surface must be parallel to the bottom at the entrance section. The depth, therefore, at this point would be the smallest flow depth in this region.

Seven variables were used to describe the non-uniform flow which existed between the entrance and tailwater sections. These variables and the flow boundaries are shown in Figure 5. F , L_s/D_1 , and D/D_1 were the independent variables studied, while S/D_1 and L_t/D_1 were the dependent variables which were determined.

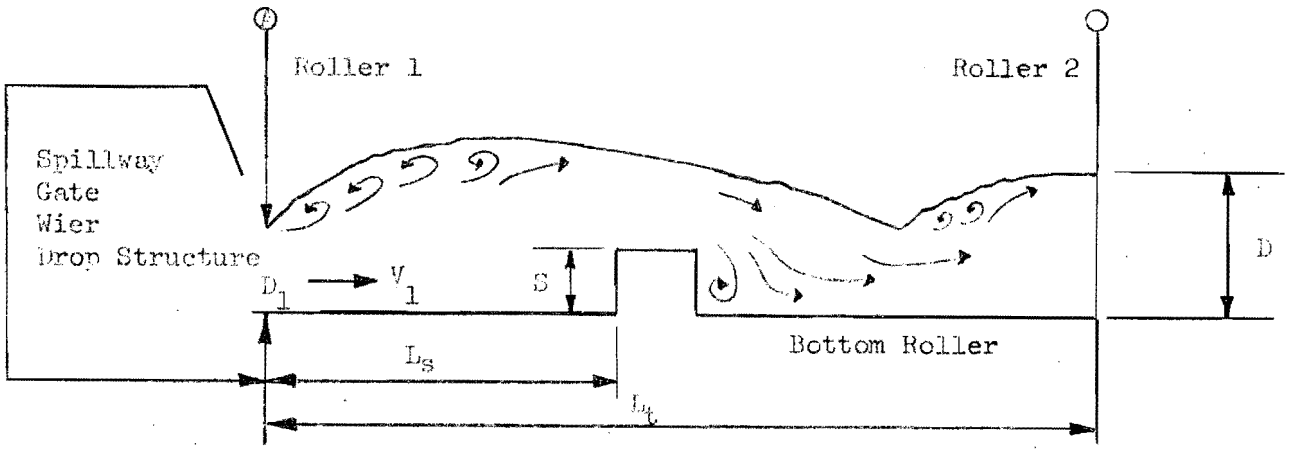

Figure 5. Flow boundaries and variables for vertical sill model [after Rand, (18)].

A forced hydraulic jump was stabilized at the entrance section of the flow by proper adjustment of tailwater depth for any given L_s and S . The forced hydraulic jump which was studied produced either supercritical or subcritical tailwater depths. When subcritical tailwater conditions existed, two rollers were observed, one upstream and one downstream of the sill. It was established that the jump could be stabilized in the basic position at the flow entrance provided a particular height of the sill was used. If the sill, S_j , is allowed to approach the entrance section, it was discovered that L_s and S_j decrease simultaneously until a minimum

L_s and a critical sill height S_c are reached. A slightly lower sill would produce a ski jump flow over the sill and the jump surface roller would vanish. When the sill was allowed to move in the downstream direction and its height increased to hold the jump in its basic position, a maximum L_s and maximum S value were obtained. The sill, in this position, acted in the manner of a true weir. The forced hydraulic jump became nearly a natural hydraulic jump. The upstream depth remained practically constant when the sill was moved further downstream from this point. Computed values of the maximum sill height, based on the papers of Forster and Skrinde, and Kandaswamy and Rouse, agreed closely with the experimentally determined values from Rand's study. The maximum sill height is normally computed on the basis of the sill being considered as a low weir.

DESIGN AND CONSTRUCTION OF MODEL

The model utilized in this study was identical to the one used by Aguirre[1], with the exception that a rise or sill was added to the stilling basin section. The components of this model as used by Aguirre are a horizontal bottom stilling basin and downstream channel, an entrance channel with a curved bottom and a tank for stilling and control of the upstream flow. The horizontal bottom and vertical sides of the stilling basin and downstream channel were constructed of 3/4-inch plywood. Control of the tailwater depth was accomplished by means of a 36-inch long flap gate placed at the end of the channel.

As mentioned previously in the review of Aguirre's work, he varied the geometric configuration of the model in order to determine the most effective design. Based on his evaluation of these variations, one particular scheme was selected for use in the present investigation. This scheme consisted of two fixed parallel channel walls, 26 inches long, and 36 inches apart. The angle of the flared walls at the upstream portion of the stilling basin was 45° measured from the channel centerline.

Two removable bottoms were utilized as a part of the model during the experimental work, as shown in Figure 6. One of the bottoms with the angle $\beta = 60^{\circ}$ as shown, was used in conjunction with testing of the model with a sill installed. The other bottom with $\beta = 0$ was placed in the model for the majority of the testing which incorporated an abrupt rise at the end of the apron. The bottom with $\beta = 0$ is preferable since it produces results which are comparable to those obtained with the other bottom and it is simpler and more economical to construct.

The removable bottom of the entrance channel used with the abrupt rise consisted of 3/4-inch plywood sides which were used as templates set 6 inches outside to outside. A horizontal bottom 6 inches above the stilling basin bottom was formed by these templates. Downstream and tangent to the

horizontal portion, the bottom formed a circular vertical curve with a 9-inch radius and 60° deflection angle. The downstream end of the vertical curve and the horizontal basin floor were connected by a short tangent. This removable bottom was of such a shape that, at any point along its surface, a transverse horizontal line would be a straight line. The other removable bottom which was used in testing the sill consisted of a sheet metal template placed along the bottom centerline with a vertical curve and end tangent identical to those of the plywood template on the sides. The point of curvature and point of tangency of the center template were at the same elevation as the corresponding points on the side templates but were displaced a fixed distance downstream. This distance was such that, when projected on a horizontal plane, a horizontal line connecting any point on the center template to a similar point on the outside curve of the side template would form an angle of 30° with a horizontal straight transverse line. Therefore, two such horizontal lines from corresponding points on the side templates would intersect at the center template forming a 60° deflection angle shown as angle β in Figure 6. The bottom was constructed in such a manner that the intersection of either side slope with the stilling basin bottom was 1/2-inch downstream from the intersection of the entrance channel walls and the flaring basin walls, measured parallel to the channel centerline.

A center section of the apparatus is shown in Figure 7. As seen in this figure, a 6-inch-wide control tank containing five wire mesh screens was used for stilling action. The tank outlet was an opening 6 inches wide by 6-1/4 inches high. A sluice gate constructed of 1/8-inch-thick brass was installed to control the depth of flow out of the tank. An instrument carriage was provided to aid in measurement of water depths as well as positions of the jump and flow velocities. The carriage was composed of two separate frames, consisting of a combination of steel pipe and structural steel shapes.

Measurements of water depths and the location of jump positions were made with a Lory Type "A" point gage mounted on the top frame of the instrument carriage. Velocity measurements were taken by a Prandtl-type Pitot tube, mounted also on the top frame of the instrument carriage.

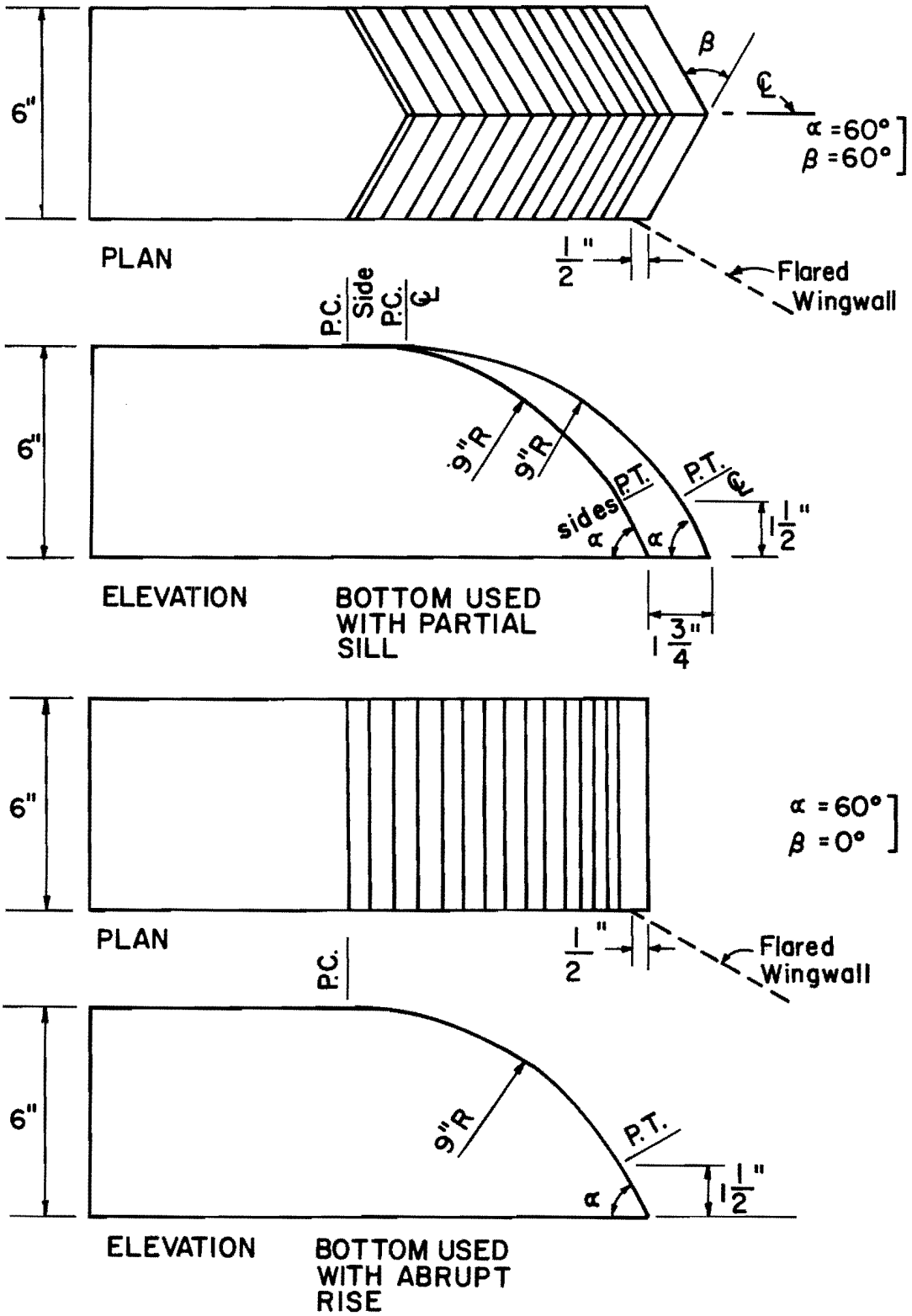

FIGURE 6 - DETAILS OF REMOVABLE ENTRANCE CHANNEL BOTTOMS

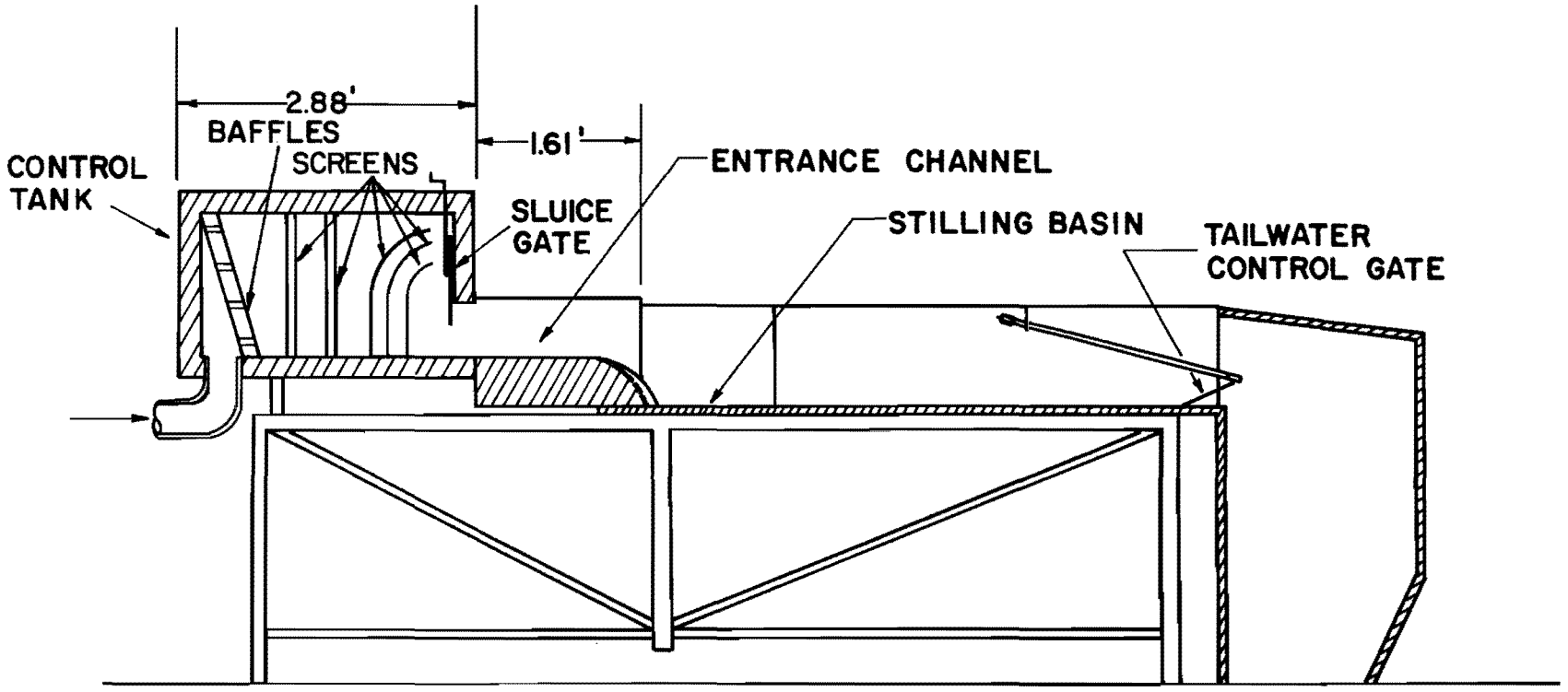

FIGURE 7 - CENTER SECTION OF THE APPARTUS

Tailwater depth measurements were made with a piezometer installed in the downstream channel bottom. The piezometer was located 8 inches upstream of the control gate, on the channel centerline. It was connected to an open manometer which was supported on one of the channel sides.

The model was connected to the laboratory constant head tank. Flow into the model from this tank was regulated by means of a 3-inch gate valve. Discharge measurements were made using a Venturi-orifice type meter connected to a differential water manometer.

The first geometric feature which was added to the model scheme previously described was a partial transverse sill. This sill built of wood was rectangular in cross section and was 3/4-inch high and 3/4-inch thick. The sill was two feet long and left an opening of 6 inches between the end of the sill and the channel walls at either end. The face of the sill was placed at the downstream end of the flare of the stilling basin wingwalls, at the section where the wingwalls intersected the parallel channel walls. The sill was waterproofed with fiberglass and painted. All joints were caulked and smoothly finished. As previously noted, the sill was placed in the model which included the entrance channel bottom with a 60^{o} deflection angle. Figure 8 shows a plan view of the model stilling basin with the sill included.

The sill was removed from the model after completion of testing with it in place. Tests were then made using a succession of four abrupt rises. The first test was on a rise approximately 1/2-inch high. Following these tests, the rise was increased successively to 1, 1-1/2, and 2 inches nominal height. Each rise was installed and tested at two different positions. One position of the rise was at a distance of 6 inches from the section where the flared wingwalls intersected the parallel channel walls, measured parallel to the channel wall. The second position of the rise was such that this distance was 9 inches. The rise extended continuously the entire width and length of the downstream channel. The rises were constructed of 1/2-inch-thick plywood and were waterproofed with a fiberglass coating and then painted. All joints were caulked and smoothly finished. Figure 9 shows a plan view of the model stilling basin with the rise in the two positions at which it was tested.

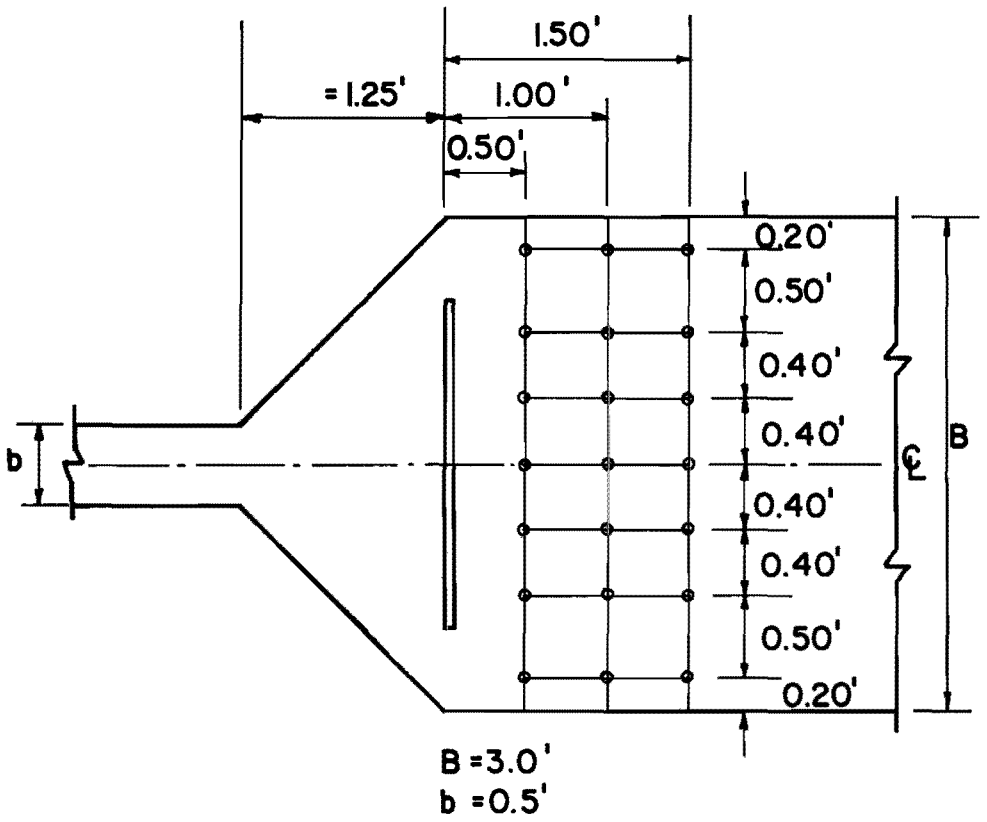

FIGURE 8 - PLAN VIEW OF THE MODEL WITH SILL SHOWING LOCATION OF VELOCITY MEASUREMENTS

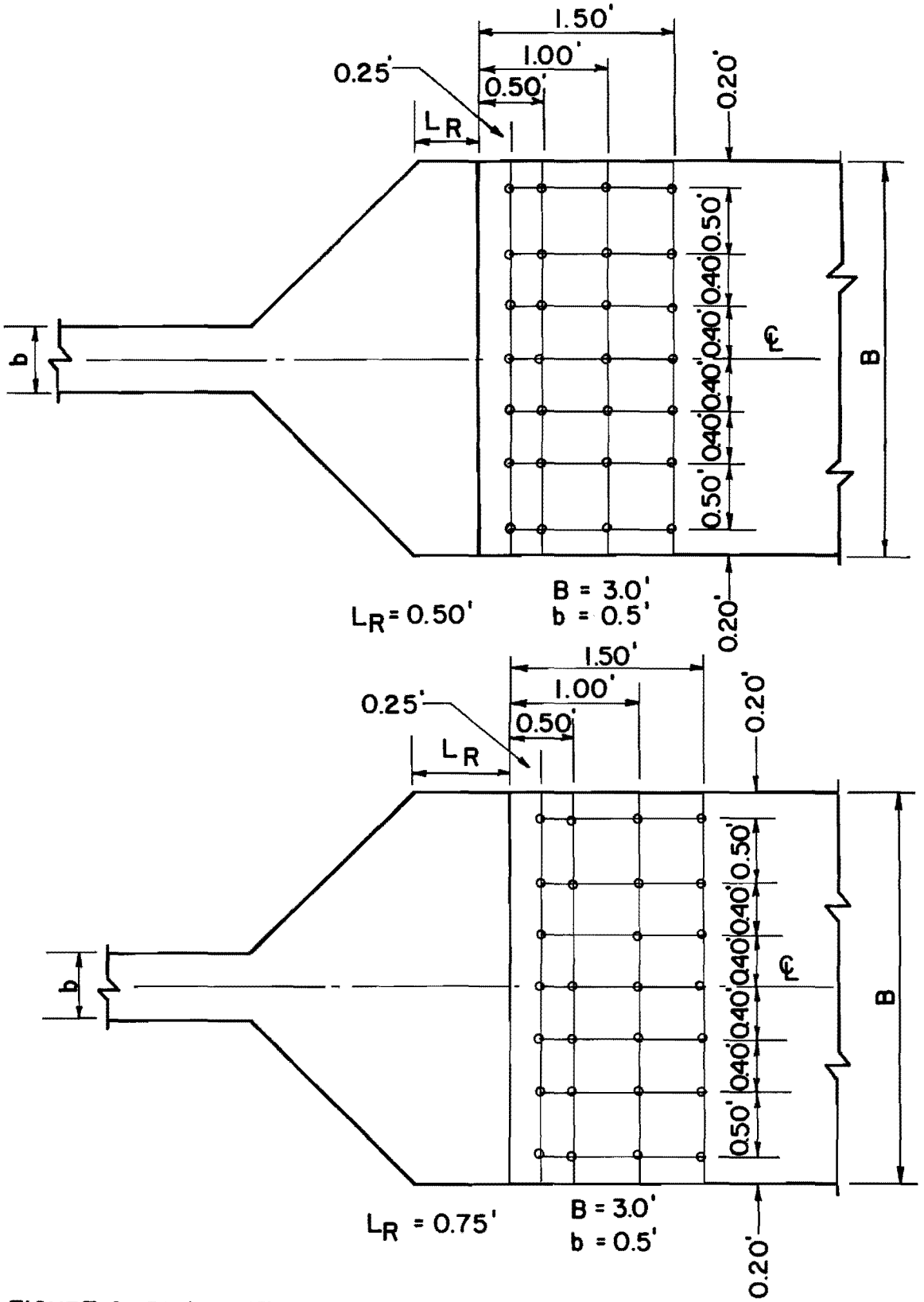

FIGURE 9- PLAN VIEW OF THE MODEL WITH ABRUPT RISE SHOWING LOCATION OF VELOCITY MEASUREMENTS ON RECTANGULAR GRID

At the completion of the experiments with the 2-inch rise, a beveled face at a 45° angle was added to the rise at its position 9 inches from the end of the flared wingwalls. The beveled face intercepted the basin bottom at a vertical angle of 45°. A side view as well as a plan view is shown in Figure 10. This approach was the last feature added for the experimental program.

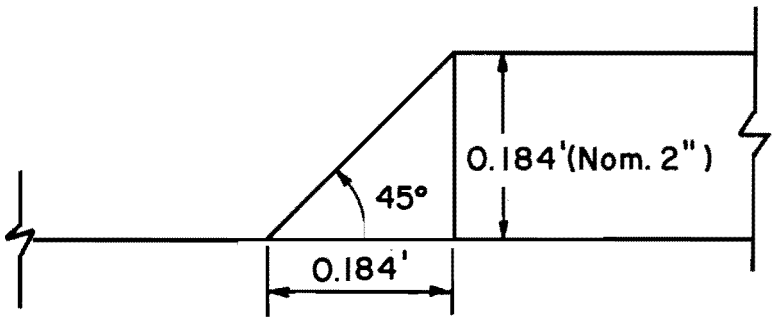

SECTION A-A

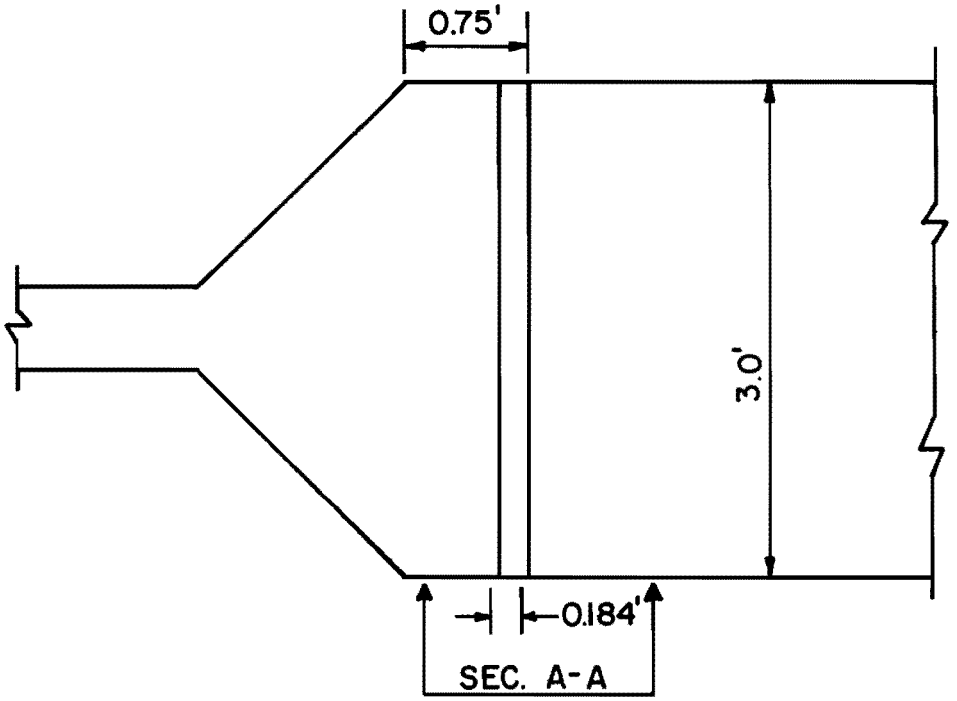

PLAN VIEW

FIGURE 10 - DETAILS OF NOMINAL 2-INCH HIGH RISE WITH 45° BEVELED FACE

ANALYSIS

Analysis of the radial flow stilling basin with an abrupt rise indicated the significance of a number of variables. The tailwater depth, y_3, is expressed as a function of the other variables as follows:

$$y_3 = f(V_t, y_t, H_R, L, L_R, x, B, b, Z, r, \alpha, \beta, g, \text{and } \theta)$$

where

y_3 = tailwater depth,

V_t = velocity of flow at the beginning of the vertical curve. Location of this point is shown in Figure 9 as the P.C. of the vertical curve of the entrance channel bottom,

y_t = the depth of flow measured at the section where V_t occurs,

g = gravitational acceleration,

H_R = height of abrupt rise,

L_R = distance from the downstream end of the flared wingwalls to the abrupt rise, measured parallel to the channel centerline,

L = distance between the upstream and downstream end of the flared wingwalls measured parallel to the channel centerline, and

x = distance from the upstream end of the flared wingwalls to the leading edge of the hydraulic jump measured parallel to the channel centerline.

θ, B, b, Z, r, α, and β* are constant in this model and are defined in Figure 11.

*$\beta = 60^{\circ}$ for tests with partial sill, $\beta = 0^{\circ}$ for tests with abrupt rise.

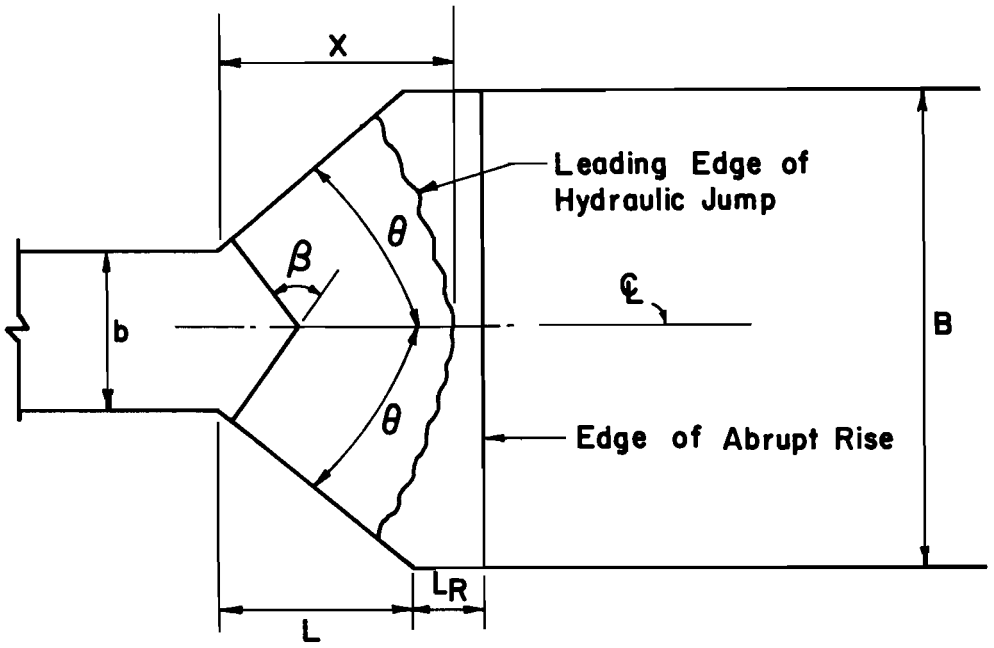

PLAN

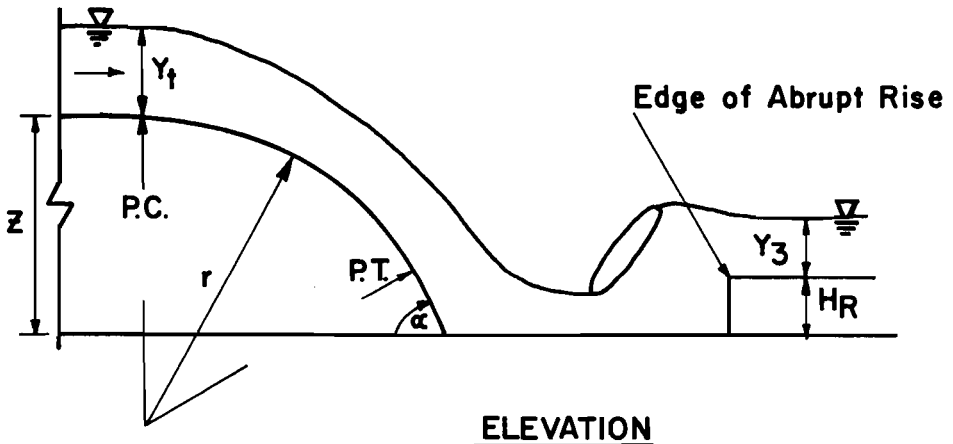

ELEVATION

FIGURE II - DEFINITION OF PARAMETERS

From these variables the following dimensionless variables were obtained from dimensional analysis:

$$\frac{y_3}{y_t}\ ,\ F_t\ ,\ \frac{x}{y_t}\ ,\ \frac{y_t}{b}\ ,\ \frac{L_R}{L}\ ,\ \frac{H_R}{L}\ ,\ \frac{B}{b}\ ,\ \beta\ ,\ \theta\ ,\ \alpha\ ,\ \frac{Z}{y_t}\ ,$$

$$\frac{V_t^2}{r_g}\ ,\ \text{and}\ \frac{r}{Z}\ .$$

In this experimental work, B/b , β , θ , α , and r/Z were held constant, while the effects of changes in Z/y_t and V_t^2/r_g were not of significance in this study. Therefore, the dimensionless parameters which were of interest in this study were:

$$\frac{y_3}{y_t}\ ,\ F_t\ ,\ \frac{x}{y_t}\ ,\ \frac{y_t}{b}\ ,\ \frac{L_R}{L}\ ,\ \text{and}\ \frac{H_R}{L}\ .$$

The Froude number is included as one of the dimensionless variables since the flow is governed primarily by gravity forces in both the model and prototype structure. The fluid property of viscosity must be considered as to its significance. Reynolds number is the dimensionless parameter used to ascertain the relative importance of viscosity. Viscous effects can be neglected if the minimum Reynolds numbers are sufficiently high so that completely turbulent flow exists. Preliminary analysis of the expected flow conditions in the model indicated a minimum Reynolds number of approximately 1×10^5 which is well into the turbulent flow range for the model.

The pressure on the face of the abrupt rise may be due to both dynamic pressure and hydrostatic pressure. Dynamic pressure is created as a result of the thrust on the face of the rise by the high velocity upstream jet. The pressure distribution on the face of the rise will be predominately hydrostatic if the toe of the jump is sufficiently far away from the face of the rise. If this pressure distribution is assumed to be hydrostatic for the model reported herein under a head of h_D , if the shear stress along the solid boundaries between the sections at y_t and y_3 is

neglected, and if the momentum coefficients at these sections are assumed as unity, the momentum equation for the sections at y_t and y_3 may be written as:

$$\frac{\gamma y_t^2 b}{2} - \gamma \left(h_D - \frac{H_R}{2} \right) H_R B - \frac{\gamma y_3^2 B}{2} = \frac{\gamma}{g} Q(V_3 - V_t) \qquad (1)$$

in which γ is the specific weight of the fluid and Q is the discharge.

The continuity equation may be written as:

$$Q = V_t Y_t b = V_3 Y_3 B \qquad (2)$$

Combining Equations 1 and 2 and reorganizing, the following equation may be written relating the aforementioned variables:

$$F_t^2 = \frac{1 - 2 \left(\frac{H_D}{Y_t} \right) \left(\frac{H_R}{Y_t} \right) \frac{B}{b} - \left(\frac{Y_3}{Y_t} \right)^2 \frac{B}{b}}{2 \left[\left(\frac{Y_t}{Y_3} \right) \frac{b}{B} - 1 \right]} \qquad (3)$$

The pressure head on the face of the rise, h_D, was not measured in this experimental program, however, it may be calculated by assuming hydrostatic pressure conditions at the rise, with the tailwater depth y_3 assumed to be approximately equal to the water depth at the face of the rise. This variable is not mentioned in the preceding dimensional analysis, since it will be another dependent variable and will be a function of the other variables.

As in the work of Aguirre[1], values selected in the experimental program for dimensionless variables were such that they would be compatible with normal field conditions, and in the case of the geometric variables would lead to a design that would be relatively simple and economical to construct.

EXPERIMENTAL PROCEDURE

Tests were conducted to determine the performance of rises of four different heights as well as the performance of a sill. The rise heights tested were 0.042 feet (nominal 1/2 inch), 0.092 feet (nominal 1 inch), 0.137 feet (nominal 1-1/2 inch), and 0.184 feet (nominal 2 inch). Each rise was tested at two positions, 6 inches and 9 inches away from the downstream end of the flare. After the rise of 2-inch nominal height was tested, a 45^{o} beveled end sill was added to the face of this rise at its positon 9 inches from the end of the flare.

Measurements were made to determine jump stability and selected velocities in the channel for each rise at both positions. The hydraulic jump stability was determined by measuring the longitudinal change in jump position resulting from a change in tailwater depth. The jump position was measured by placing the point gage directly over the leading edge of the jump. The jump position was indicated on a calibrated tape placed on the side of one of the longitudinal tracks. Since the jump position oscillated somewhat, a visual temporal average of its position was observed. The tape on which the jump position was indicated was read to the nearest 0.01 foot, but the actual average position was determined to approximately ±0.04 feet. A tailwater depth was measured by means of a piezometer for each adjusted jump position. The piezometer was located at $x = 6.0$ ft. and was connected to a manometer which was read to the nearest ±0.002 foot.

The tailwater was adjusted for each magnitude of rise so that the leading edge of the jump moved from an initial position of $x = 0.17$ feet near the beginning of the flared basin to the fartherest position downstream where a true jump would be maintained. Several intermediate jump positions were set and the corresponding tailwater depths measured.

Jump stability determinations were made in this manner for six values of F_t the Froude number at the downstream end of the horizontal

position of the entrance channel. F_t ranged from a low of 1.63 to a high of 2.94. The different values of F_t were obtained by varying both the discharge and the depth of flow y_t.

Two values of discharge, 0.64 and 0.72 cubic feet per second were used. For each discharge setting, three values of y_t were used to obtain the desired F_t. The minimum y_t setting was 0.195 feet, while the maximum y_t setting was the free entrance flow depth with no sluice gate control.

Velocity measurements were made in the channel section past the rise to determine the velocity distribution in the channel and the energy reduction created by the action of the hydraulic jump and the abrupt rise. Velocity measurements were taken at a Froude number of 2.94, in order to observe the maximum velocity conditions. It was of primary interest to investigate the velocity near the channel bottom which was taken as an indicator of the potential for scour. For this reason all but one set of velocity measurements were taken at a height of 0.02 feet, measured from the bottom of the Pitot tube to the channel bottom. The vertical distance from the channel bottom to the centerline of the Pitot tube was approximately 0.025 feet.

Prior to the reading of velocity measurements for each rise, the jump was stabilized at its fartherest position downstream in order to determine the worst velocity conditions which could occur. In the case of the two larger rises, 0.137 feet and 0.184 feet high respectively, excessive ski jump flow resulted in a large concentration of flow as far as 1.5 feet downstream from the face of the rise with the jump in its fartherest downstream position. For this reason, the jump was moved back upstream by adjustment of the tailwater depth until the flow was more uniformly distributed and also of a reduced velocity in the channel section. In this position velocity measurements were again taken in the channel. Velocity measurements were also taken for the rise .042 feet high with the jump positioned back upstream from its maximum possible downstream setting. For this rise, with the jump at its maximum downstream position, velocities as high as 4 feet per second were recorded near the face of the rise.

As shown in Figure 9, the principle velocity measurements were taken on a rectangular grid. Measurements were taken at longitudinal distances

of 0.25, 0.50, 1.00, and 1.50 feet from the face of the rise. Velocity measurements were taken at the channel centerline and at lateral distances of 0.40, 0.80, and 1.30 feet to the left and right of the centerline. To give a better indication of the velocity distribution in the channel resulting from the spreading action of the radial stilling basin, a number of radial velocity profiles were obtained. As shown in Figure 12, the velocity measurements were taken at the intersection of a circular arc of radius 2.125 feet with the previously established lateral stations. The circular sector was one with a central angle of 90°, the same angle as the one formed by the projected intersection of the flared wingwalls. Radial measurements were made in the region of concentrated flow. For the rise 0.042 feet high, the arc was constructed so that it intersected the channel walls 0.25 feet from the face of the rise, while the arc constructed for measurements points for the 0.137 foot and 0.184 foot high rises intersected the channel walls 0.50 feet from the face of the rise.

Another special velocity profile was taken for the 0.137 foot high rise in its position 0.50 feet from the downstream end of the flare. Velocities were determined for this rise with the centerline of the Pitot tube 0.055 feet above the channel bottom. A lateral profile was taken for the seven lateral stations at a longitudinal distance of 1.0 feet from the face of the rise. The purpose of these measurements was to compare the velocity distribution in the middle of the flow stream at this height with the velocity distribution obtained at the measurement height of 0.02 feet.

In the case of the model with the partial transverse sill included, the experimental program consisted of a series of velocity measurements taken in the channel section past the sill. As shown in Figure 8, velocity measurements were taken on a rectangular grid similar to the one for the abrupt rise. The lateral points of measurement were at the centerline, and 0.40, 0.80, and 1.30 feet to the right and left of the centerline. Longitudinal points were 0.50, 1.00, and 1.50 feet from the intersection of the flared wingwalls with the parallel channel walls measured parallel to the centerline. Measurements of velocity were taken 0.02 feet from the bottom of the Pitot tube to the channel bottom, except for one special set of measurements.

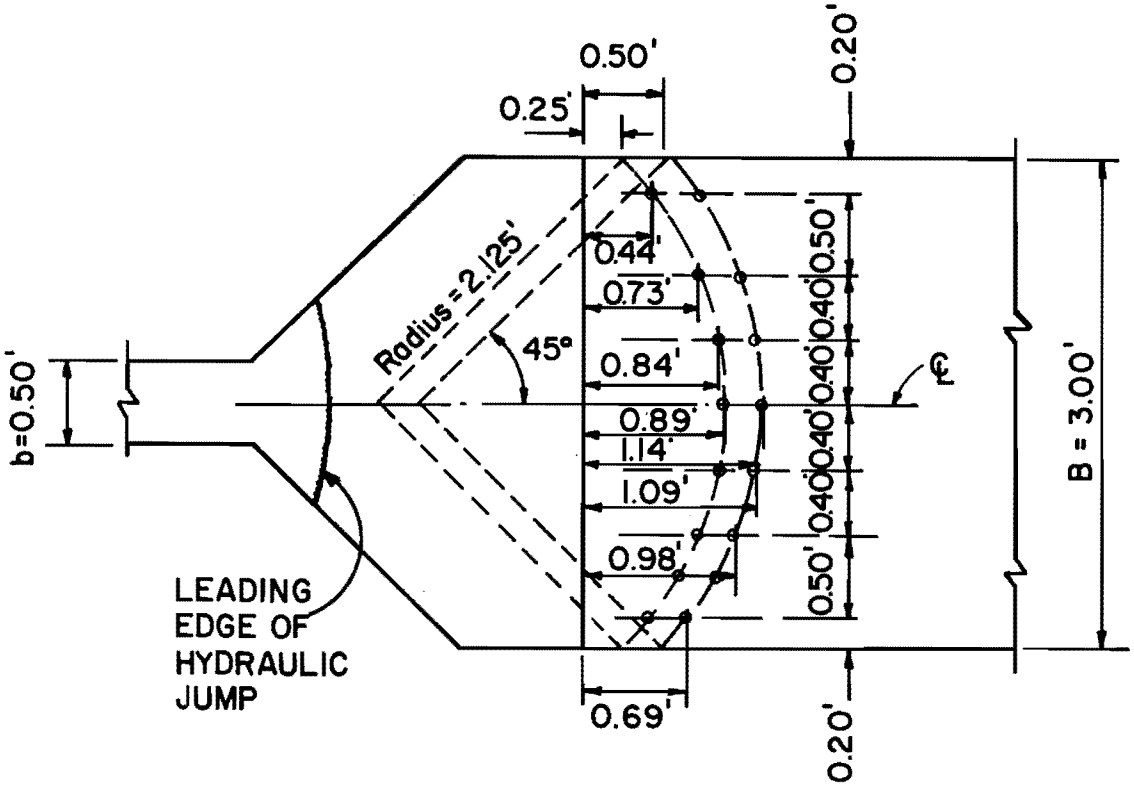

FIGURE 12 - PLAN VIEW OF MODEL WITH ABRUPT RISE SHOWING LOCATION OF RADIAL VELOCITY MEASUREMENTS

Velocity measurements were obtained for six different values of Froude number, F_t, ranging from 1.76 to 2.94. The Froude number was varied in a manner similar to that for the abrupt rise, in that the different values of F_t were arrived at by varying both the discharge and the depth of flow y_t. The minimum y_t setting was 0.195 feet, while the maximum y_t setting was the free entrance flow depth with no sluice gate control. For each value of F_t, velocity measurements were taken with the jump at three different positions.

EVALUATION OF RESULTS

Performance characteristics of both the abrupt rise and partial transverse sill will be discussed in the following portion of the report:

I. Structure With Abrupt Rise

Performance of the abrupt rise was evaluated on the basis of jump stability characteristics and tailwater requirements as well as the magnitude and distribution of velocities.

A. Tailwater Requirements and Jump Stability

1. General Characteristics

One indication of the performance of the structure with the abrupt rise is the degree of stability of the jump position for a variable tailwater depth. This characteristic was studied for each of the four rises (1/2, 1, 1-1/2, and 2 inches nominal height) at two positions, 6 and 9 inches from the downstream end of the flare. Stability of the jump is represented by the change in position of the hydraulic jump corresponding to a given change in tailwater depth. The jump position denoted as x, was defined as the distance from the beginning of the flared wingwalls to the leading edge of the jump.

As mentioned previously in the analysis, the required tailwater depth, y_3, for the specific basin and channel geometry required to stabilize the jump at the position x depends on V_t, y_t, g, L, L_R, and H_R. The entrance channel width, b, was added to these variables to form the dimensionless variables y_3/y_t, x/y_t, F_t, y_t/b, L_R/L, and H_R/L.

To investigate jump stability, the parameter x and correspondingly y_3 were varied for each rise at each of the two positions, while V_t and

y_t were maintained constant. From this procedure, y_3/y_t could be expressed as a function of x/y_t for several constant values of F_t and y_t/b, in the case of each value of H_R/L and L_R/L. As cited in the procedure, for each of two discharge rates, three values of y_t were set, so that for each rise in one of its positions, six different values of F_t were investigated. These functions for each rise including the ones for the 2-inch nominal high rise with the 45^o beveled face are shown in Figure 21-29.

As was demonstrated in the results presented by Aguirre[1], the degree of jump stability may be expressed by the absolute value of the slope of each curve of x/y_t vs y_3/y_t. Several general characteristics of these curves may be observed which were similar to those for the structure without the rise. For each rise, curves of y_3/y_t vs x/y_t indicate that for a certain value of x/y_t, a higher value of y_3/y_t is required to stabilize the jump in a certain position as F_t is increased. The absolute slope of these curves for constant values of H_R/L and L_R/L, appears to be approximately the same for each value of F_t. All of the curves indicate that as x/y_t is increased, the absolute value of the slope decreases. This change in slope is much more pronounced, however, for the lower rises of 1/2-inch ($H_R/L = 0.034$) and 1-inch height ($H_R/L = 0.074$).

2. Use of y_3/y_t vs F_t Curves

Another expression of these parameters is that of y_3/y_t vs F_t. For a particular Froude number, F_t, y_3/y_t values were determined for each corresponding x/y_t value, with the jump position ranging from a nearly submerged position close to the entrance channel to its extreme downstream position. The limiting values of y_3/y_t within which the jump would form at given entering flow conditions are thus shown, as seen in Figures 13-20, for each H_R/L and L_R/L value. In the case of the rises of 1/2-inch, 1-1/2-inch, and 2-inch nominal height, the lowest y_3/y_t values designated by a dashed line are not desirable for purposes of satisfactory design, since high velocities near the bottom are encountered in a portion of the channel with the jump in its extreme downstream position. This concentration

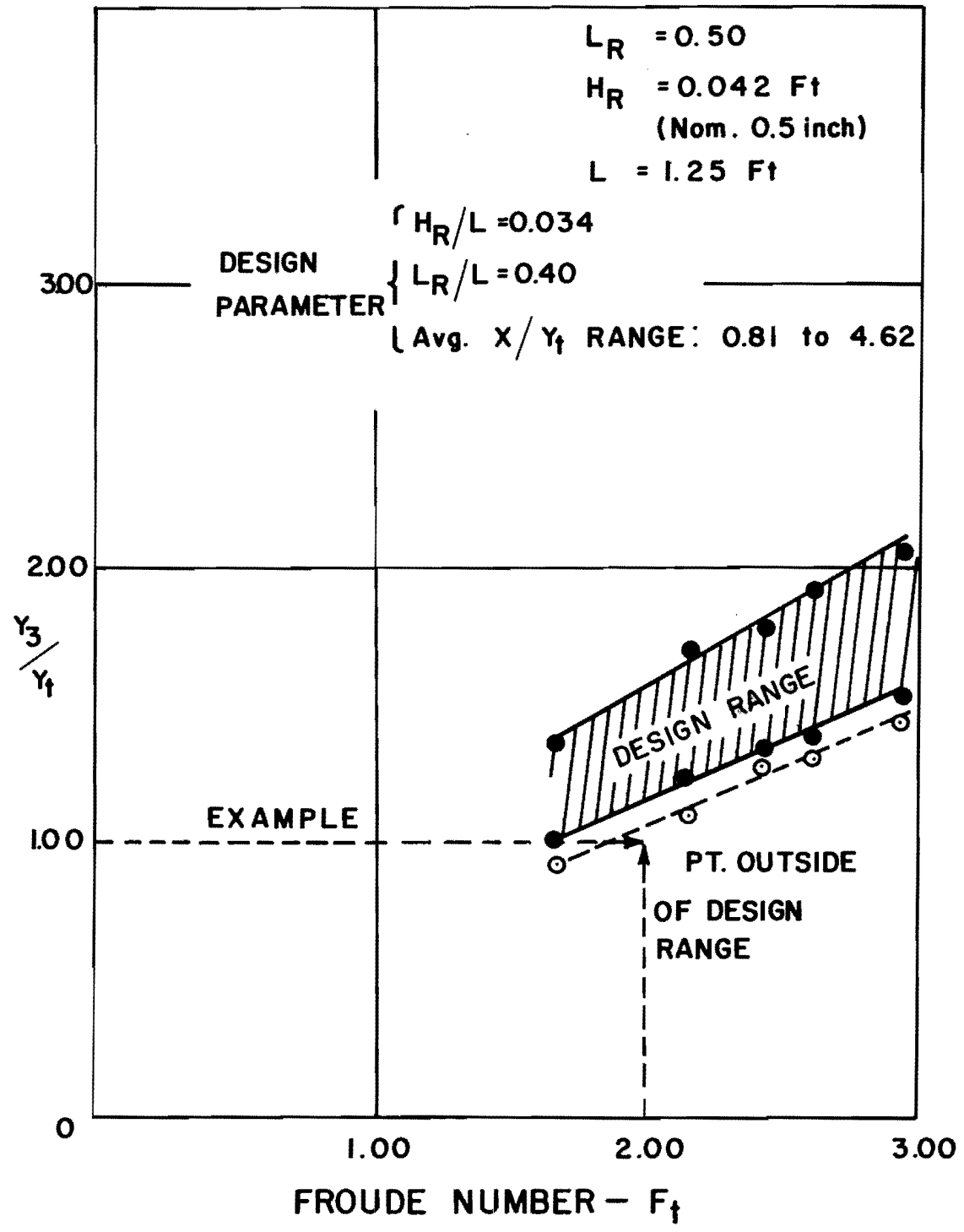

FIGURE 13 - VARIATION OF Y_3/Y_f vs. F_f FOR H_R/L = 0.034, L_R/L = 0.40

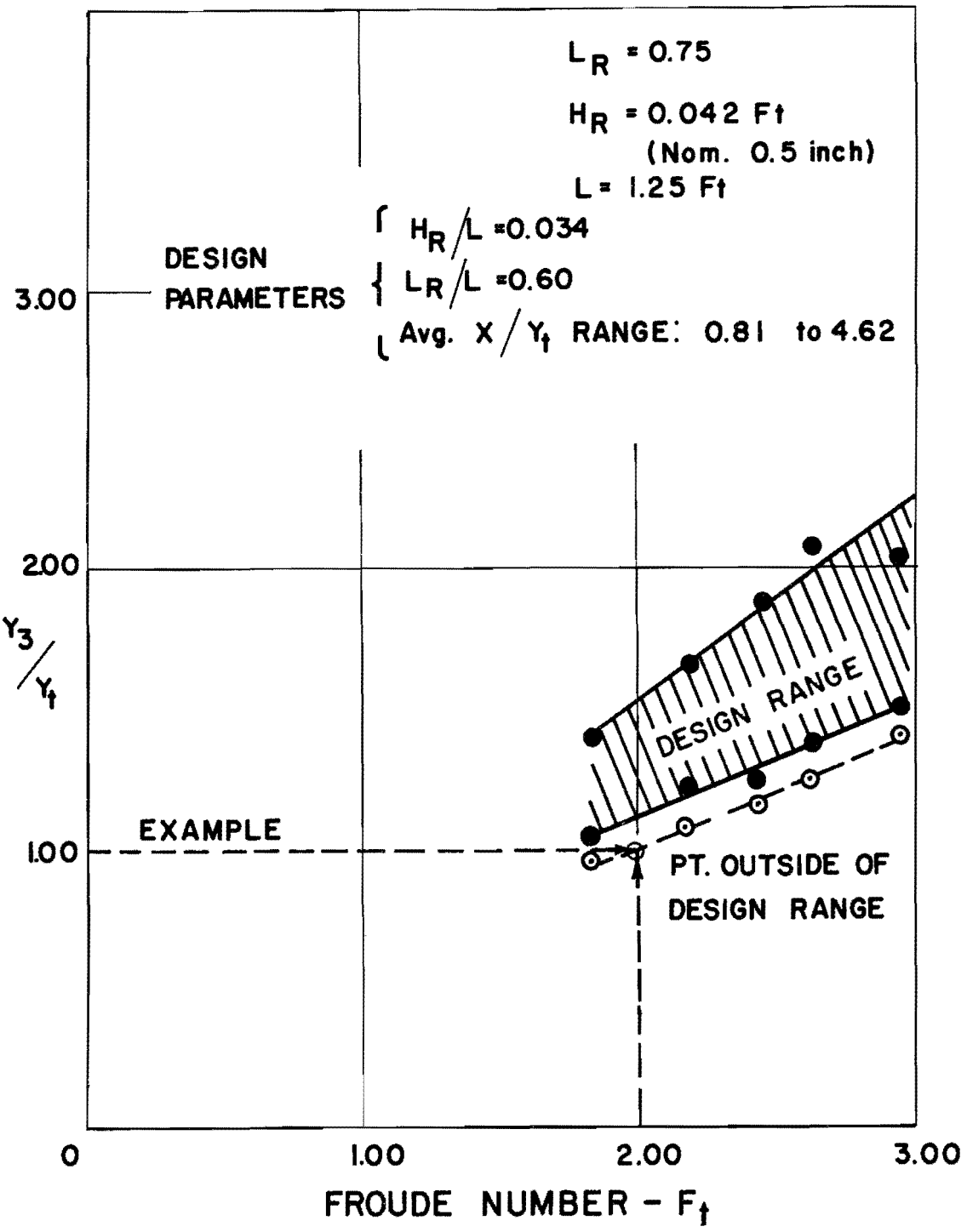

FIGURE 14 - VARIATION OF Y_3/Y_1 vs. F_1 FOR H_R/L=0.034, L_R/L=0.60

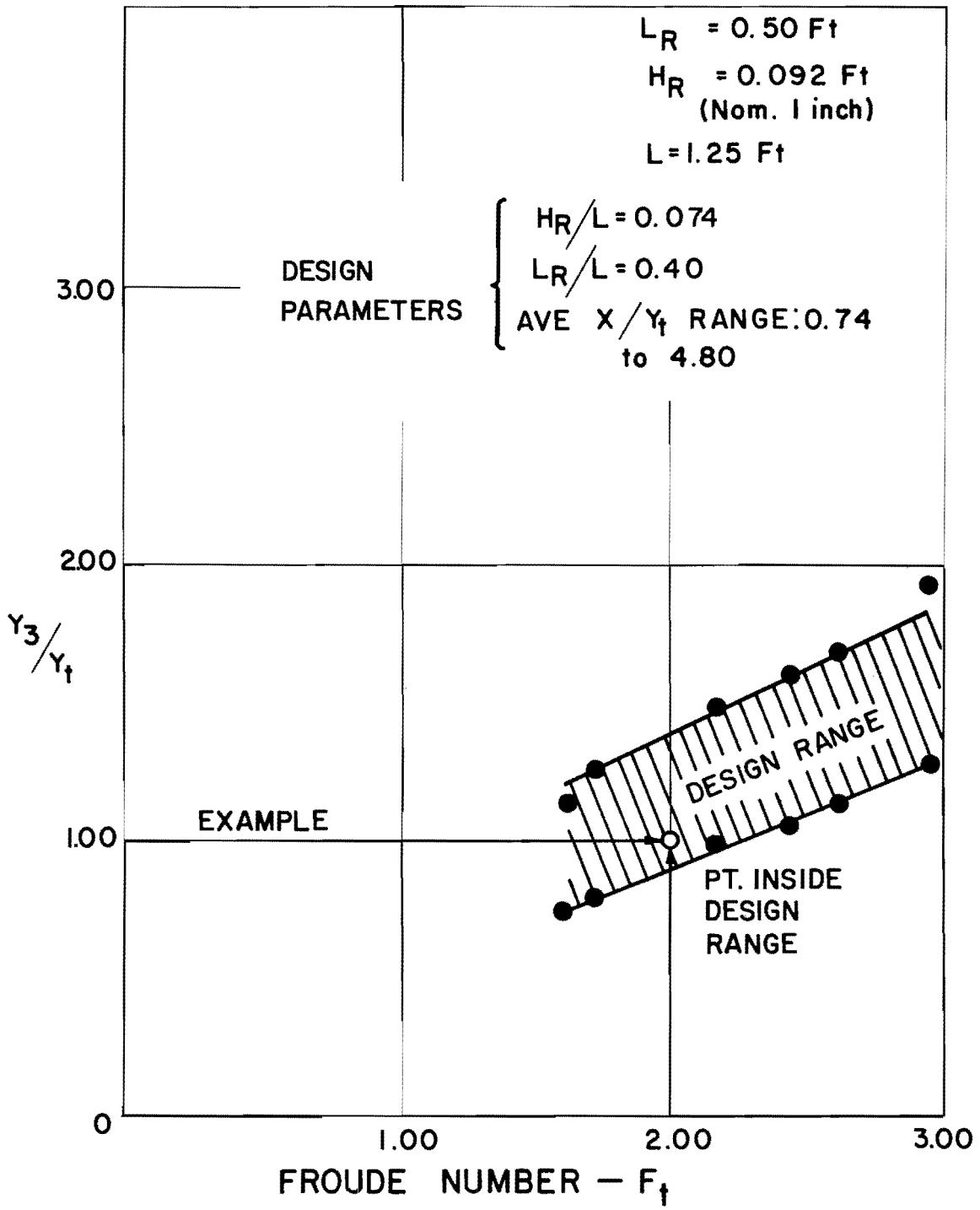

FIGURE 15 – VARIATION OF Y_3/Y_t vs. F_t FOR H_R/L=0.074, L_R/L = 0.40

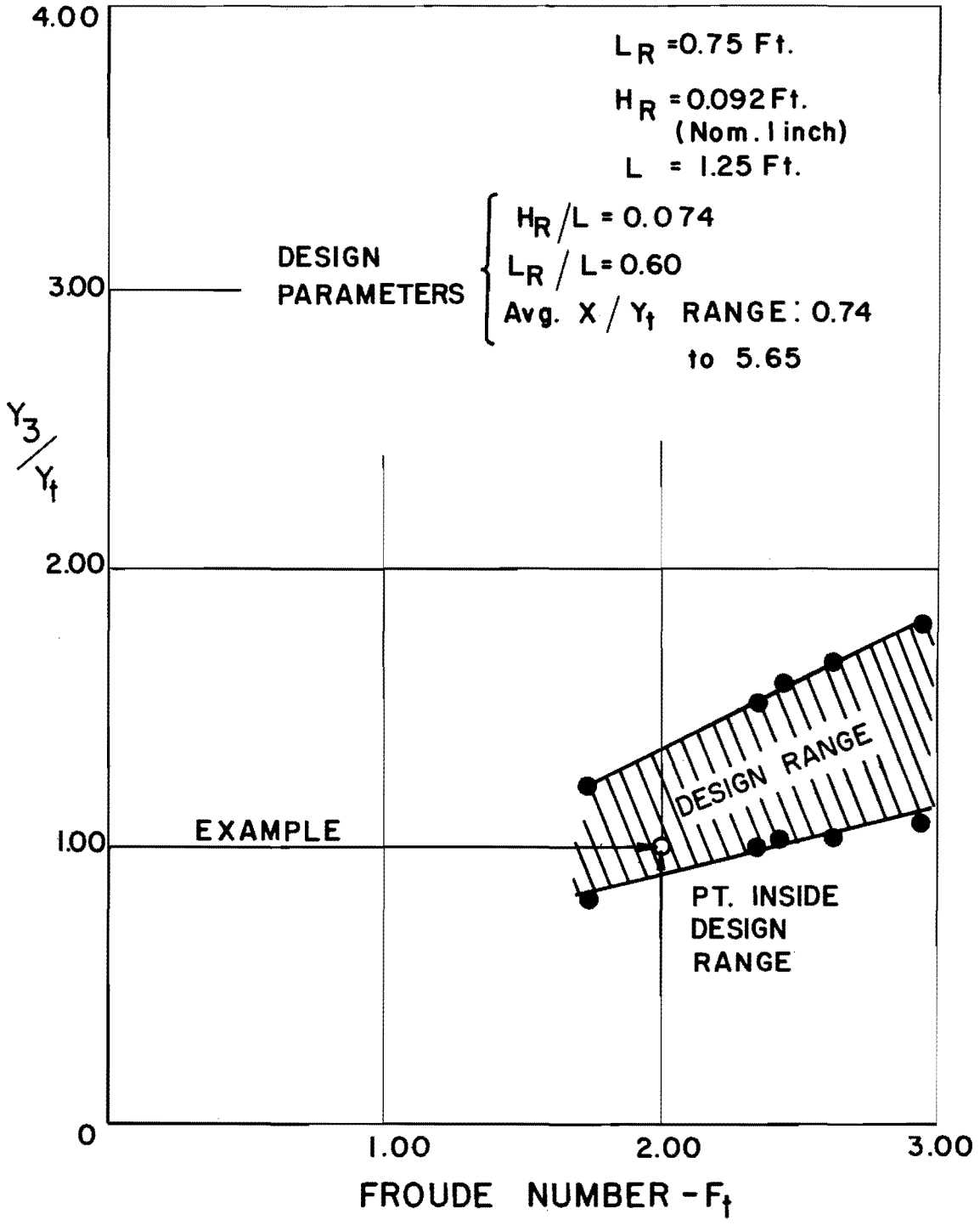

FIGURE 16 - VARIATION OF Y_3/Y_f vs. F_f FOR H_R/L =0.074, L_R/L = 0.60

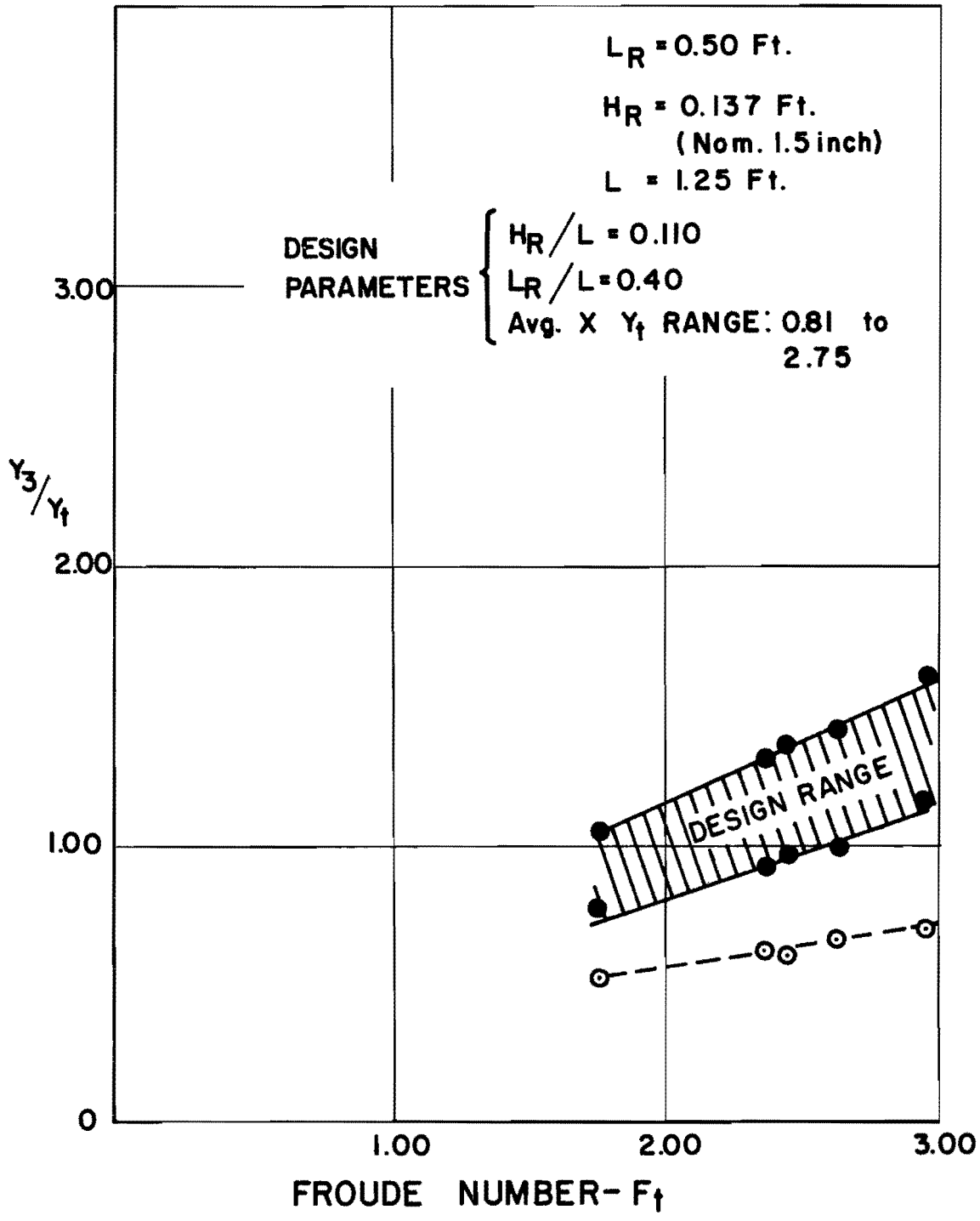

FIGURE 17 - VARIATION OF Y_3/Y_f vs. F_f FOR H_R/L=0.110, L_R/L =0.40

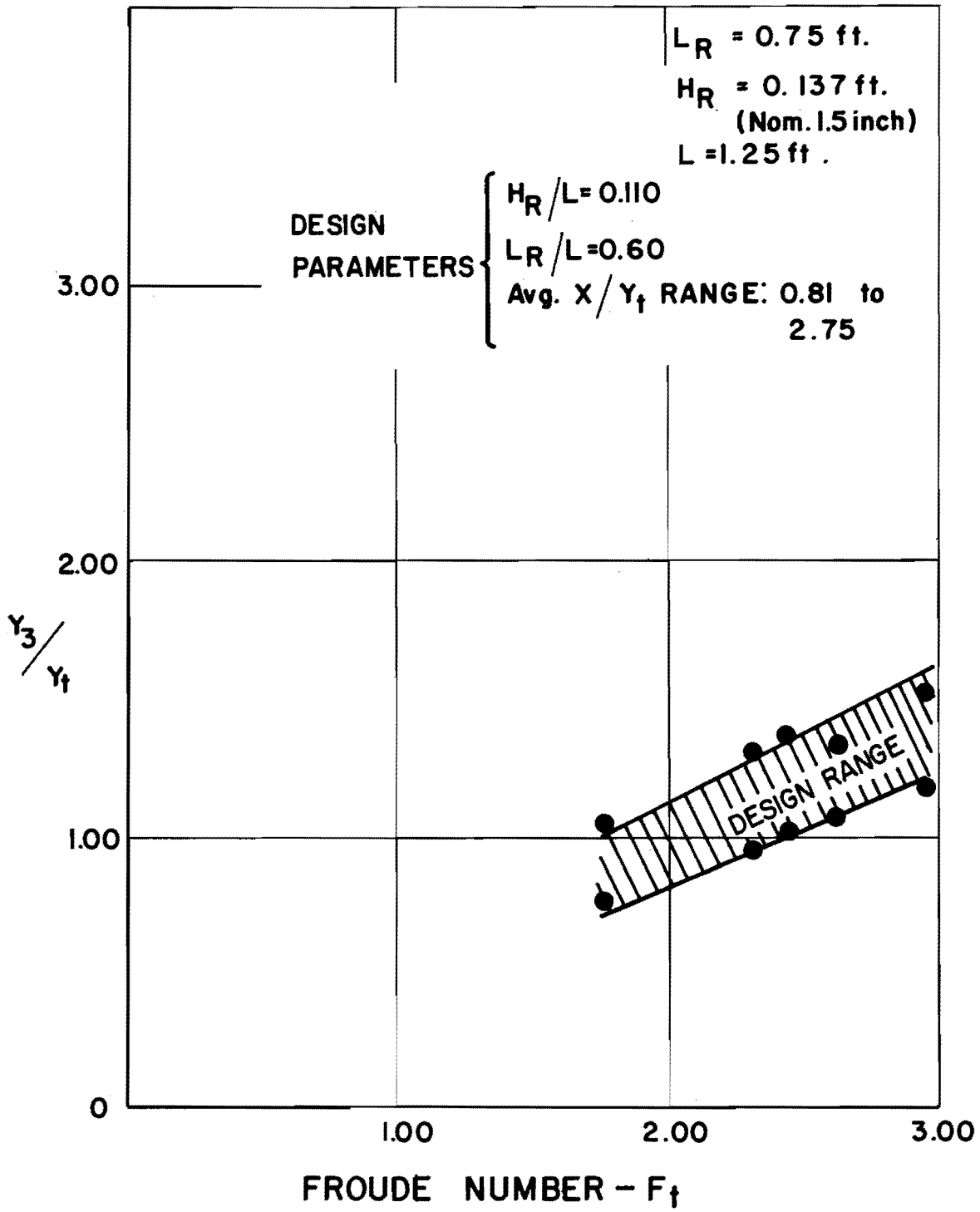

FIGURE 18 - VARIATION OF Y_3/Y_f vs. F_f FOR $H_R/L = 0.110$, $L_R/L = 0.60$

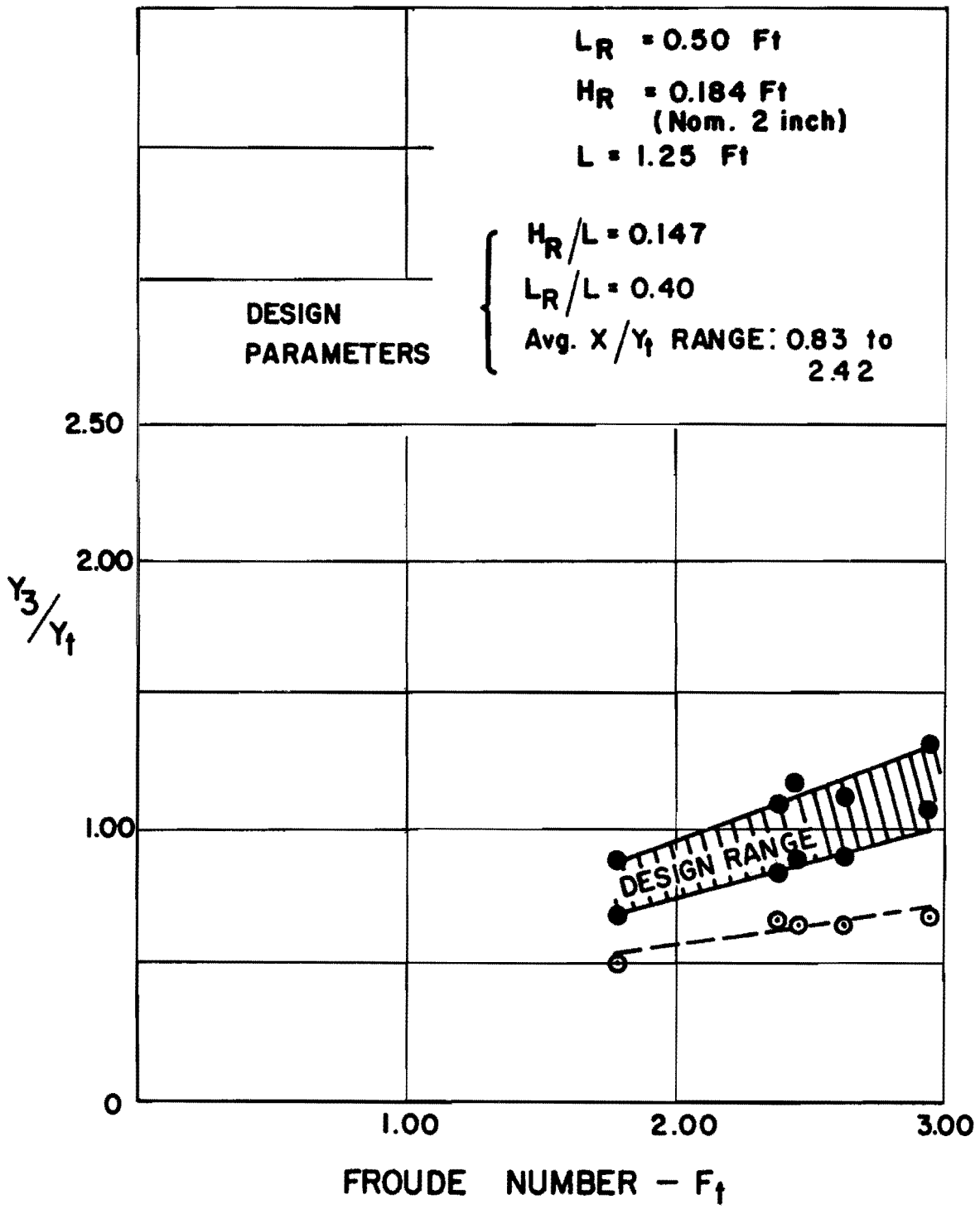

FIGURE 19 - VARIATION OF Y_3/Y_f vs. F_f FOR H_R/L=0.147, L_R/L = 0.40

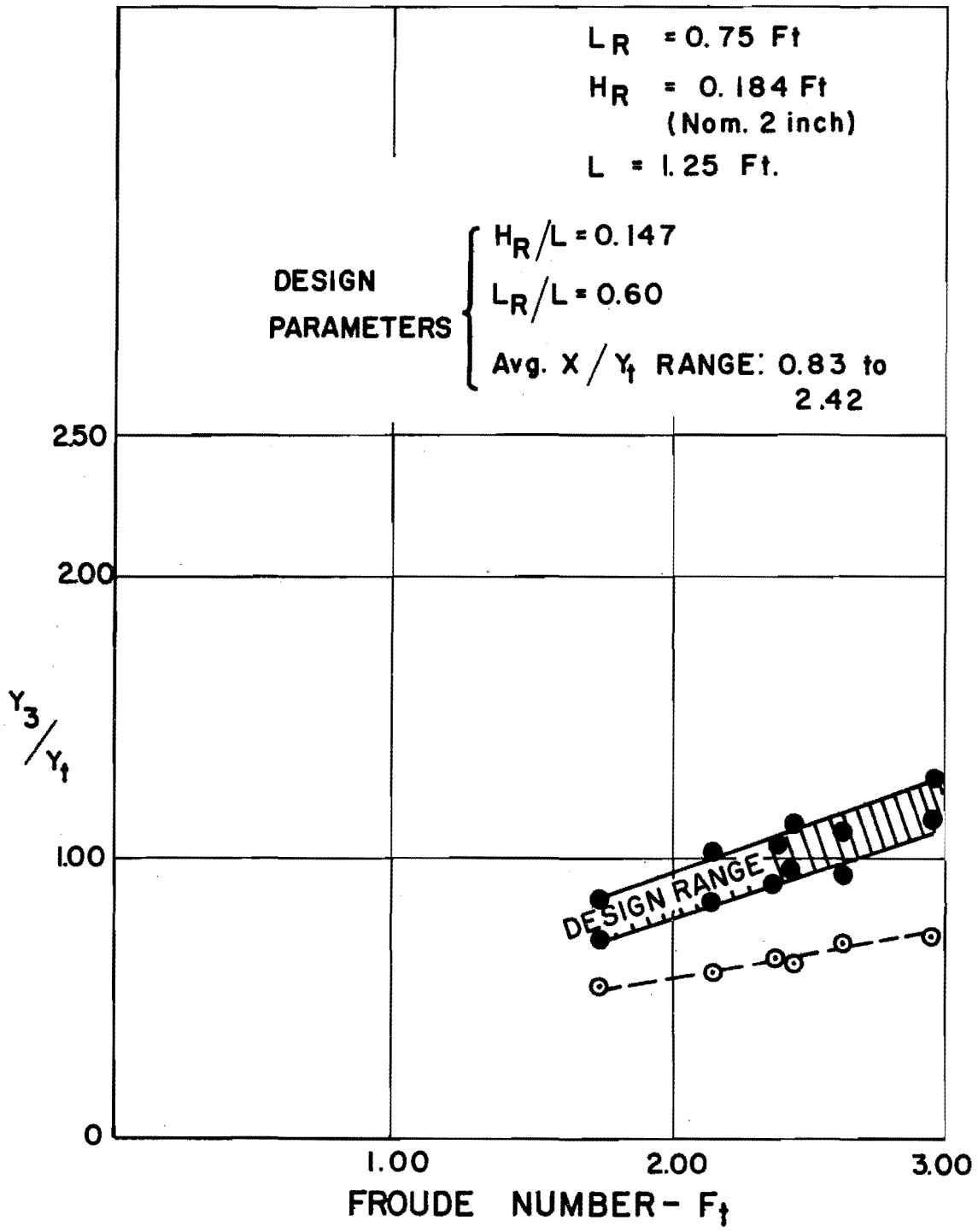

FIGURE 20 - VARIATION OF Y_3/Y_1 vs. F_1 FOR H_R/L=0.147, L_R/L = 0.60

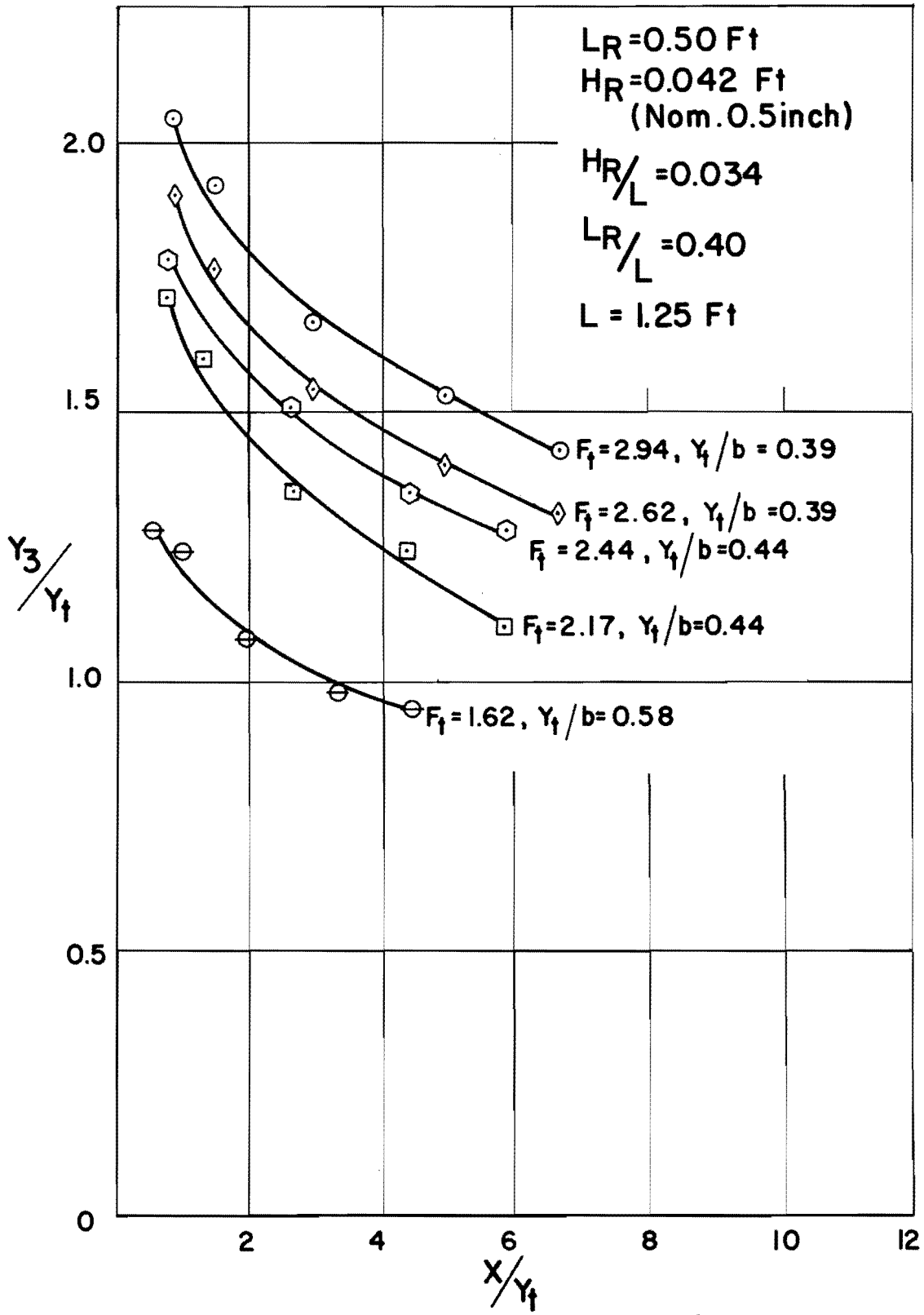

FIGURE 21 - VARIATION OF Y_3/Y_1 vs X/Y_1 FOR H_R/L = 0.034, L_R/L = 0.40

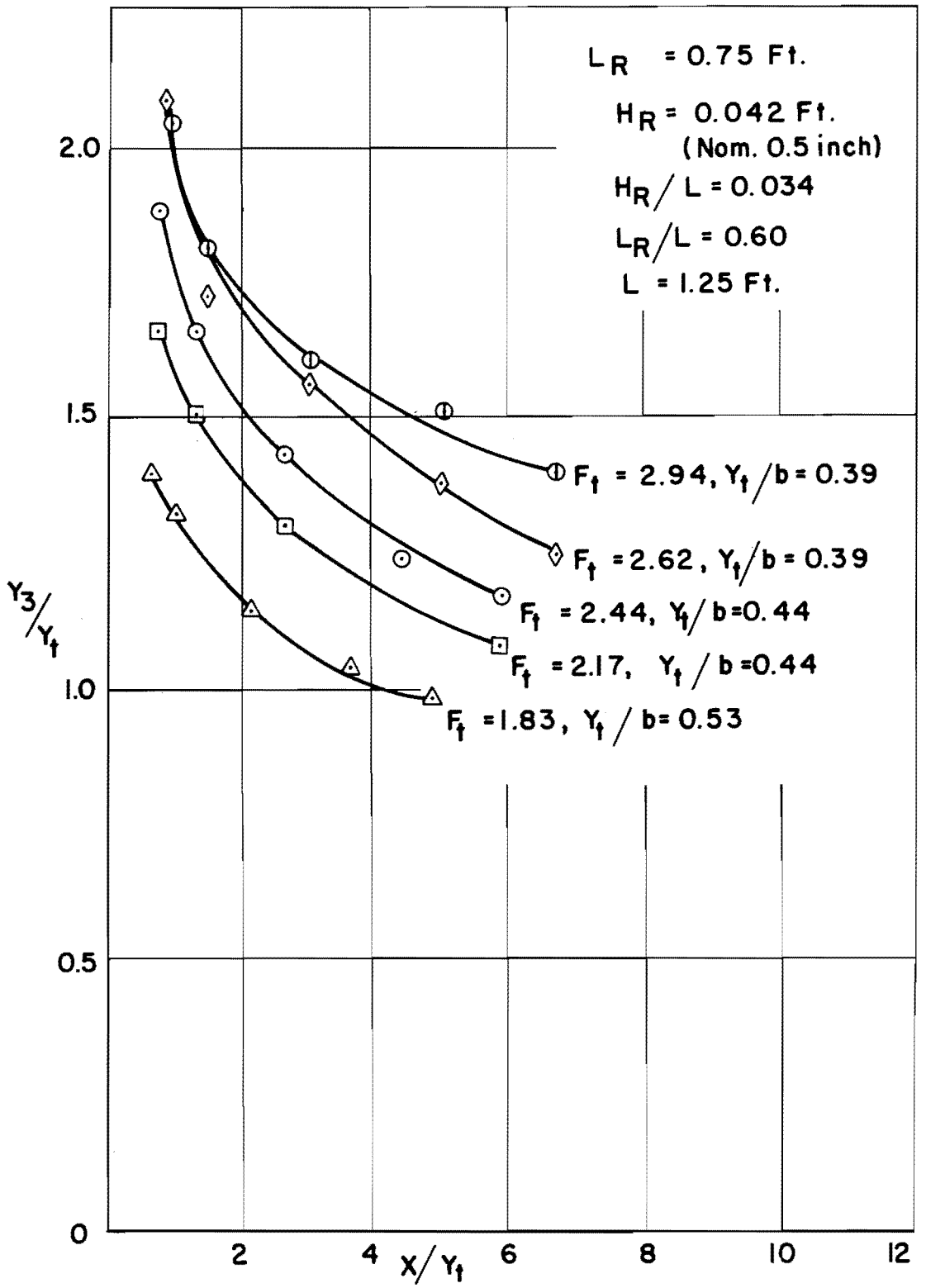

FIGURE 22 - VARIATION OF Y_3/Y_f vs. X/Y_f FOR H_R/L=0.034, L_R/L = 0.60

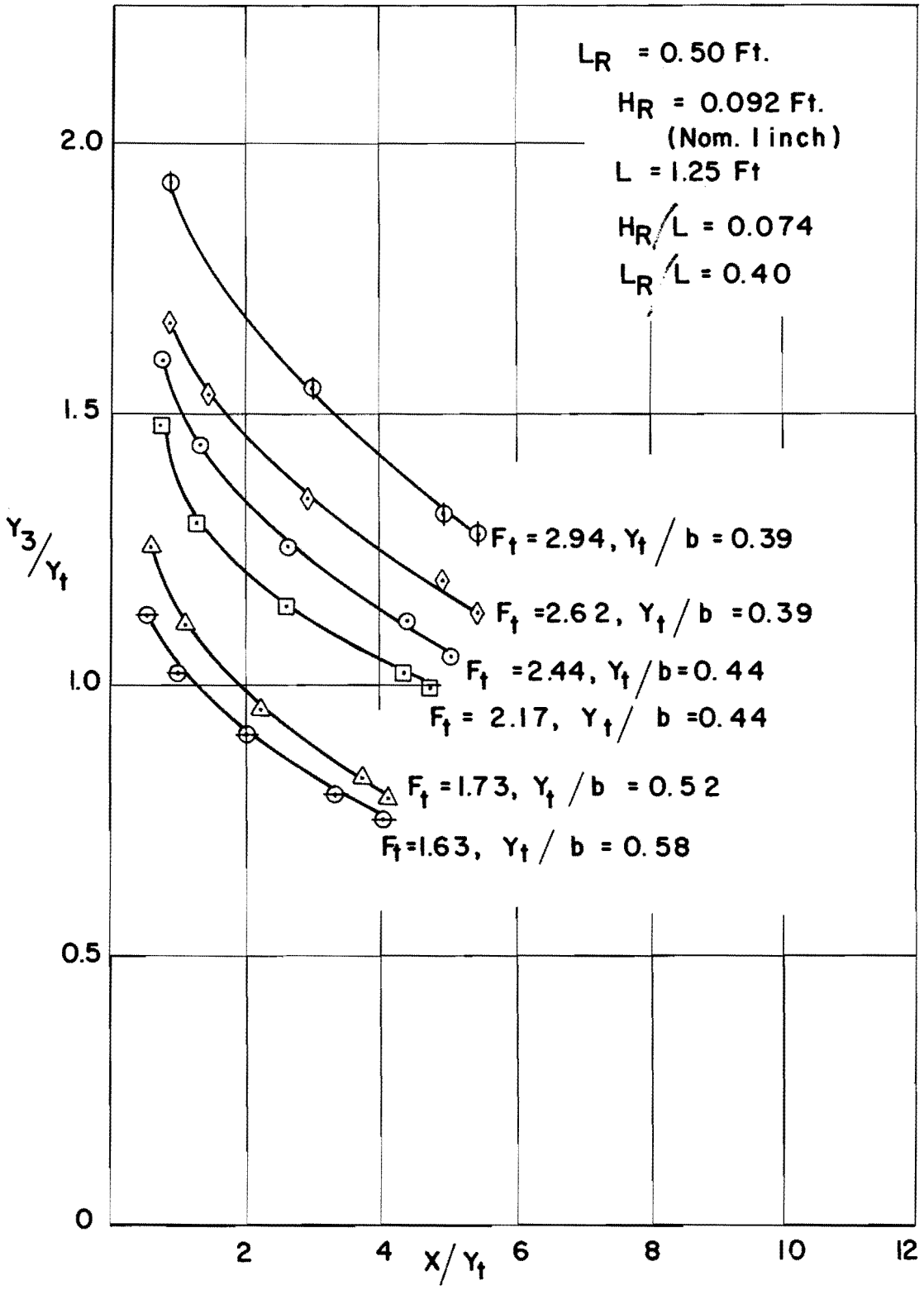

FIGURE 23 - VARIATION OF Y_3/Y_t vs. X/Y_t FOR $H_R/L = 0.074$, $L_R/L = 0.40$

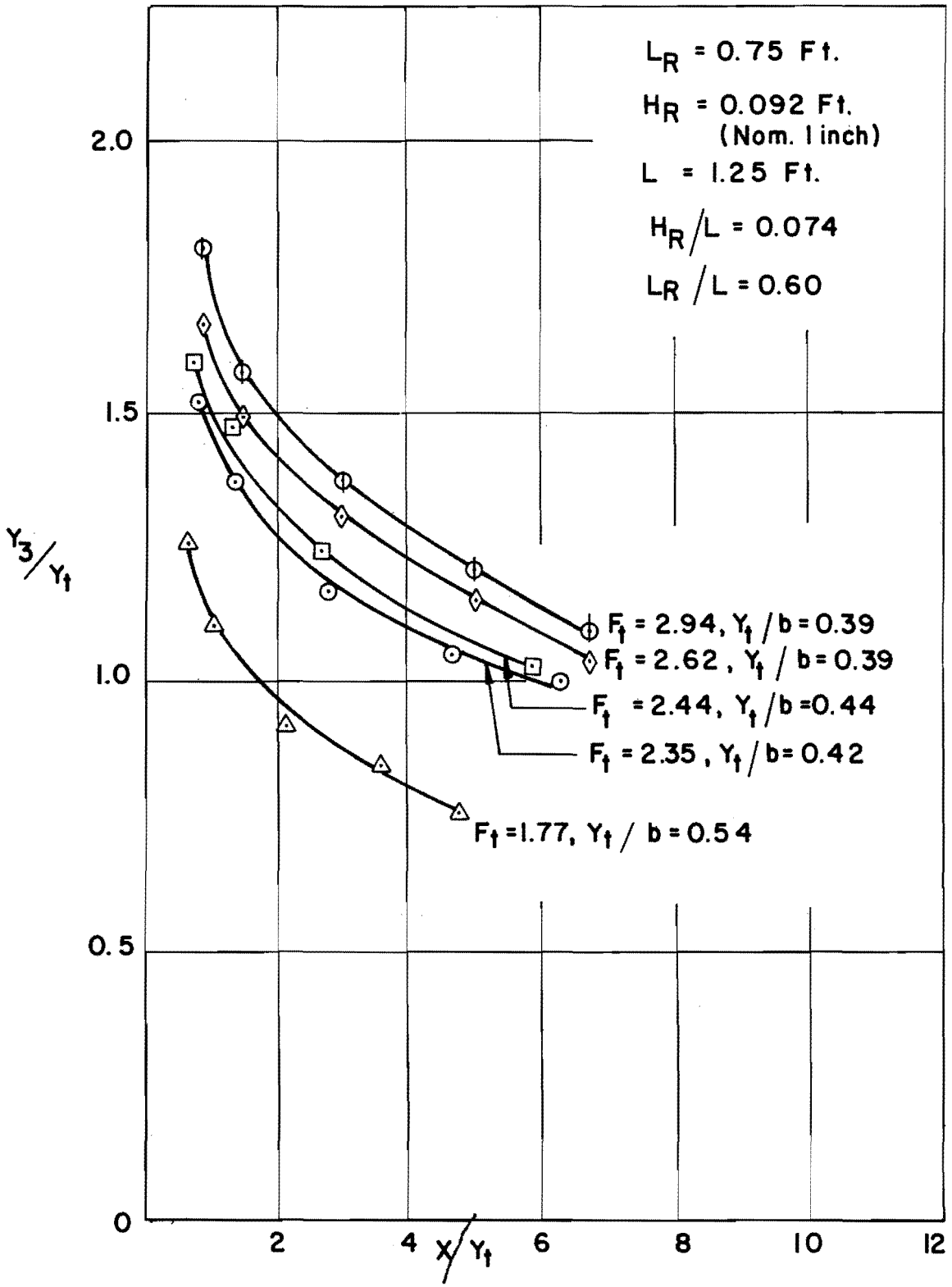

FIGURE 24 - VARIATION OF Y_3/Y_1 vs. X/Y_1 FOR $H_R/L = 0.074$, $L_R/L = 0.60$

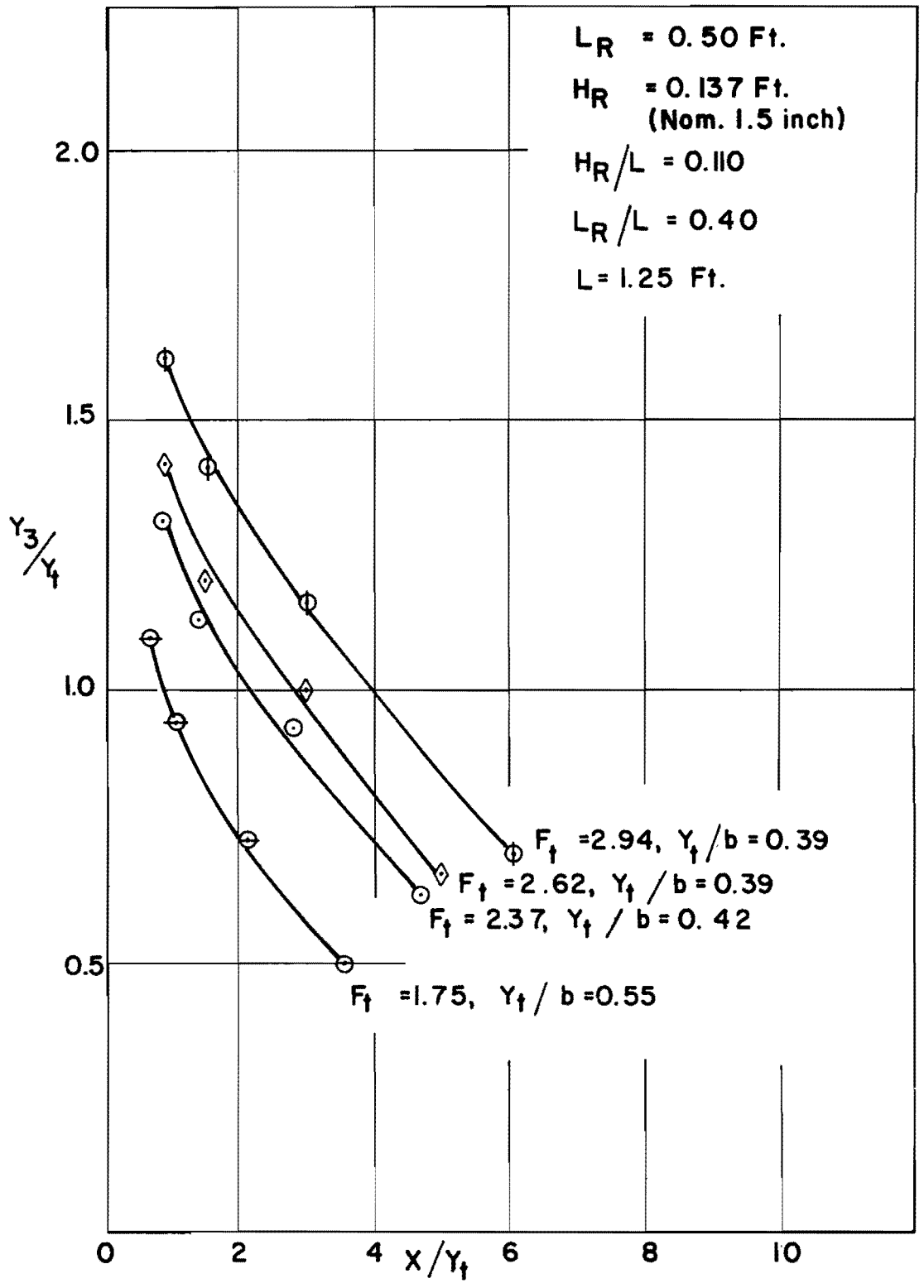

FIGURE 25 - VARIATION OF Y_3/Y_t vs. X/Y_t FOR H_R/L =0.110, L_R/L= 0.50

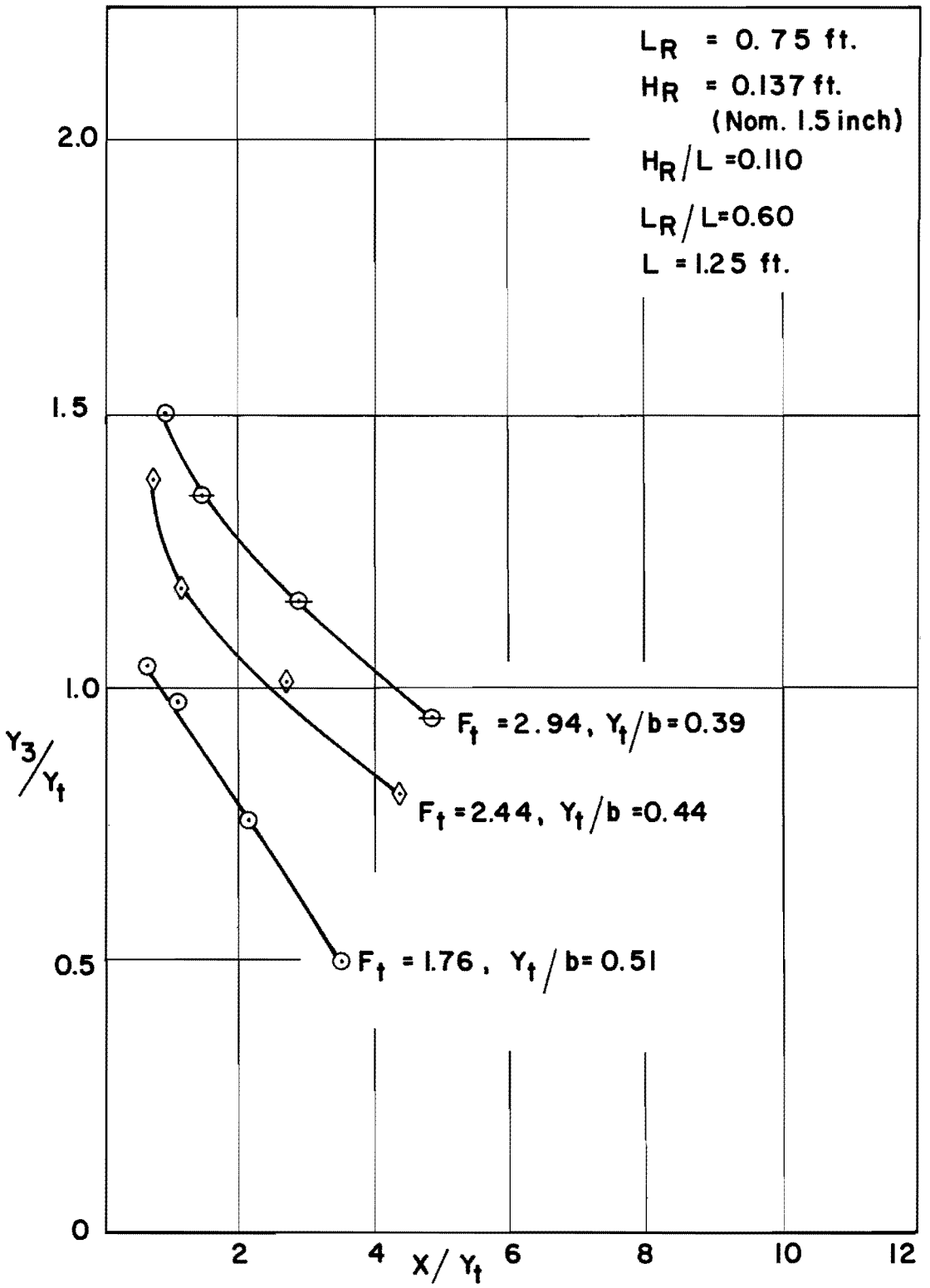

FIGURE 26 - VARIATION OF Y_3/Y_t vs. X/Y_t FOR H_R/L=0.110
L_R/L =0.60

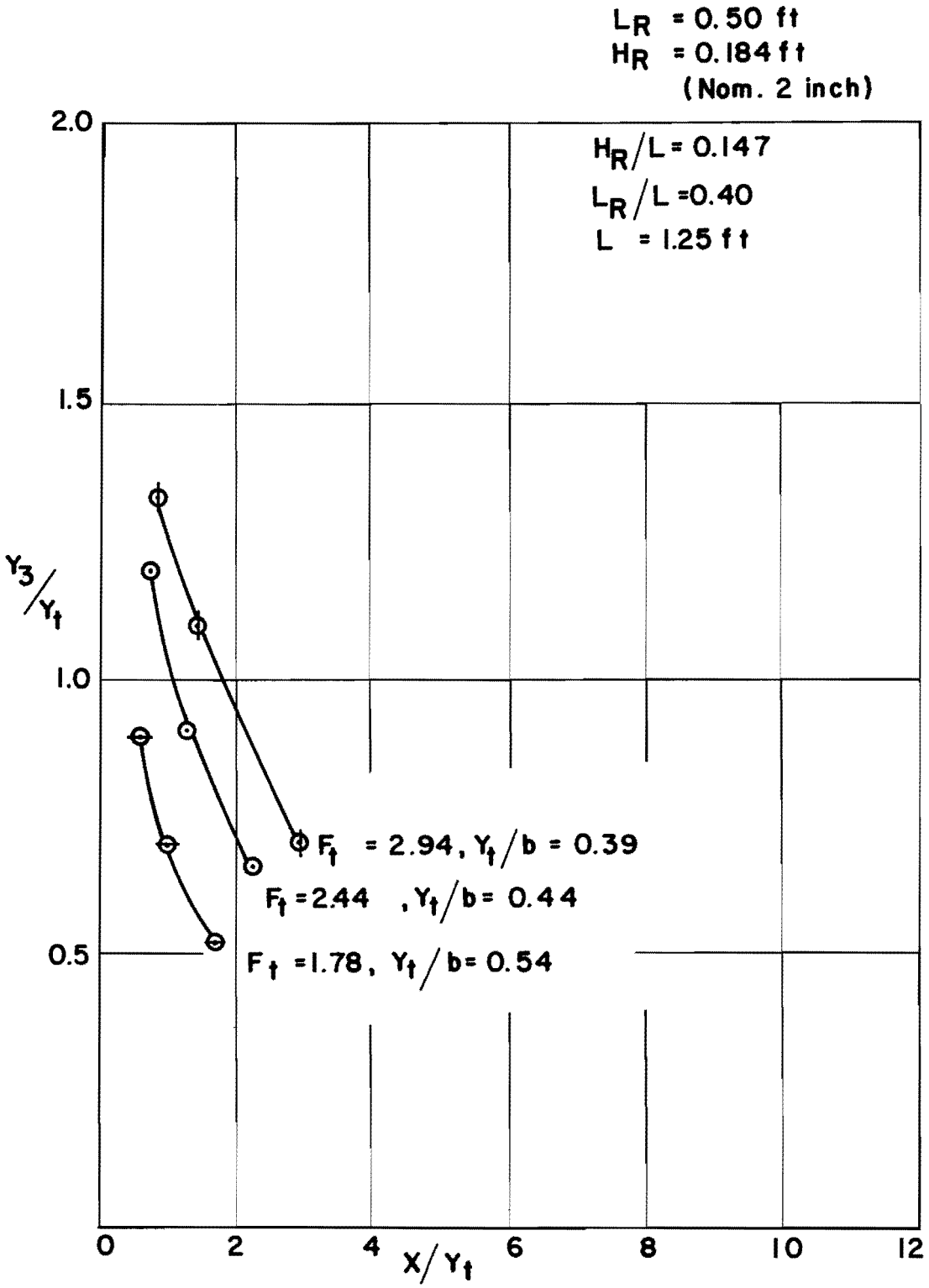

FIGURE 27 - VARIATION OF Y_3/Y_1 vs. X/Y_1 FOR H_R/L=0.147, L_R/L =0.40

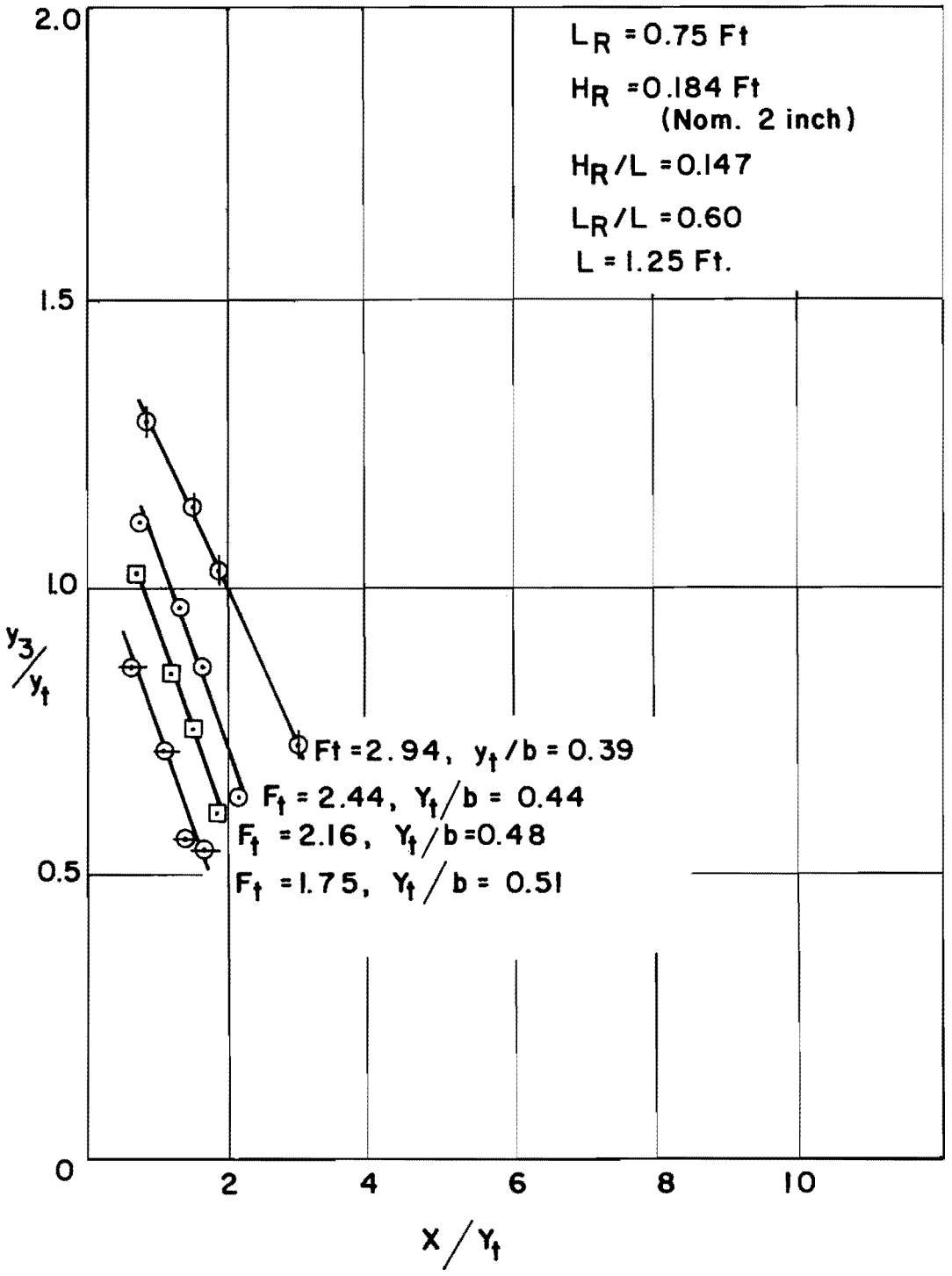

FIGURE 28 - VARIATION OF Y_3/Y_t vs. X/Y_t FOR H_R/L=0.147, L_R/L=0.60

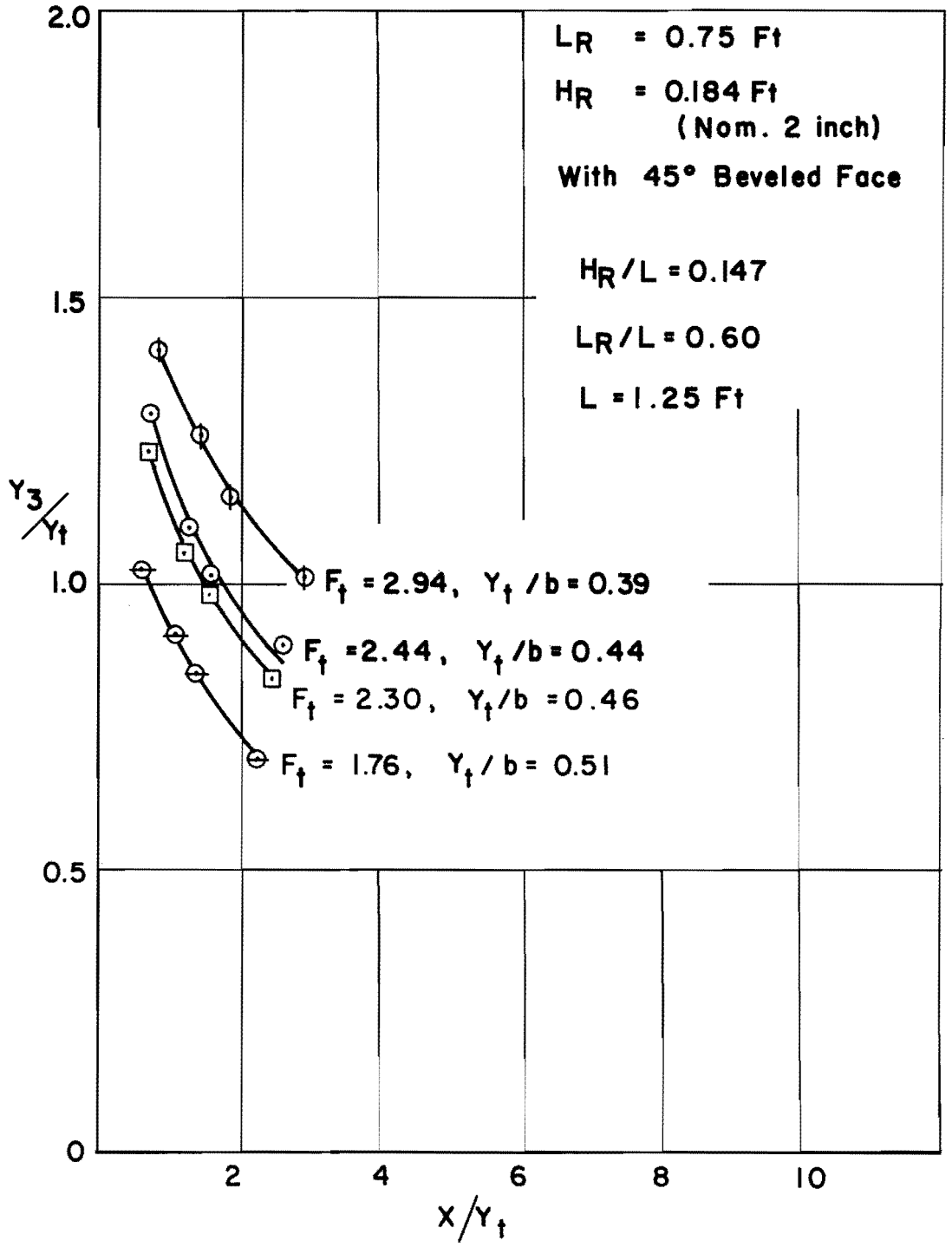

FIGURE 29 - VARIATION OF Y_3/Y_f vs. X/Y_f FOR H_R L=0.147, L_R L=0.60 WITH 45° BEVELED FACE

of velocity is a result of ski jump action by the flow jet after it strikes the rise. A more satisfactory velocity distribution was obtained with the jump further upstream, as reflected by higher values of y_3/y_t. This position of the jump has been designated as the extreme downstream position for optimum design. It is indicated on the graphs of y_3/y_t vs F_t as a solid line, denoting the lower limit of y_3/y_t for best performance.

The results presented in this manner are directly applicable to the design of a stilling basin structure of this geometric configuration, incorporating an abrupt rise. These results may be applicable in two basic situations. The range of permissible tailwater depths for a given entering discharge and water depth, y_t, may be obtained for a rise of given height. In addition, these results may be utilized to determine the most suitable rise height and position, if the range of tailwater depths and entrance flow conditions are known.

If a value of y_3/y_t lies to the left and above the upper limiting line of the design band, the rise is too high, and the jump will be forced upstream and may finally be drowned. If the y_3/y_t point is to the right and below the lower limiting line of the design band, either the jump will be forced downstream toward the abrupt rise and be washed out or a true jump will essentially disappear and flow will shoot over the rise.

As mentioned, a y_3/y_t point may be high enough to permit a jump to be held within the basin but may result in excessive velocities near the bottom of the channel past the rise, due to the close proximity of the jump to the rise. An example of this type of application of the curves of y_3/y_t vs F_t for values of H_R/L and L_R/L is as follows:

Given: Q and y_t such that $F_t = 2.00$

and min $y_3/y_t = 1.00$

Trying $H_R/L = 0.034$ for both $L_R/L = 0.40$ and 0.60 it is seen in Figures 13 and 14 that the point is outside of the design range.

Utilizing Figures 15 and 16 for $H_R/L = 0.074$ with $L_R/L = 0.40$ and 0.60, respectively it is seen that the point is within the design range for both rise positions.

3. Comparison of the Four Test Rise Heights

A comparison of the minimum tailwater requirements for the various rise heights from the plots of y_3/y_t vs F_t shows that significantly lower values of tailwater are required to hold the jump in the basin as the rise height is increased. A part of this difference in tailwater requirement is a result of the increased elevation of the channel bottom in relation to the total head. However, the effect of dynamic pressure also appears to account for some of this difference. An indication of the effect of increased dynamic pressure as the rise height is increased is given in Figure 30, where $(H_R + y_3)/y_t$ is plotted as the ordinate with x/y_t, the dimensionless jump position variable as the absicca. A comparison is made between rises of $H_R = 0.042$ feet (nominal 1/2-inch height), and $H_R = 0.184$ feet (nominal 2-inch height) for each of the two rise positions. The spreading of the two curves, as the jump is allowed to move downstream toward the rise, indicates that dynamic pressure acts in addition to the hydrostatic pressure to resist the movement of the jump downstream. In this figure, $H_R + y_3$ is only an approximation of the hydrostatic head on the face of the rise, since the elevation of the water surface drops somewhat from the face of the rise to the point where the tailwater was measured. As would be expected, the spread between the curves was greater for $L_R/L = 0.40$ than for $L_R/L = 0.60$. This is a result of the rise being closer to the jump with $L_R/L = 0.40$ for a given value of x.

A comparison of the performance of the various rise heights in stabilizing the jump can also be accomplished by comparing the absolute value of the slope of the y_3/y_t vs x/y_t curves for a given value of F_t. In general, these curves displayed a sharp degree of curvature for low values of x but approached a nearly linear slope for larger values of x as the jump proceeded farthur downstream. For this reason $\frac{\Delta y_3/y_t}{\Delta x/y_t}$ ratios are compared for the various rise heights over the linear portion of the curves, where the x/y_t values are larger as the jump approaches the rise. This comparison is shown in Table 1 for $L_R/L = 0.40$ and 0.60 at $F_t = 2.94$.

Comparison of the jump stability characteristics of these rise heights for the same rise position clearly shows that improved jump stability is

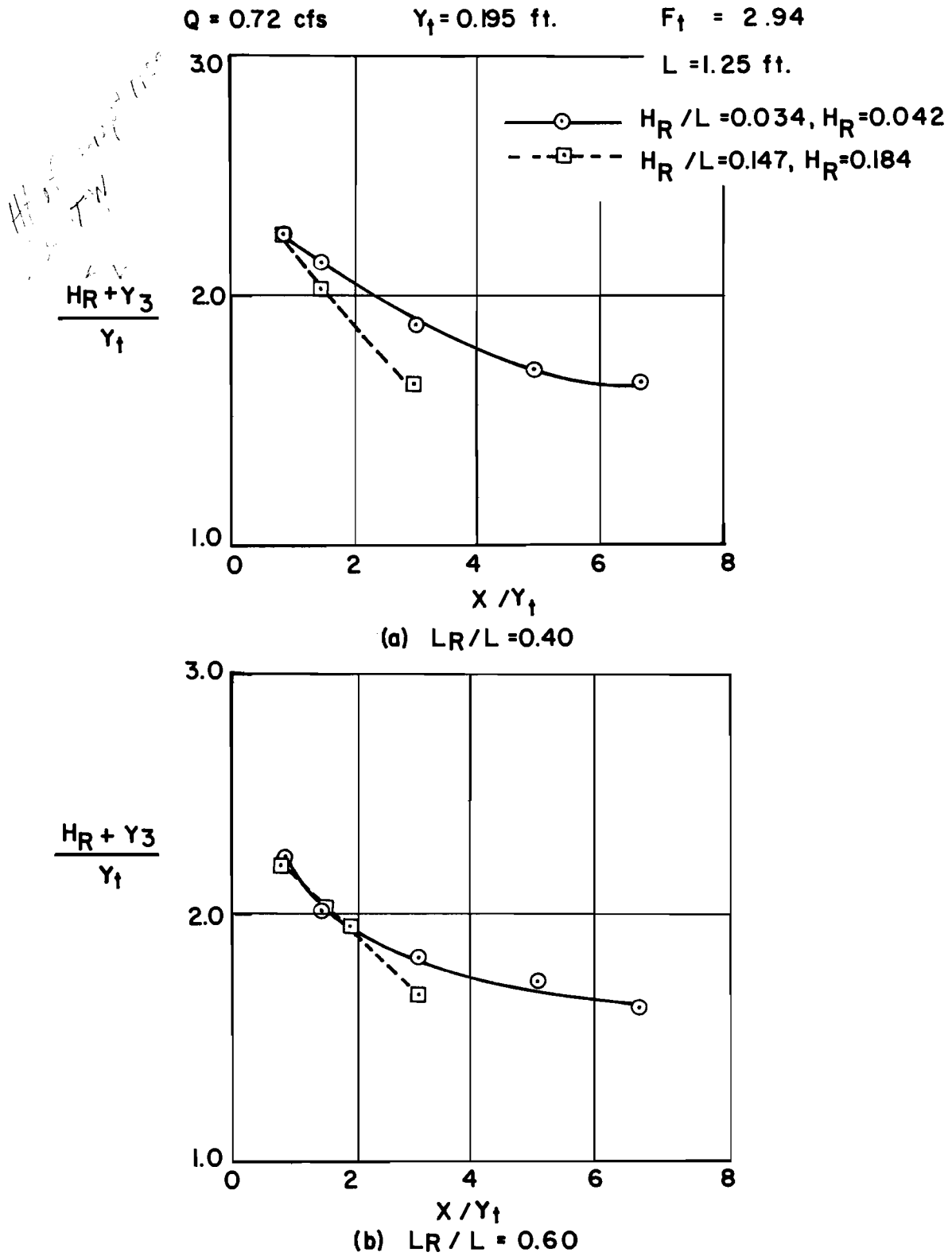

FIGURE 30-VARIATION OF $(H_R+Y_3)/Y_t$ vs. X/Y_t FOR DIFFERENT VALUES OF H_R/L

TABLE 1. COMPARISON OF JUMP STABILITY

H_R	$\frac{H_R}{L}$	$\frac{L_R}{L}$	$\frac{x}{y_t}$ Range	$\left[\frac{\Delta x}{y_t}\right]$	$\frac{\Delta y_3}{y_t}$	$\left[\frac{\Delta y_3/y_t}{\Delta x/y_t}\right]$
0.042	0.034	0.40	4.0 - 6.0	2	0.13	0.065
		0.60	4.0 - 6.0	2	0.10	0.050
0.092	0.074	0.40	3.2 - 5.2	2	0.21	0.105
		0.60	4.0 - 6.0	2	0.15	0.075
0.137	0.110	0.40	2.8 - 4.8	2	0.30	0.150
		0.60	2.8 - 4.8	2	0.22	0.110
0.184	0.147	0.40	1.8 - 2.8	1	0.25	0.250
		0.60	1.6 - 2.6	1	0.26	0.260

achieved by increasing the rise height. From the standpoint of jump stability characteristics, the rise of 0.184 feet (nominal 2-inch height) is the most desirable of the rises which were tested. One undesirable feature of the 0.184 foot and 0.137 foot high rises is the demonstrated fact that they are applicable over a more limited range of tailwater values.

4. Comparison of the 2-inch Nominal Rise With and Without the 45° Beveled Face

Figure 31 gives a comparison of the tailwater requirements of the 0.184 foot high rise, ($H_R/L = 0.147$), with those of this rise with a 45° beveled face added. The jump stability performance of this rise is also compared to that of the rise with the 45° beveled face. Plots of y_3/y_t vs x/y_t are shown for $F_t = 2.44$ and 2.94 . Noticeably lower tailwater values are required for this rise without the sloping face. In addition, the absolute values of the slope of the curves, which is indicative of the jump stability, are somewhat greater for the rise without the sloping face as the jump moves closer to the rise.

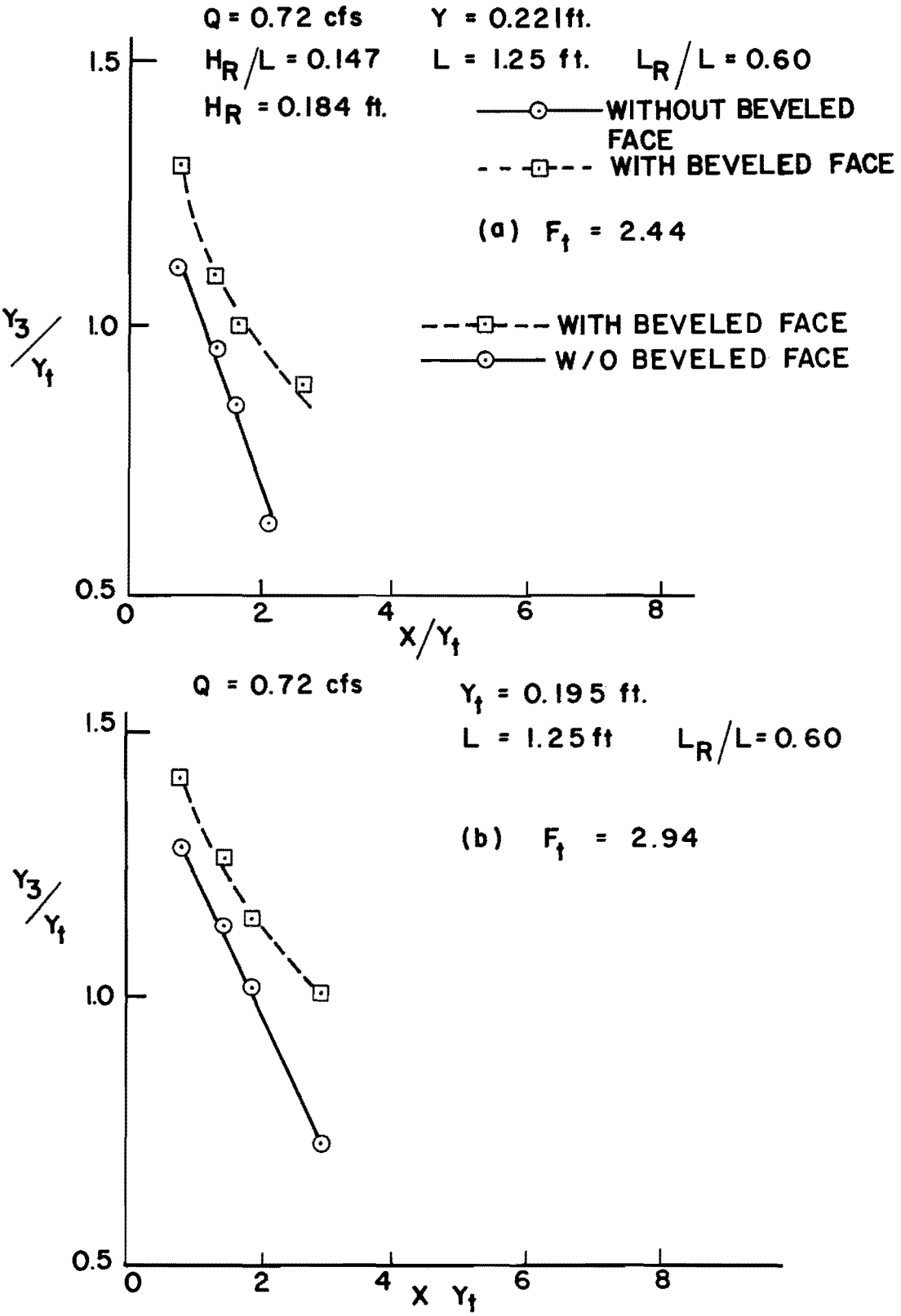

FIGURE 31- VARIATION OF Y_3/Y_t vs. X/Y_t FOR RISE, H_R/L = 0.147, WITH AND WITHOUT 45° BEVELED FACE

5. Comparison of the Two Rise Test Locations

As is shown in Table 1, significantly better jump stability is achieved for an L_R/L of 0.40 in the case of the rises 0.042, 0.092, and 0.137 feet high. However, for the highest rise, 0.184 feet high, there is virtually no improvement in jump stabilization at the more upstream rise position with $L_R/L = 0.40$.

A comparison of tailwater requirements for the two rise positions is shown in Figure 32, for $H_R = 0.092$ feet and $H_R = 0.184$ feet. The two lower rises, 0.042 and 0.092 feet high, both require lower tailwater values for a given jump position with the rise located 9 inches away from the end of the flare at $L_R/L = 0.60$. This behavior is contrary to what might be expected. One reason for this might be the reduced effect of dynamic pressure with the smaller rises. For the two higher rises, 0.137 and 0.184 feet high, however, this behavior reverses and slightly lower tailwater values are required for the rise location of $L_R/L = 0.40$. The difference in tailwater requirements is more pronounced for larger x/y_t values. The most desirable rise location, therefore, based on jump stability and tailwater requirements is dependent to some degree, upon the height of rise desired. The rise location, $L_R/L = 0.40$, is definitely more desirable for a rise height of $H_R/L = 0.110$ ($H_R = 0.137$ feet) and slightly more desirable for $H_R/L = 0.147$ ($H_R = 0.184$ feet) . The most desirable location of the rise for the two lower rises, based on these two characteristics, will be at $L_R/L = 0.40$, if the minimum tailwater conditions expected are high enough to permit the jump to be held in the basin.

B. Magnitude and Distribution of Velocities

As mentioned in the experimental procedure, velocity measurements were obtained at several sections in the channel to ascertain the longitudinal and transverse distribution of velocities for each of the rises tested. Velocity measurements for each rise were taken at $F_t = 2.94$ and with the jump stabilized at its farthest position downstream in order to determine the worst velocity conditions which could occur. As discussed in the

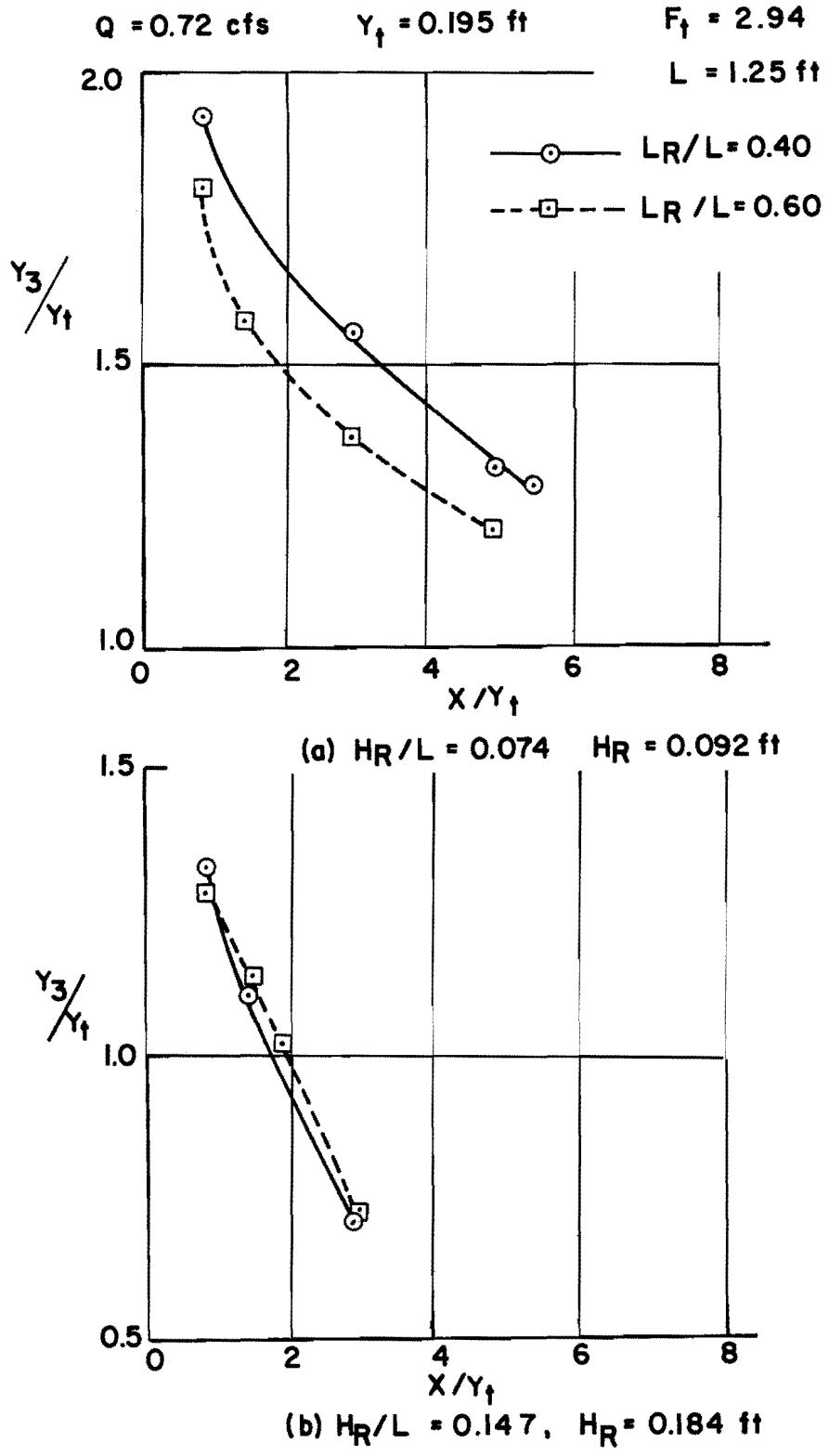

FIGURE 32 - VARIATION OF Y_3/Y_t vs. X/Y_t FOR DIFFERENT VALUES OF L_R/L

procedure, measurements were taken also for the rises 0.042, 0.137, and 0.184 feet high with the jump positioned farther upstream in a location where velocities were significantly reduced and more uniformly distributed. Measurements were taken, with the various rises located at each of the two test locations of $L_R/L = 0.40$ and 0.60..

All velocity measurements downstream from the jump were taken with the Pitot tube aligned parallel to the channel centerline. Since flow with lateral velocity components continues into the downstream channel, the Pitot tube was not always aligned in the direction of the principal velocity vector. This error in measurement becomes more pronounced in the flow regions near the channel walls, where the principal velocity vector deviates the most from a direction parallel to the centerline. Trial measurements indicated, however, that this error was not of great significance in this study since in the region near the walls the magnitude of the velocity was small.

1. Evaluation of the Transverse Distribution of Velocities

Figures 33 through 36 demonstrate the transverse distributions of velocities for each rise at the sections where the highest velocities were encountered. Except in the case of the nominal 1/2-inch high rise, velocities are indicated with the jump located in the downstream position for optimum design, as previously described, where velocities were significantly reduced and fairly uniformly distributed as compared with more extreme downstream location of the jump. The velocity distribution shown for the nominal 1/2-inch high rise ($H_R = 0.042$ feet) was with the jump positioned in its extreme downstream position so that the velocities although reduced were not as well distributed as if the jump were positioned farther upstream. Velocities are shown for both rise positions. Velocities are plotted in terms of the mean channel velocity, V_m .

The velocity distributions clearly indicate the concentration of flow velocities in the center portion of the channel, with a sharp velocity reduction toward the sides of the channel. Radial velocity measurements taken, as described in the procedure section, showed a more uniform transverse distribution of velocities in the center portion of the channel but

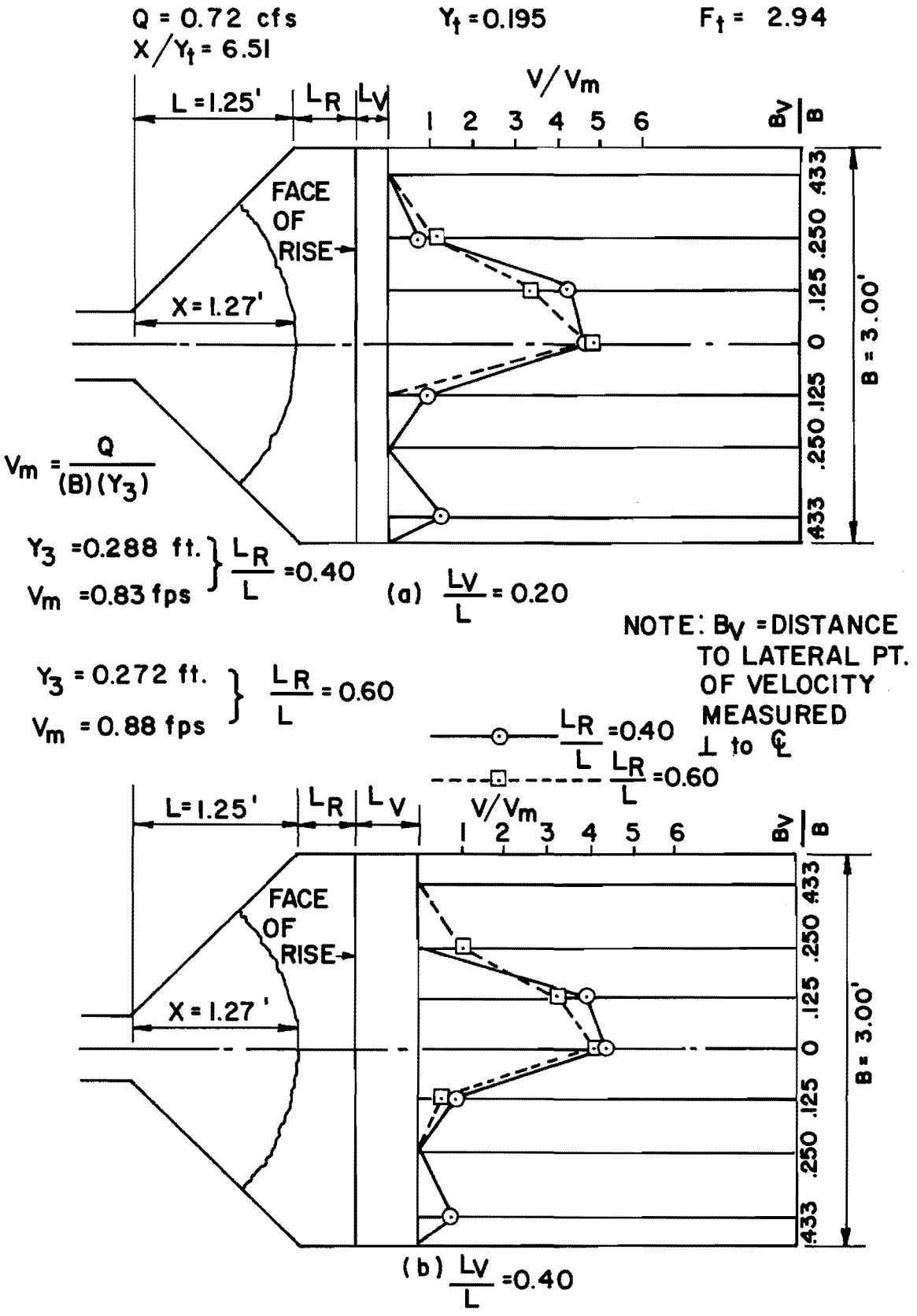

FIGURE 33 - V/V_m vs B_V/B FOR $H_R/L = 0.034$

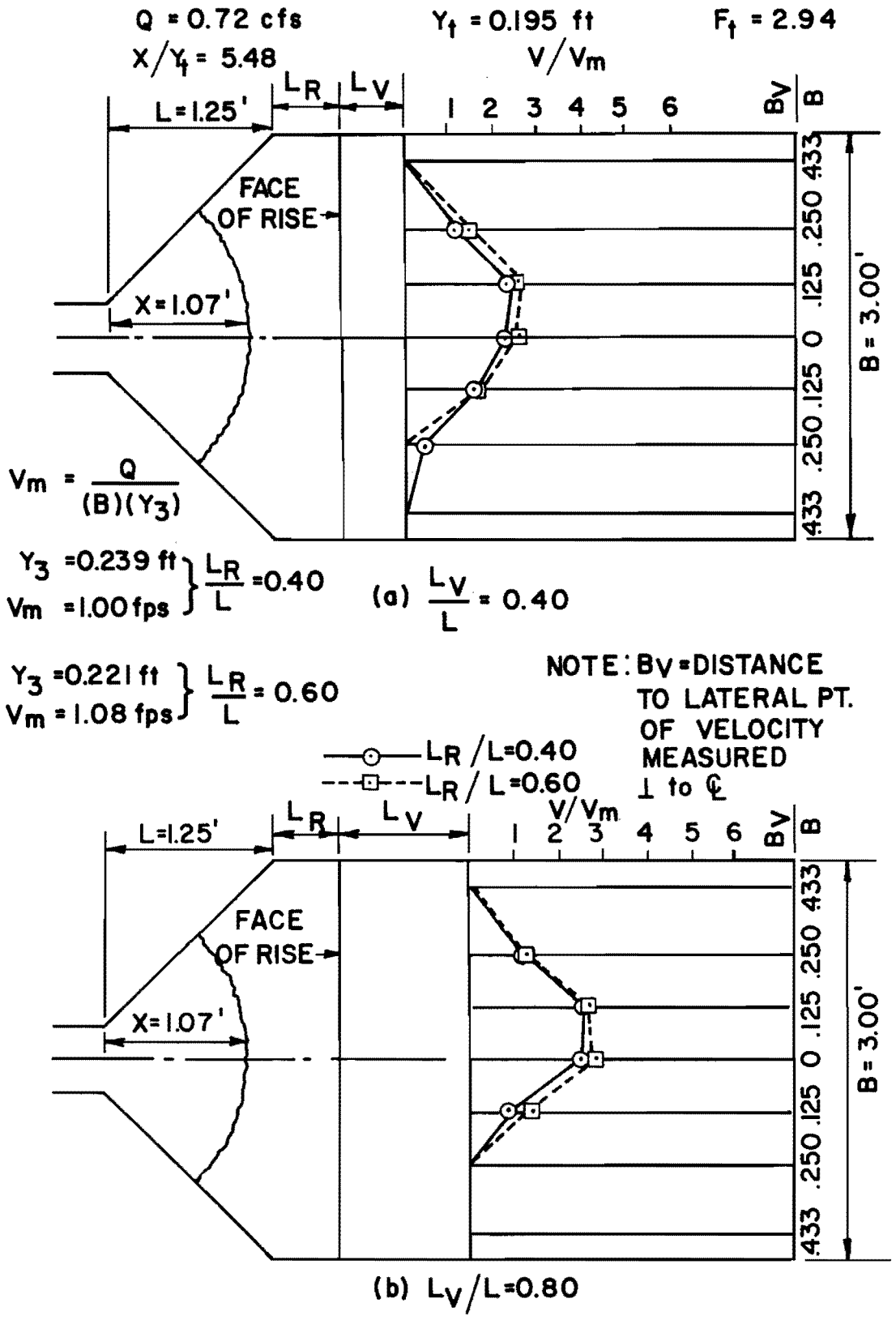

FIGURE 34 - V/V_m vs. B_V/B FOR $H_R/L=0.074$

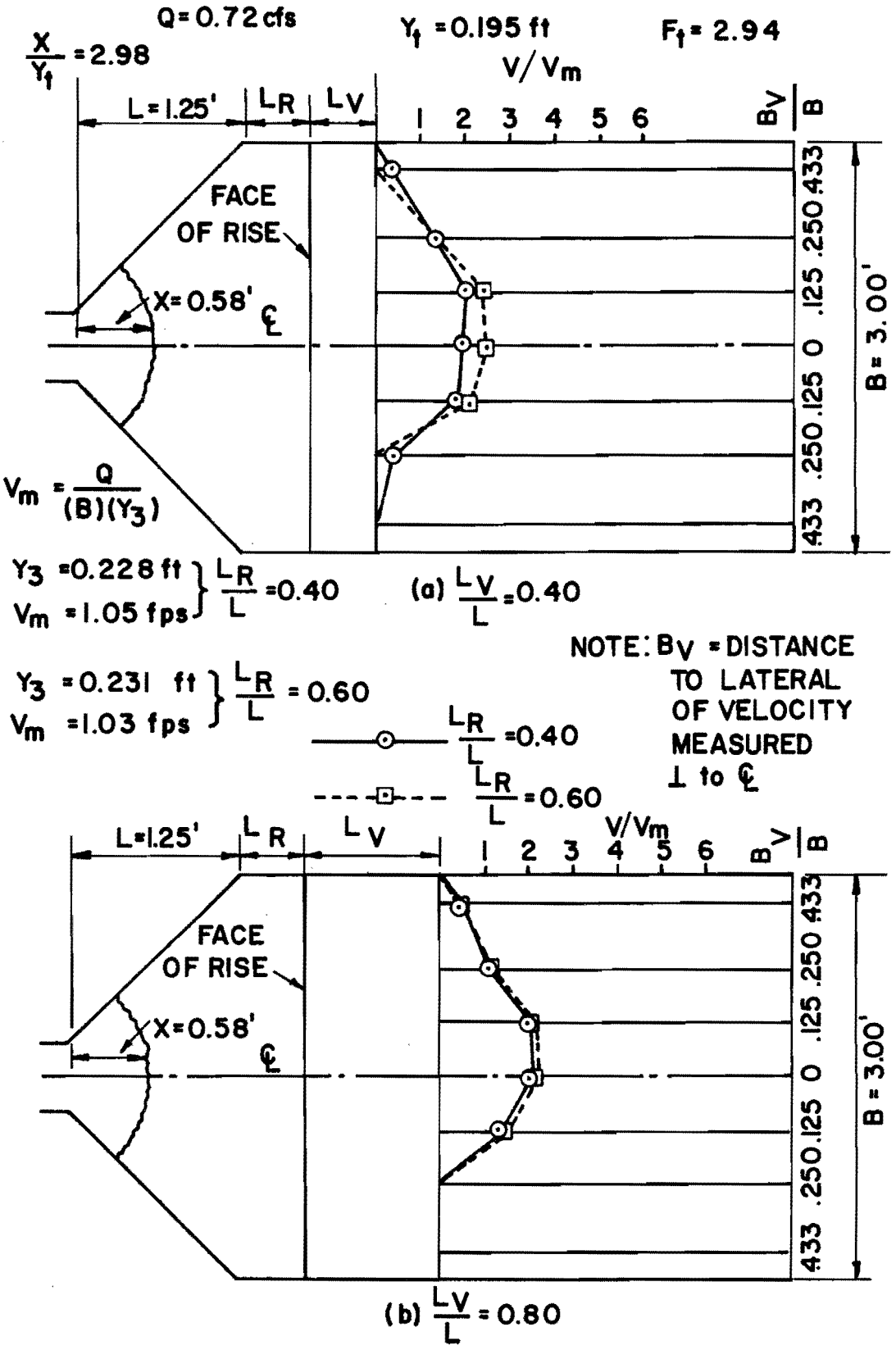

FIGURE 35 - V/Vm vs. B_V/B FOR H_R/L = 0.110

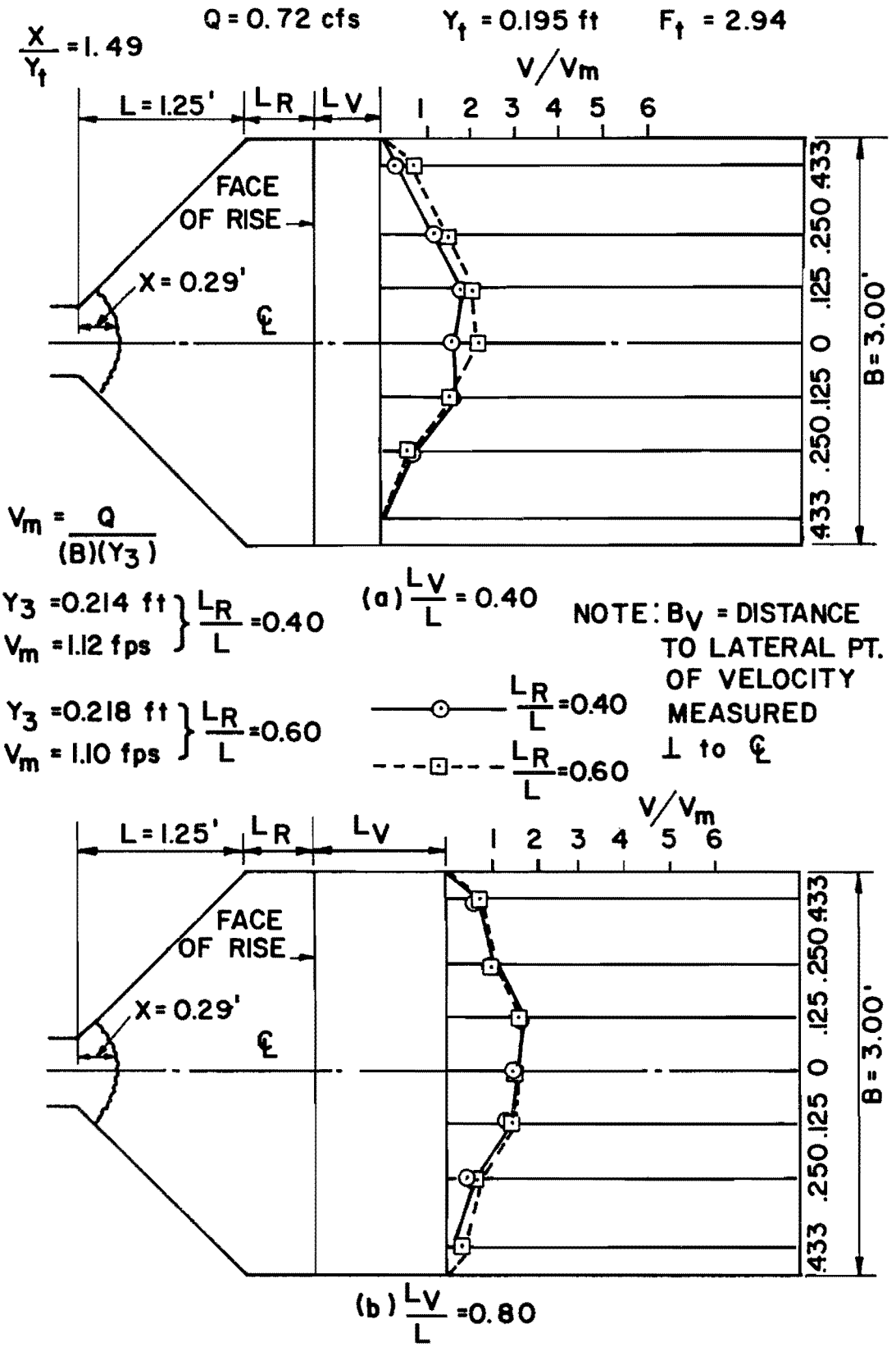

FIGURE 36 – V/V_m vs. B_V/B FOR H_R/L = 0.147

also indicated a sharp reduction in velocities toward the channel sides. Part of this concentration of flow in the center is a result of non-uniform spreading in the supercritical flow region of the basin, with more flow proceeding parallel to the basin centerline down the center of the basin. Another factor which appears to add to the concentration of flow in the center of the basin is reflection of the supercritical flow off of the radial side walls. Since the flow following impact on the channel bottom is not spread to the outside perfectly, so that streamlines are exactly parallel with the radial basin walls, a portion of the spreading supercritical flow will strike the walls forming a wave reflection back toward the center of the basin. This effect although not of a large magnitude increases the flow concentration in the center and helps to create a zone of very low velocity along the channel walls.

2. Variation of the Longitudinal Distribution of Velocities With Jump Location

Variation of the longitudinal velocity distribution with jump position is shown in Figure 37, for the rises of height, $H_R = 0.042$ feet and 0.137 feet at the rise location $L_R/L = 0.60$. A centerline profile is shown of V/V_m , comparing its longitudinal distribution at the extreme downstream jump position with its longitudinal distribution at the extreme downstream position for optimum design. Although velocities are reduced in the case of $H_R = 0.042$ feet , the velocity distribution is virtually unchanged by moving the jump upstream. In the case of the rise with $H_R = 0.137$ feet , for both jump positions, the flow shoots over the rise giving high velocities downstream from the face of the rise. As the jump is moved upstream from the rise, this concentration of velocity is moved upstream and reduced in magnitude. Since the variation of V/V_m is shown in this figure, a larger difference would exist between the actual velocities in feet per second of the two jump positions than is indicated by the V/V_m curves.

The velocities, V for the more downstream jump positions, are significantly higher than velocities for the more upstream jump position. This difference is more pronounced than for V/V_m since the jump in the

$Q = 0.72$ cfs $\quad Y_t = 0.195$ ft $\quad F_t = 2.94$

$L = 1.25$ ft. $\quad L_R/L = 0.60$ $\quad V_m = \frac{Q}{(B)(Y_3)}$

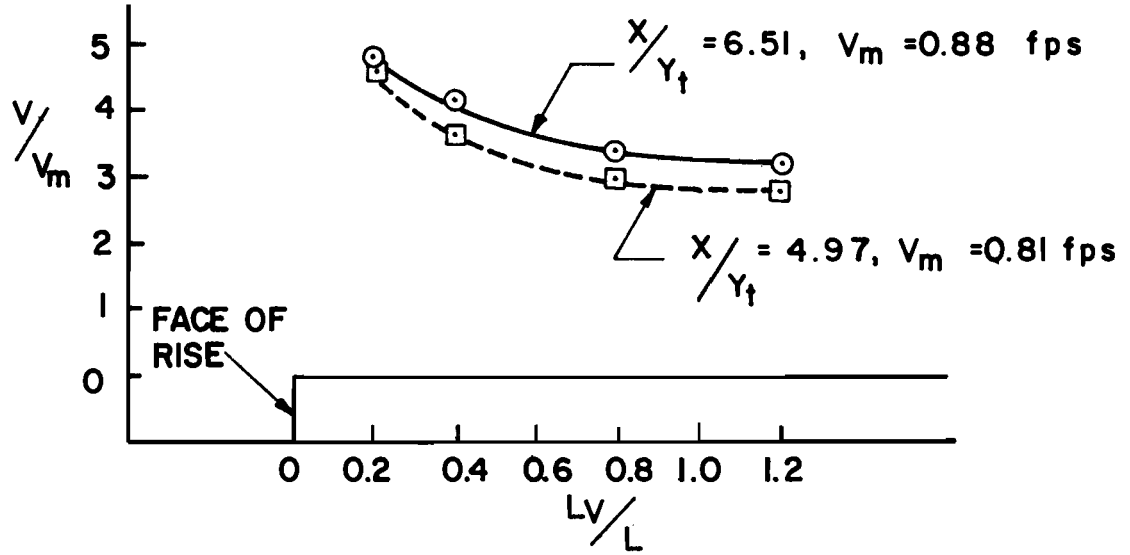

(a) $H_R/L = 0.034$, $H_R = 0.042$ Ft.

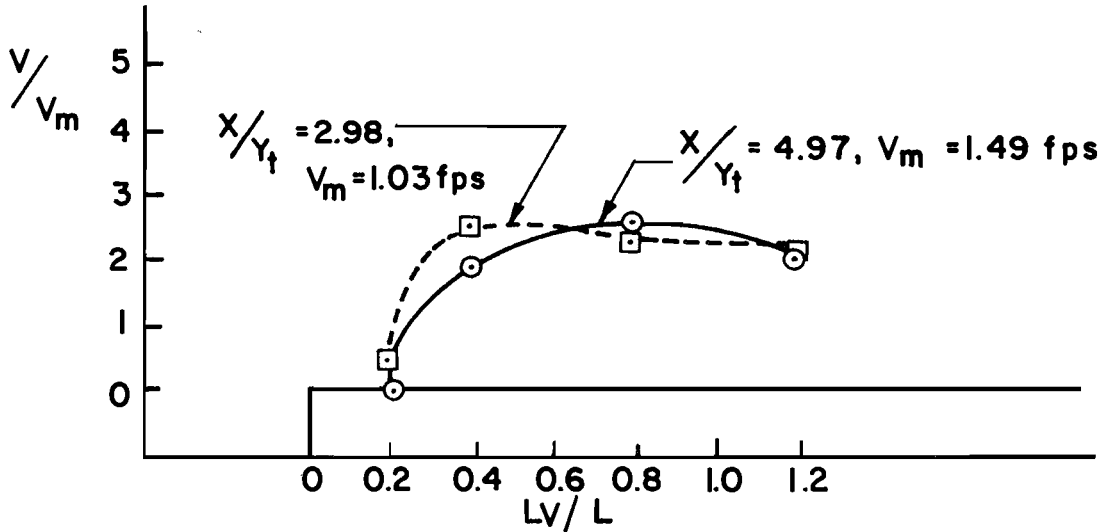

(b) $H_R/L = 0.110$, $H_R = 0.137$ Ft.

FIGURE 37 - CENTERLINE PROFILE SHOWING VARIATION OF V/V_m vs. L_v/L WITH JUMP POSITION

more downstream position also results in a higher value of V_m than the jump in the more upstream position.

3. Comparison of the Four Test Rise Heights

Figure 38 shows the centerline profile of the actual flow velocities in feet per second for the four rise heights tested at $L_R/L = 0.60$. Profiles are shown for the jump in its extreme downstream position as well as at the position for optimum design. For both jump positions, the rise with $H_R/L = 0.034$ shows high velocities near the face of the rise. The extreme downstream jump position is taken also as the best design position for the rise with $H_R/L = 0.074$, since a comparatively uniform distribution of velocity is achieved with the jump in this position. The two higher rises of $H_R/L = 0.110$ and 0.147 indicate significantly lower velocities with the jump positioned farther upstream. If the jump is allowed to proceed no further than its indicated extreme position for optimum design, the highest rise of $H_R/L = 0.147$ will be the most desirable since it exhibits lower velocities. At the extreme downstream jump positions, the rise of $H_R/L = 0.074$ shows the lowest maximum velocity.

4. Comparison of the 2-inch Nominal Rise With and Without the 45^o Beveled Face

Figure 39 gives a comparison of the distribution of V/V_m for the rise $H_R/L = 0.147$, ($H_R = 0.184$ feet) with and without the 45^o beveled face, for the jump in its extreme downstream position. Both the longitudinal and transverse profiles indicate significantly lower velocities are obtained in the channel for this rise without the beveled face. Better velocity distribution is also achieved without the beveled face.

5. Comparison of the Two Rise Test Locations

From Figures 33 through 36 a comparison can be made of the performance of each of the rise locations $L_R/L = 0.40$ and 0.60, by comparison of their lateral distribution of velocities for each rise height. There is apparently

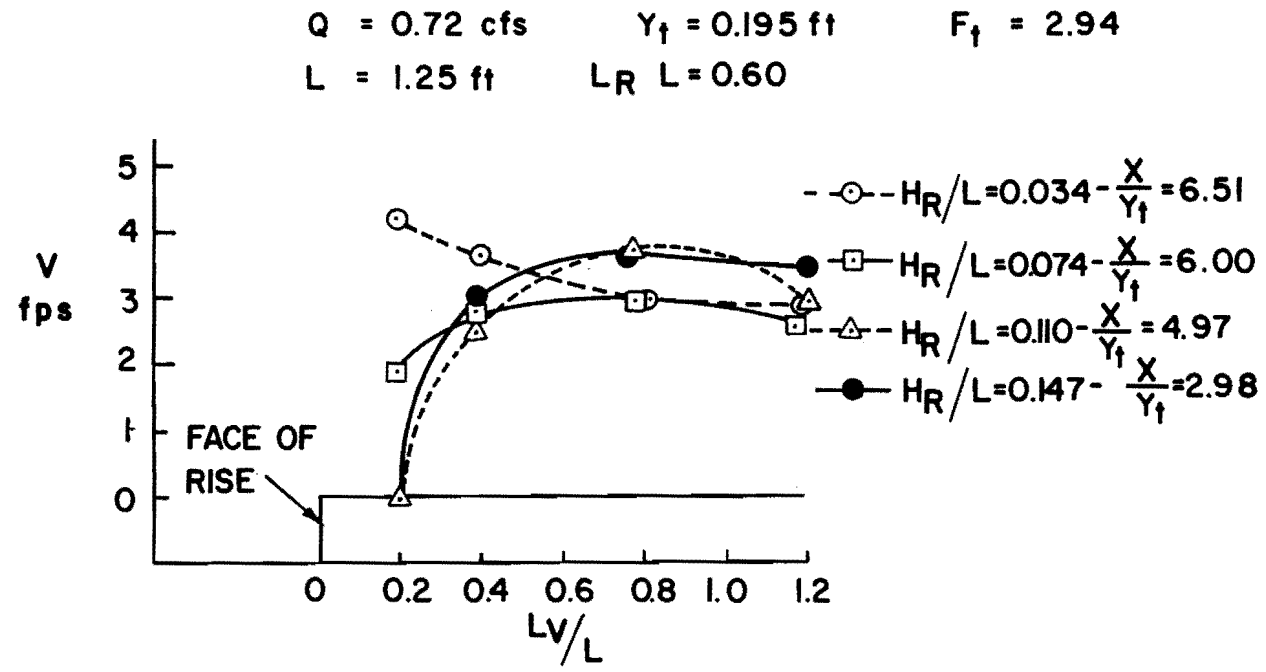

(a) HYDRAULIC JUMP AT EXTREME DOWNSTREAM POSITION

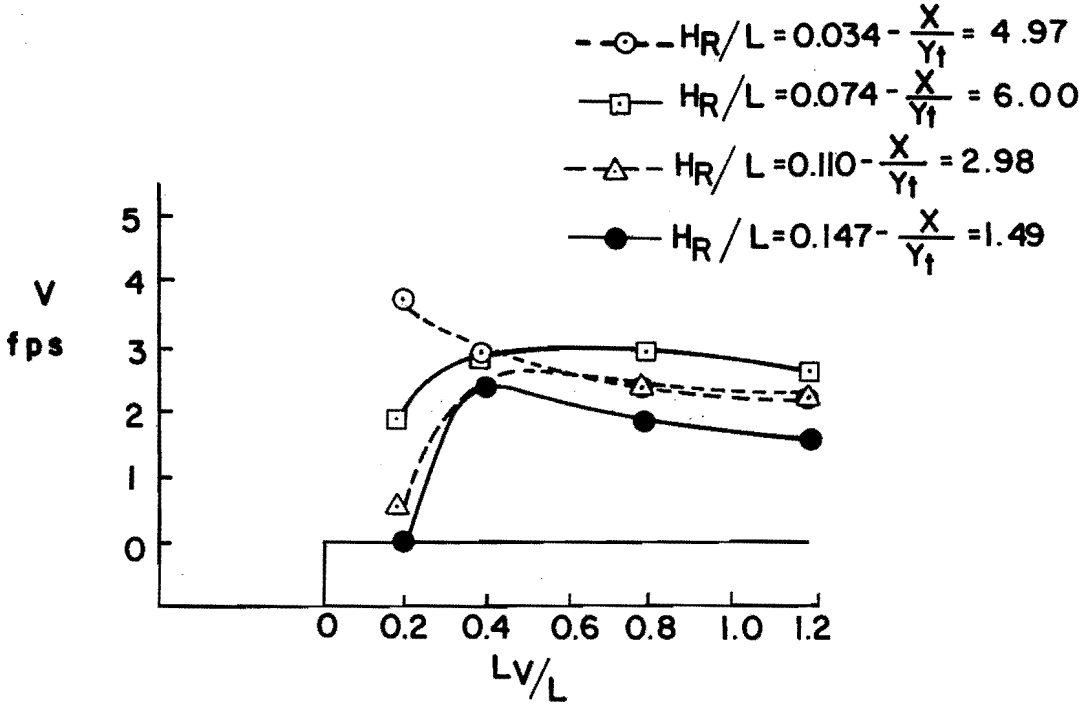

(b) HYDRAULIC JUMP AT POSITION FOR OPTIMUM DESIGN CONDITIONS

FIGURE 38 - CENTERLINE PROFILE SHOWING VARIATION OF V, FPS vs. LV/L FOR DIFFERENT VALUES OF H_R/L

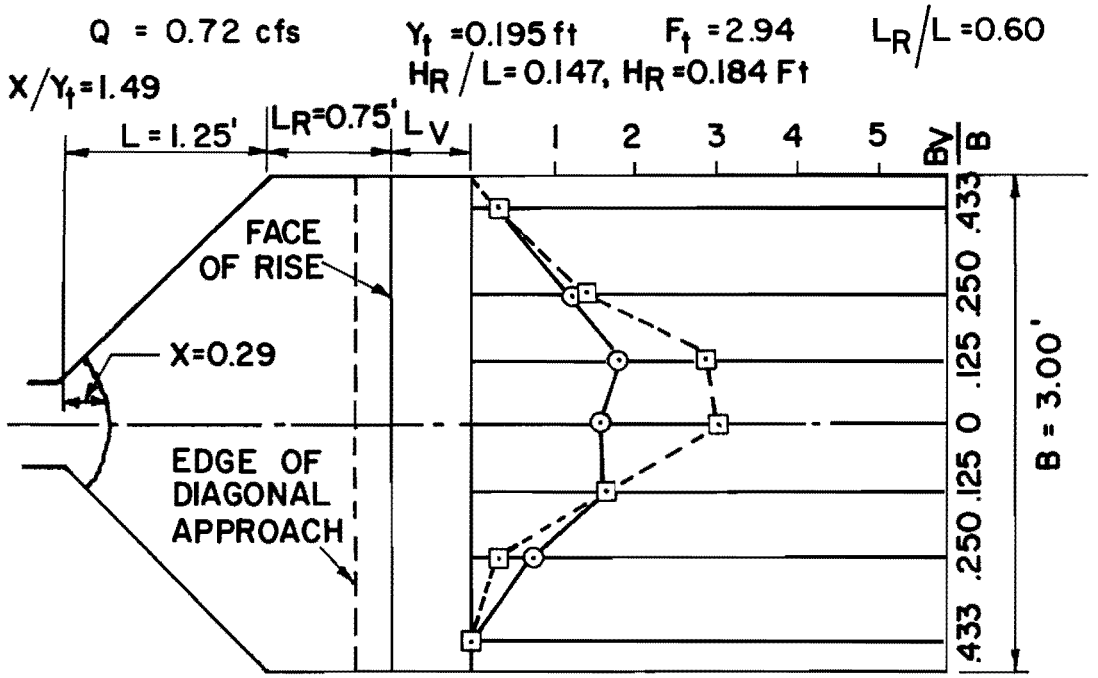

(a) V/V_m vs. B_V/B FOR $L_V = 0.50'$, $\frac{L_V}{L} = 0.40$

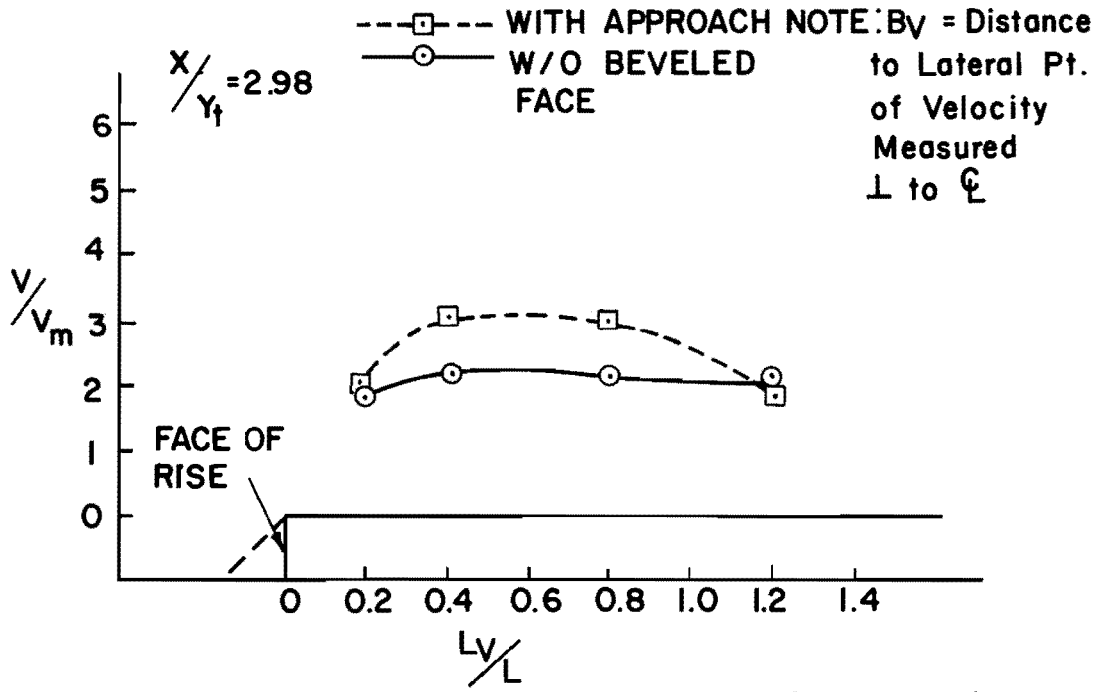

(b) Centerline Profile Showing V/V_m vs. L_V/L

FIGURE 39 - COMPARISON OF RISE, $H_R/L = 0.147$, WITH AND WITHOUT 45° BEVELED FACE

no great difference between the transverse velocity profiles for the two positions. Slightly better distribution and generally lower velocities are noted in the case of the lowest rise of $H_R/L = 0.034$ with the rise 9 inches from the end of the flare at $L_R/L = 0.60$. For the other three rise heights, however, the rise position 6 inches from the end of the flare at $L_R/L = 0.40$ produces slightly lower velocities and somewhat better distribution.

6. Comparison of the Velocity Profiles at Transverse Sections for Two Heights of Measurement at $H_R = 0.137$ Feet

Figure 40 gives a comparison of the lateral distribution of velocities for two different heights of measurement with the rise height = 0.137 feet. Velocities were taken 1.00 feet from the face of the rise at the section of maximum velocities. The measurement height of 0.05 feet is very close to the center of the flow stream. Although a somewhat more uniform velocity profile was noted in the center portion of the channel at the higher measurement position, a sharp drop off in velocity was noted at both measurement heights as the Pitot tube was stationed progressively closer to the channel walls.

C. Comparison of the Performance of the Radial Flow Energy Dissipation Structure With and Without an Abrupt Rise in the Apron

The radial flow energy dissipator with an abrupt rise is superior in tailwater requirements, jump stability, as well as velocity reduction to this same energy dissipator without a rise. This can be seen in Table II, which gives a typical comparison of the performance of the structure with and without the rises for $F_t = 2.94$. This table indicates that there is only slight improvement in tailwater requirement with the addition of a rise of $H_R/L = 0.034$. No improvement in jump stability as indicated by the absolute slope of the y_3/y_t vs x/y_t curves is achieved by the addition of this rise. Reduction in channel velocities is achieved, however, as seen in Table II by addition of this rise.

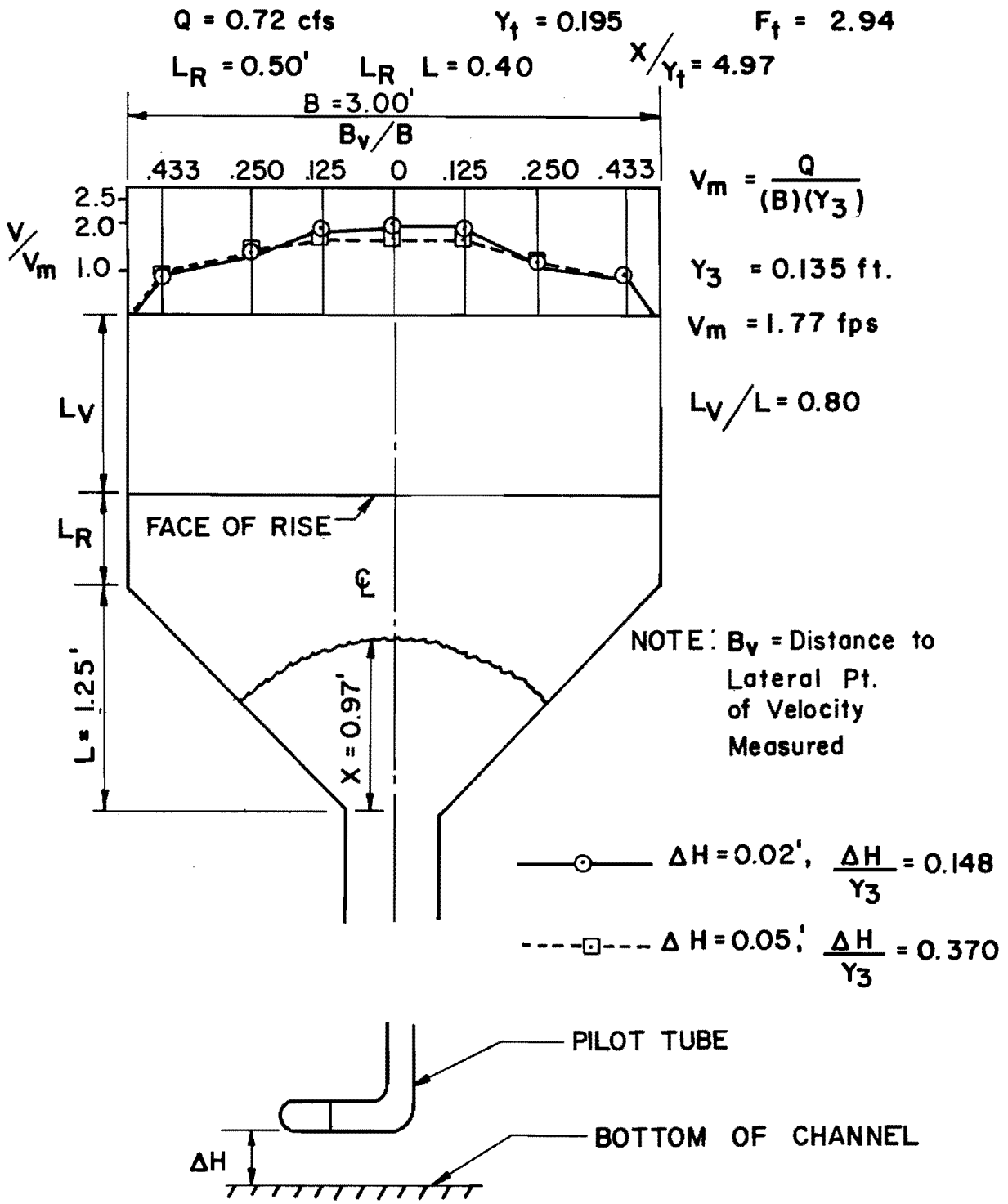

FIGURE 40 - COMPARISON OF THE LATERAL DISTRIBUTION OF VELOCITY (V/V_m vs. B_v/B) FOR DIFFERENT HEIGHTS OF MEASUREMENT FOR H_R=0.137 Ft., H_R/L=0.110

TABLE II. COMPARISON OF PERFORMANCE OF THE RADIAL FLOW ENERGY DISSIPATOR WITHOUT RISE TO PERFORMANCE OF DISSIPATOR WITH VARIOUS RISES AT $F_t = 2.94$, $y_t/b = 0.39$.

Structure	Tailwater Requirements y_3/y_t for $x/y_t = 3$	Jump Stability $\left[\frac{\Delta y_3/y_t}{\Delta x/y_t}\right]$	Channel Velocities $x/y_t = 5$ V_c, fps	$L_v/L = 0.60$ V_c/V_m
Without Rise	1.75	0.065	5.45	6.85
$H_R/L = 0.034$				
$L_R/L = 0.40$	1.68	0.065	----	----
$L_R/L = 0.60$	1.61	0.050	2.60	3.21
$H_R/L = 0.074$				
$L_R/L = 0.40$	1.54	0.105	----	----
$L_R/L = 0.60$	1.37	0.075	----	----
$H_R/L = 0.110$ ft				
$L_R/L = 0.40$	1.14	0.150	----	----
$L_R/L = 0.60$	1.14	0.110	3.40	2.28
$H_R/L = 0.147$ ft				
$L_R/L = 0.40$	0.70	0.250	----	----
$L_R/L = 0.60$	0.72	0.260	----	----

The centerline velocity, Vc in fps, and V_c/V_m the mean channel velocity is shown for $x/y_t = 5$ and $L_v/L = 0.60$. L_v is the longitudinal distance from the downstream end of the flared wingwalls to the point of velocity measurement measured parallel to the channel centerline. The other three rises show definitely better performance than the structure without an abrupt rise.

D. Comparison of the Performance of the Radial Flow Energy Dissipation Structure Incorporating the Abrupt Rise With the St. Anthony Falls Basin

A better evaluation of the performance of the radial energy dissipation structure with an abrupt rise can be made if it is compared with a stilling basin which has been investigated and utilized successively in a number of applications. The St. Anthony Falls basin is recommended for use on small structures such as culvert outlet works where the incoming Froude number F_1 = 1.7 to 17 . This incompasses the smaller range of approaching Froude numbers 1.7 to 3 investigated in this study. Because of its comparatively short length of stilling basin it is frequently used under the aforementioned conditions of approaching flow. For this reason it is chosen for comparison in an example design.

For example, given $F_t = 2.94$, culvert outlet width, $b = 4$ feet , $y_t/b = 0.40$

$$y_t = (0.40)(4) = 1.60 \text{ feet}$$

$$V_t = (F_t)(\sqrt{gy_t}) = (2.94)(\sqrt{(32.2)(1.60)})$$

$$V_t = 21.1 \text{ fps}$$

$$Q = (V_t)(b)(y_t) = (21.1)(6)(2.40)$$

$$Q = 304 \text{ cfs}$$

1. St. Anthony Falls Basin (With Parallel Basin Side Walls)

L_B (length of basin) = $4.5\ y_2/F_t^{0.76}$ where y_2 is the theoretical sequent depth corresponding to y_t , assuming $y_t \approx y_1$.

(a) $$y_2 = 0.5\ y_t(\sqrt{1 + 8\ F_t^2} - 1) = 5.9 \text{ feet}$$

(b) $$L_B = 4.5\ y_2/F_t^{0.76} = \frac{(4.5)(5.9)}{(2.94)^{0.76}} = 11.7 \text{ feet}$$

(c) $y_2' = (1.10 - F_t^2/120)y_2 = 6.07$ feet where y_2' is the depth of tailwater above the stilling basin floor

(d) $V_m = \frac{Q}{(b)(y_2')} = \frac{(304)}{(4)(6.07)} = 12.5$ fps

(e) $y_2'/y_t = \frac{6.07 \text{ ft}}{1.60 \text{ ft}} = 3.8$

(f) height of chute blocks and floor blocks = y_t or 1.60 feet

(g) width and spacing of these blocks are approximately 0.75 y_t or 1.20 feet

(h) height of end sill, $c = 0.07\ y_2 = 0.413$ feet

2. Radial Energy Dissipation Structure With Abrupt Rise

(a) $B = 6b = 24$ feet

(b) $L = 1/2(B - b) = 9$ feet

(c) $L_R = (L_R/L)(L) = (0.40)(9) = 4.0$ feet

(d) $L_B = L + L_R = 14.0$ feet

(e) H_R/L chosen as 0.074 minimum, with $H_R = 0.67$ feet since this rise height parameter in general exhibits superior performance to the $H_R/L = 0.034$ in jump stabilization as well as reduction and distribution of velocities

(f) y_3/y_t range = 1.27 to 1.83
min $y_3 = (1.60)(1.27) = 2.03$ feet

(g) $V_m = \frac{Q}{(B)(y_3)} = \frac{(304)}{(24)(2.03)} = 6.25$ fps

A comparison of these two designs indicate that there is no appreciable difference in the length of basin required. The radial flow energy dissipation structure will allow much lower minimum tailwater values. Velocity data from investigation of the radial energy dissipation structure with the

abrupt rise indicates that within the design range, these low tailwater values do not result in excessive velocities near the bottom of the channel. In addition, the mean channel velocity of the St. Anthony Falls basin is twice that of the radial flow energy dissipator with the abrupt rise. This indicates that the scouring tendencies in general are probably greater for the St. Anthony Falls basin. A somewhat lower minimum tailwater would result for the St. Anthony Falls basin if the side walls were tapered.

The width ratio, B/b of 6 for the radial flow energy dissipator, may be larger than is desirable for the actual channel. A reduction in stability of the jump is inherent, however, in any decrease of the width ratio for the same length of basin. Investigation of the effect of reducing the width ratio, B/b on the performance of the basin, is a possible subject for future study.

Results of this comparison indicate that if low tailwater conditions are expected and if fairly low approaching Froude numbers not greatly in excess of 3 are expected, the radial flow energy dissipation structure with an abrupt rise appears to be more applicable than the St. Anthony Falls basin.

Since the radial flow energy dissipator with the rise was not tested at Froude numbers greater than about 3, it is not recommended for application at higher Froude numbers until further experimental investigations are carried out for these flow conditions.

E. Effect of the Abrupt Rise in Reduction of the Required Drop Between Culvert Outlet and End of Structure

The utilization of a structure incorporating an abrupt rise enables energy dissipation to be achieved without a significant drop in elevation between the culvert outlet and the stream channel. This is of importance when the topographic conditions will not permit a large drop in elevation.

F. Problems of Ponding and Debris Accumulation Immediately Upstream of Abrupt Rise

As cited in the previous study section of this report, accumulation of sediment immediately upstream of an abrupt rise has been noted in some cases.

Although sediment may settle in the pool upstream of the rise during low flow conditions, it appears that the turbulent flow conditions existing with normal discharges will quickly clean out the pool. Large pebbles dropped into the pool of the model basin for the flow conditions employed during the testing were rapidly removed and carried downstream. Ponding of water in the basin upstream of the rise may be prevented by the addition of drains.

II. Structure With Partial Transverse Sill

The performance of the radial flow energy dissipator with a partial transverse sill was evaluated on the basis of its velocity reduction and distribution characteristics. Figures 41 through 46 demonstrate these characteristics for three of the six Froude numbers, F_t which were set. Transverse distribution of velocities are shown for two of the jump positions for each Froude number. Measurements are shown at measurement distances, L_v of 0.50 feet and 1.50 feet from the end of the flared wingwalls. Velocities are expressed in terms of the mean channel velocity, V_m. Generally higher velocities are noted for each value of F_t at the measurement distance L_v of 1.50 feet. As would be expected, velocities generally increased in the channel as the jump was positioned farther downstream. In the case of F_t values of 1.76 and 2.62, flow velocities were concentrated on one side of the channel. Unusual behavior was noted for $F_t = 1.76$ with the jump at $x/y_t = 1.49$ and for $F_t = 2.62$ with the jump at $x/y_t = 1.80$, in that the lateral profile of velocity was skewed to one side of the channel at $L_v = 0.50$ feet, but was skewed to the opposite side of the channel at $L_v = 1.50$ feet. This skew in the velocity profile may be a result of poor spreading of the tranquil flow in the basin. It may also have been caused by reflection of flow from the channel tailgate which caused some eddy formation to occur. However, the severely skewed velocity distribution was observed with the partial transverse sill and not with the flat apron or the abrupt rise. Velocities measured for $F_t = 4.08$ showed a different trend. Velocities at $L_v = 0.50$ feet, for this Froude number were very low near the bottom of the channel, with some concentration of flow near the channel sides at the more downstream jump position. At $L_v = 1.50$ feet,

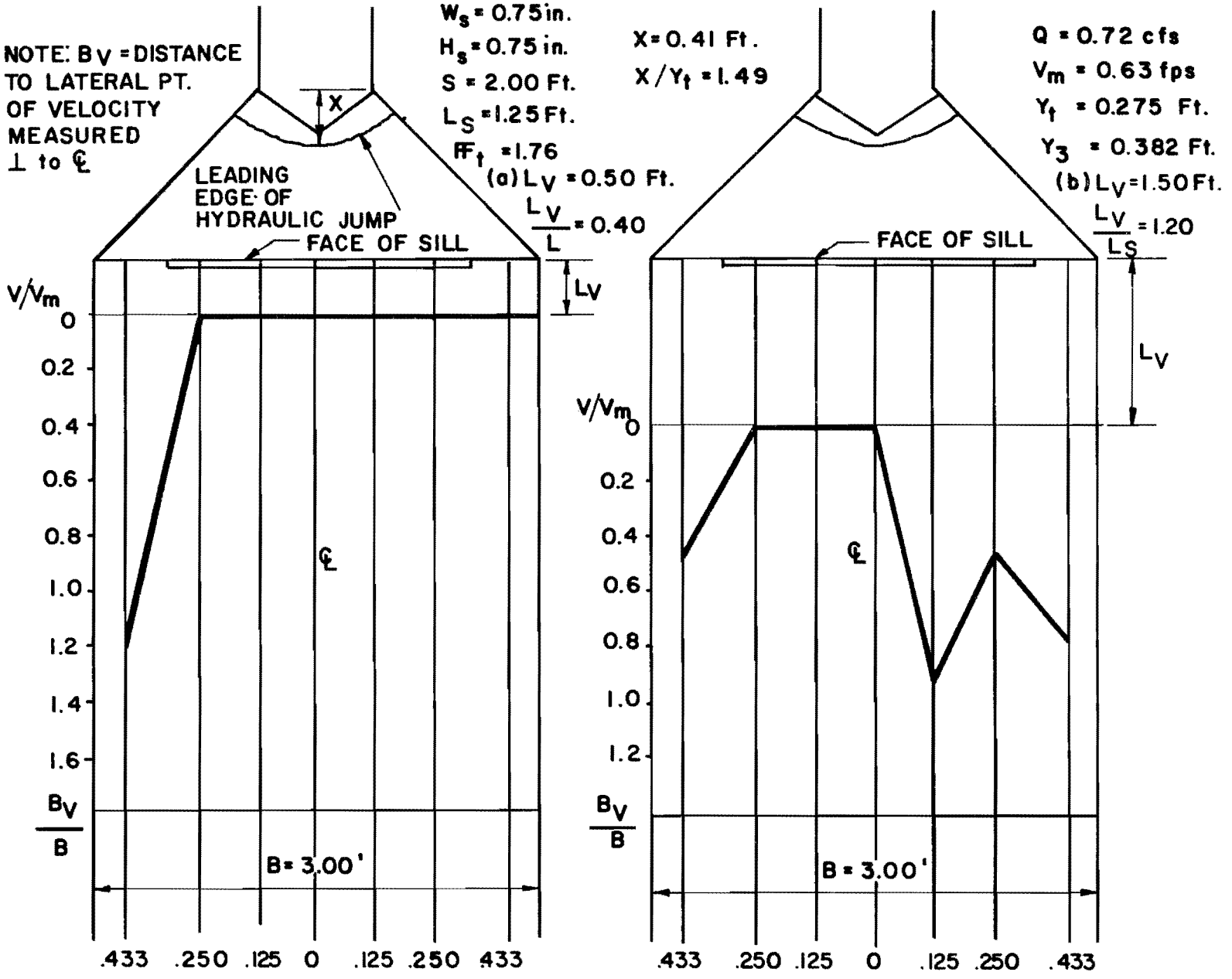

FIGURE 41 - V/V_m vs. B_V/B FOR SILL WITH F_t = 1.76, X/Y_t = 1.49

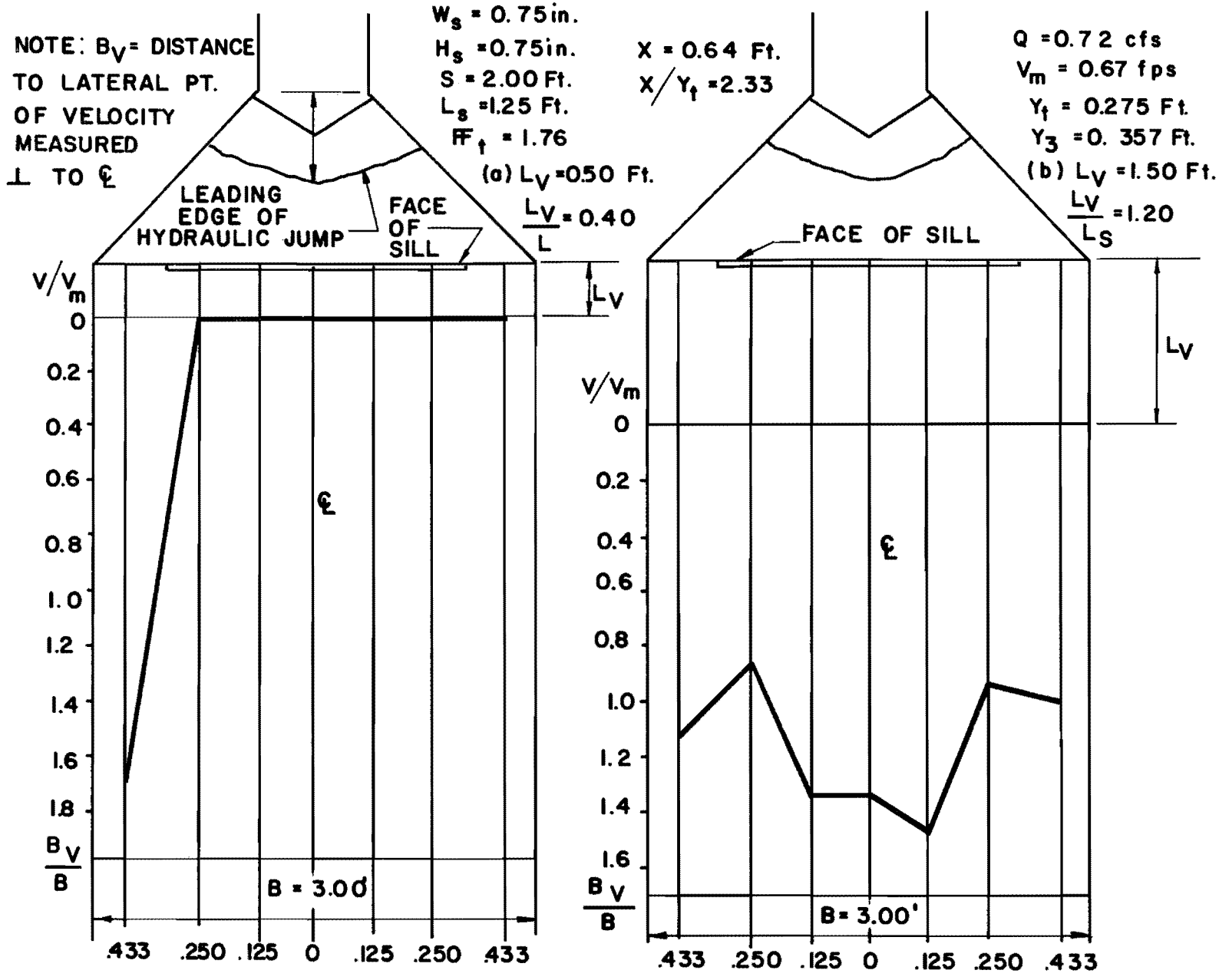

FIGURE 42 - V/V_m vs. B_V/B FOR SILL WITH F_t=1.76, X/Y_t = 2.33

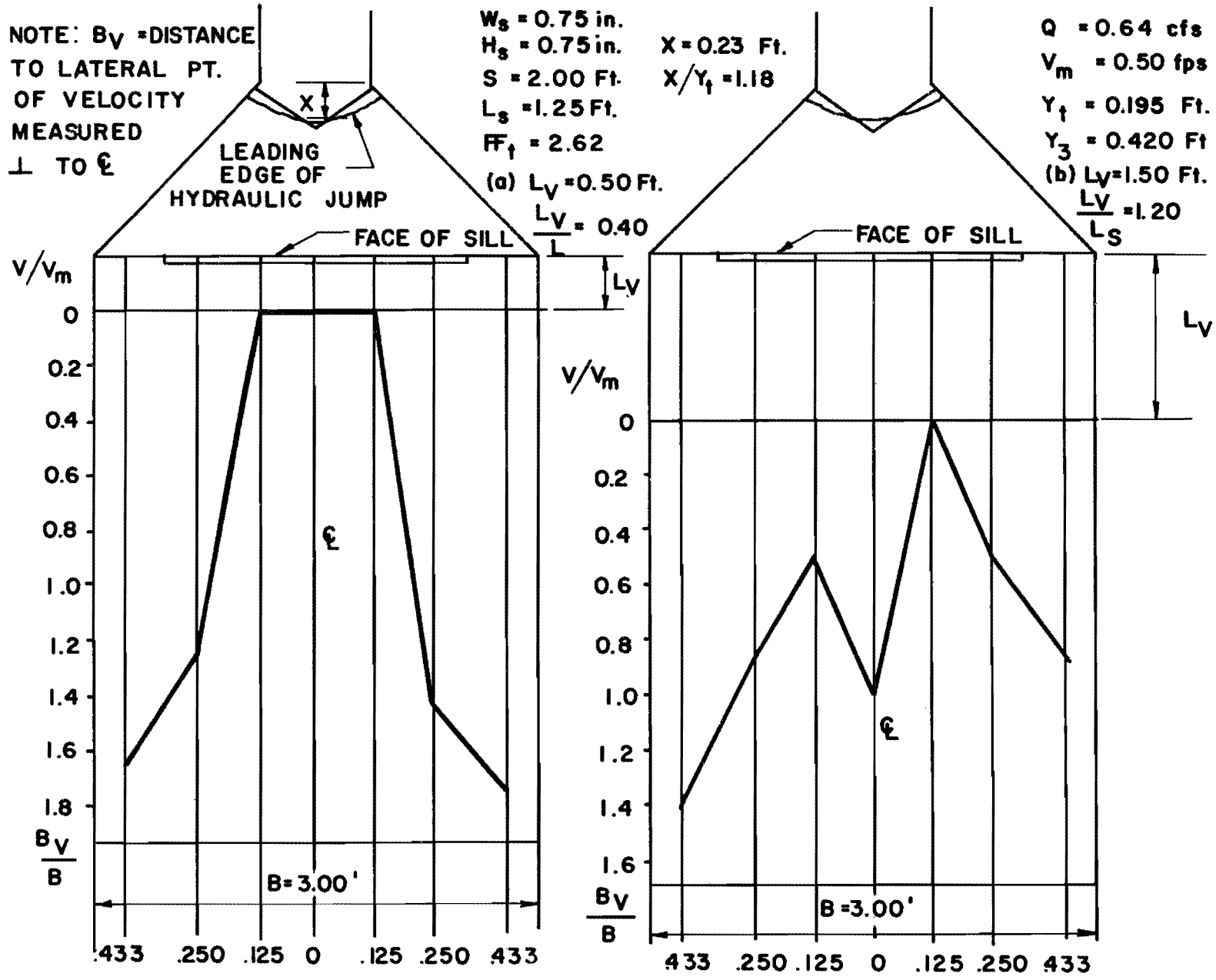

FIGURE 43 - V/V_m vs. B_V/B FOR SILL WITH F_t = 2.62, X/Y_t = 1.18

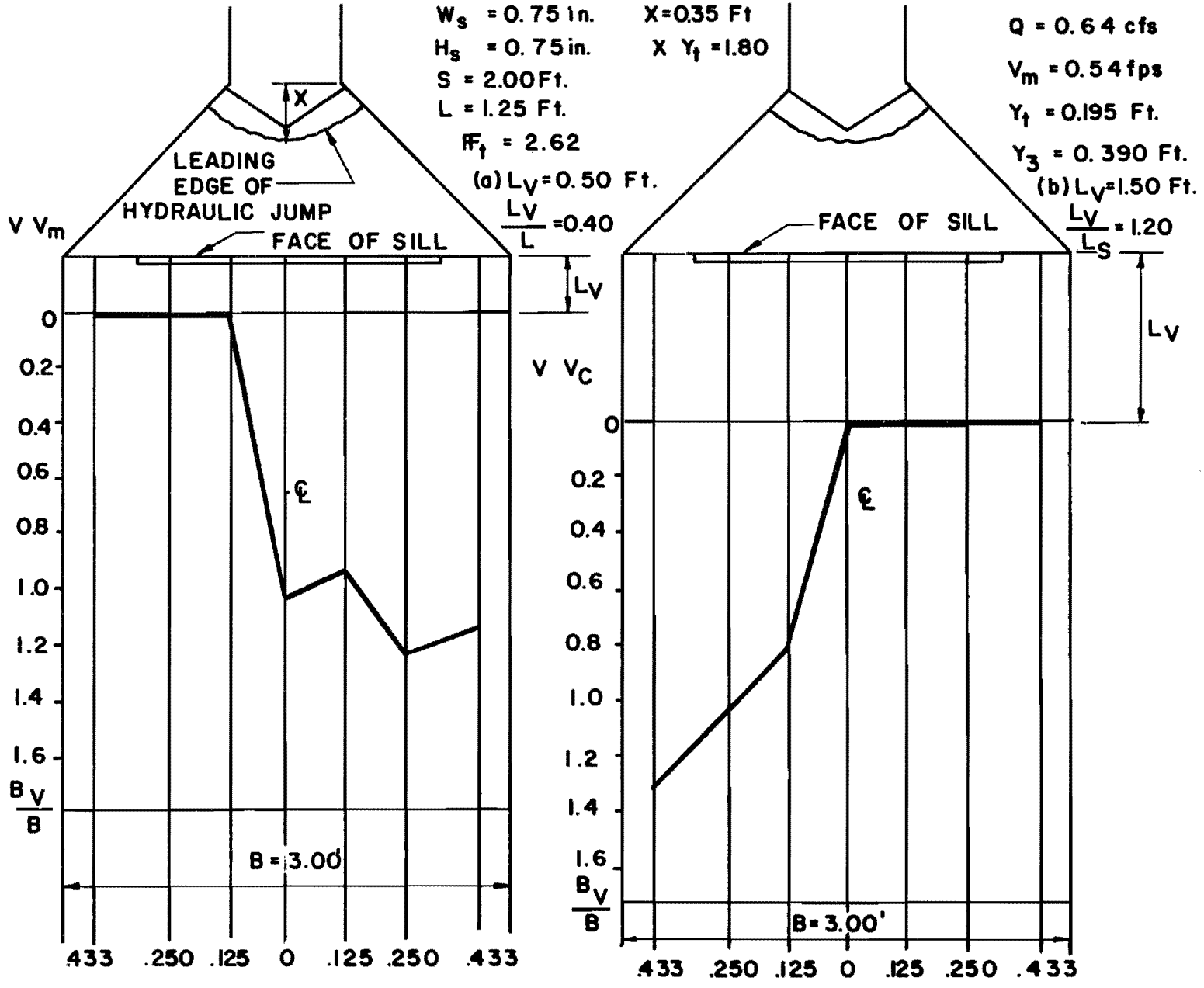

FIGURE 44 - V/V_m vs. B_V/B FOR SILL WITH F_t = 2.62, X/Y_t = 1.80

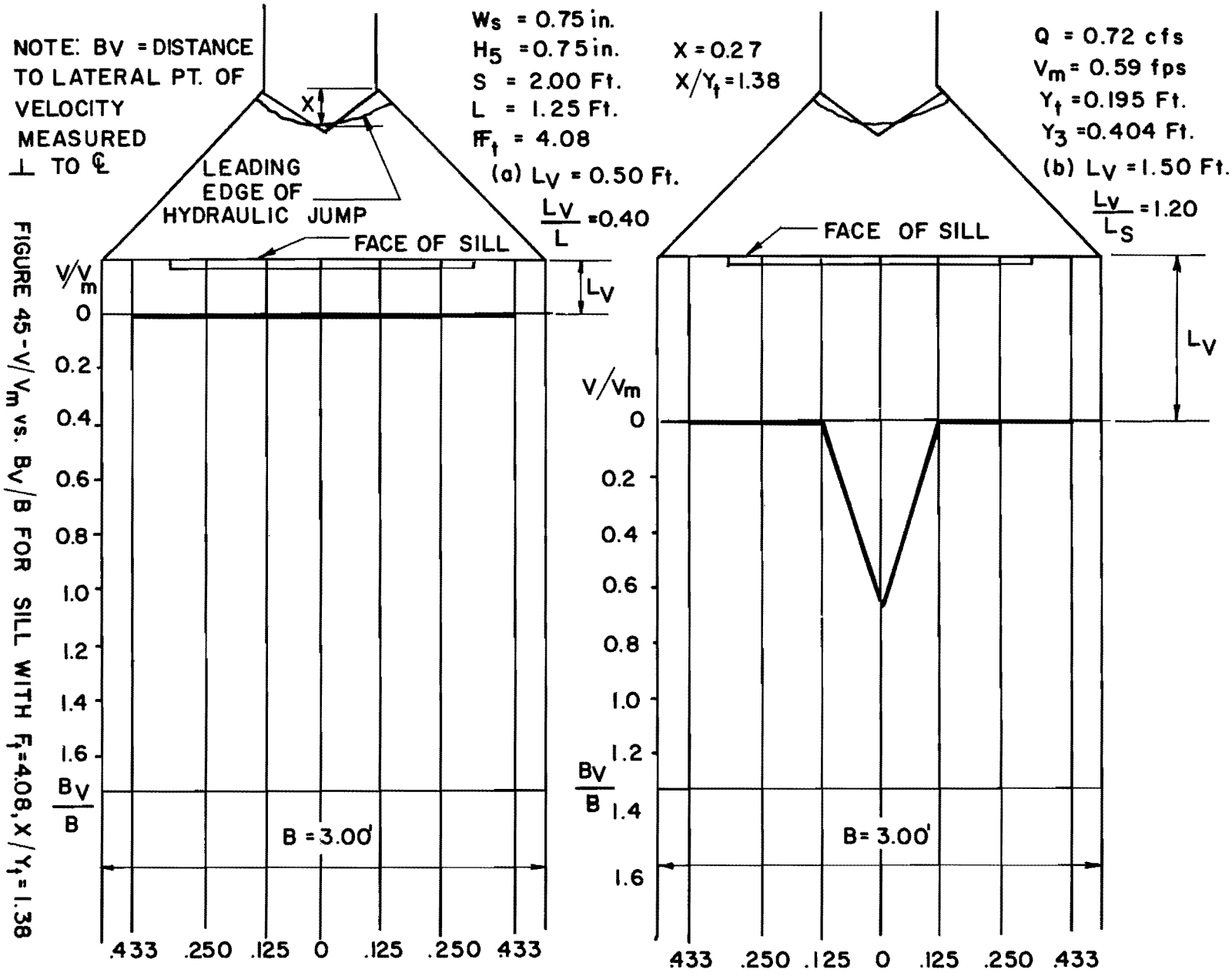

FIGURE 45 - V/V_m vs. B_V/B FOR SILL WITH F_1=4.08, X/Y_1 = 1.38

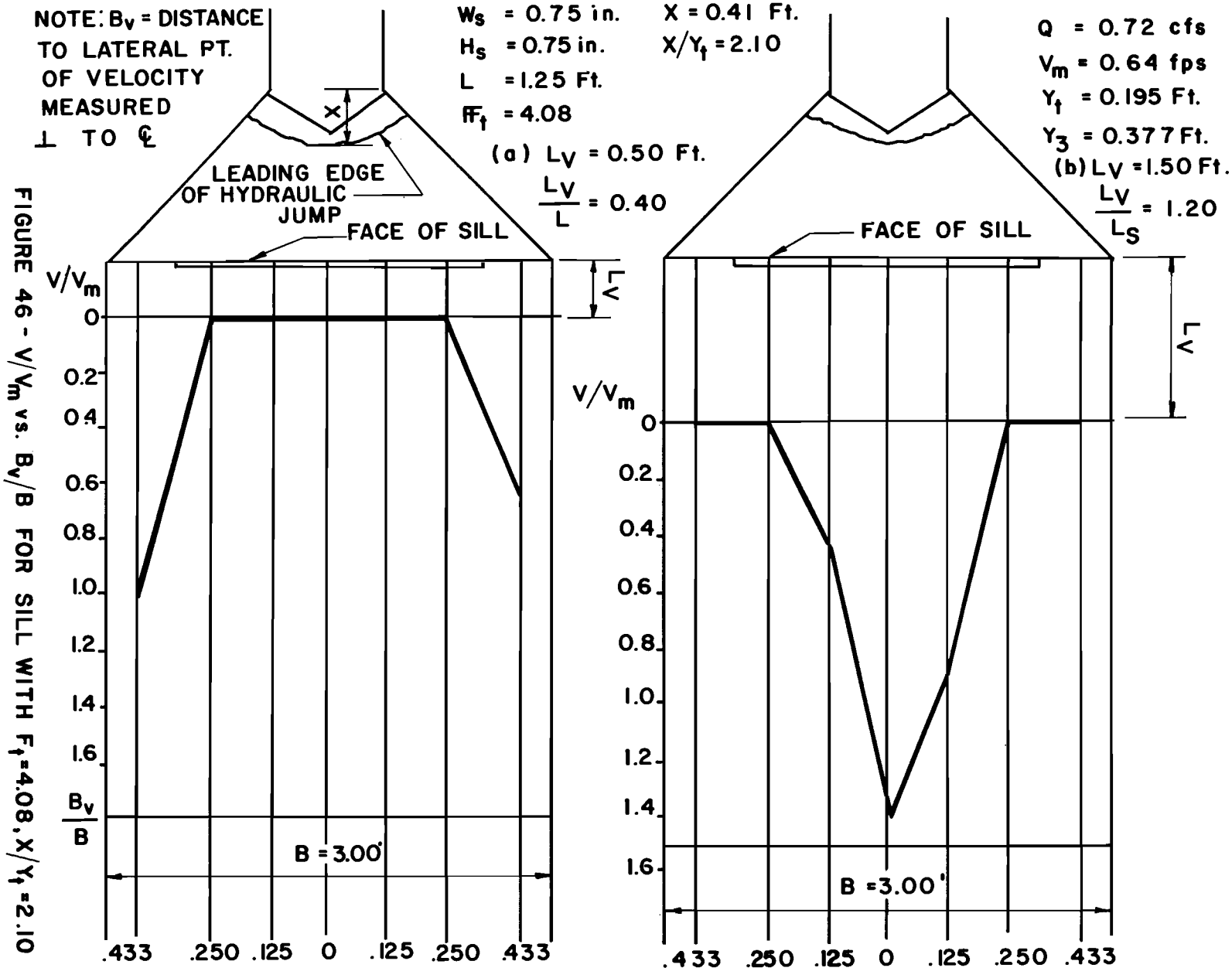

FIGURE 46 - V/V_m vs. B_v/B FOR SILL WITH F_t=4.08, X/Y_t=2.10

for this Froude number, flow was concentrated in the center of the channel. Although very low velocities were noted near the bottom of the channel in some instances at $L_v = 0.50$ feet , significantly larger velocities were measured at positions higher in the flow stream. This indicated that the major portion of the flow stream was flowing over at a higher elevation from the bottom. Maximum velocities measured for the sill were in the order of 3 feet per second, which compared favorably with the velocities measured for the abrupt rise.

Flow as noted, however, was concentrated in most cases on one side of the channel. Tailwater requirements also are greater for jump stabilization with the sill. For this reason, the partial transverse sill is believed to be less desirable as a device for energy dissipation and jump stabilization. If a transverse sill completely across the channel width, were utilized in lieu of a partial sill, it may be that better distribution of flow could be achieved in the channel.

CONCLUSIONS

(1) An abrupt rise in the bottom of the channel as a part of the radial energy dissipation structure is effective in stabilizing the hydraulic jump with satisfactory dissipation of flow energy within the range of approaching Froude numbers, 1.76 to 2.94 considered in this study.

(2) Utilization of an abrupt rise as a part of the radial energy dissipation structure permits stabilization of the hydraulic jump with low values of downstream tailwater depth.

(3) Significantly lower values of tailwater depth are required to maintain the jump in the basin as the rise height is increased. This lower tailwater requirement for abrupt rises of increased height is a result of both the increased elevation of the channel bottom and the effect of dynamic pressure on the upstream face of the rise.

(4) Comparison of the jump stability characteristics of each rise height, as indicated by the movement of the jump resulting from a given decrease in tailwater depth, clearly shows that improved jump stability is achieved by increasing the height of the abrupt rise.

(5) From the standpoint of tailwater requirements and jump stability characteristics, the two highest rises, 0.184 feet and 0.137 feet high, are the most effective of the rises tested even though they are applicable over a more limited range of tailwater values.

(6) Selection of the more desirable rise location of the two locations tested, based on jump stability and tailwater requirements, is dependent upon the height of rise chosen. The rise location, $L_R/L = 0.40$ is more desirable for the two higher rises of $H_R/L = 0.110$ ($H_R = 0.137$ feet) and $H_R/L = 0.147$ ($H_R = 0.184$ feet). The best rise location for the two lower uses tested, $H_R/L = 0.034$ ($H_R = 0.042$ feet) and $H_R/L = 0.074$ ($H_R = 0.092$ feet) will be at

$L_R/L = 0.40$ if effective jump stability is the characteristic desired. If low tailwater depths are expected for these lower two rises, however, $L_R/L = 0.60$ is a somewhat more desirable rise location, since it permits the jump to be held in the basin with lower tailwater depths than the rise location L_R/L of 0.40.

(7) Transverse distributions of velocities for each rise tested, clearly indicate that for a structure of geometry similar to the one investigated, flow will be concentrated in the center portion of the channel with a sharp velocity reduction toward the sides of the channel. An improvement in velocity distribution in the channel will be achieved as the jump is moved upstream toward the entrance channel.

(8) Based on the comparative magnitude of velocities near the bottom of the channel, which may be considered as an index of the scouring power of the flow leaving the jump, and the distribution of these velocities, the rise location L_R/L of 0.60 produces slightly better results for the smallest rise height tested, $H_R/L = 0.034$. The rise location L_R/L of 0.40 produces better results for the other three rises tested.

(9) An evaluation of the comparative performance of a rise of height $H_R/L = 0.147$, with and without a 45° beveled face, clearly shows that the rise without the sloping face is superior in both jump stability performance and reduction of flow velocities.

(10) The tailwater requirements, jump stability characteristics and velocity reduction of the radial energy dissipator are improved by the addition of rises of height, $H_R/L = 0.074$, $H_R/L = 0.110$, and $H_R/L = 0.147$. Although velocities are reduced in the channel by addition of a rise of height $H_R/L = 0.034$, there is little or no improvement in tailwater requirements or jump stability over that for a flat apron.

(11) Although debris may accumulate in the basin immediately upstream of this structure with an abrupt rise during low flow periods, it appears that the turbulent flow conditions existing with normal discharges will quickly clean out this debris.

(12) The utilization of a structure incorporating an abrupt rise enables energy dissipation to be achieved without a large drop in elevation between the culvert outlet and the stream channel.

(13) Although maximum velocities near the bottom of the channel attained with the partial transverse sill included were no greater than those attained with the rise, the partial transverse sill is less desirable than the abrupt rise as an energy dissipation device because of skewed velocity characteristics and higher tailwater requirements. For this reason the abrupt rise is recommended in lieu of the partial transverse sill.

BIBLIOGRAPHY

1. Aguirre, Raymundo G., "Radial Flow Energy Dissipator for Culvert Outlets," (Unpublished Doctoral Dissertation).

2. Blaisdell, F. W., and C. A. Donnelly, "The Box Inlet Drop Spillway and Its Outlet," Transactions, ASCE, Vol 121, pp 955-986, 1956.

3. Blaisdell, F. W., "The SAF Stilling Basin," U. S. Soil Conservation Service, Report SCS-TP-79, May 1949.

4. Bossy, H. G., "Culvert Design Manual," Bureau of Public Roads, (Unpublished Material).

5. Argue, J. R., "New Structure for Roadway Pipe Culverts," Journal of the Institution of Engineers, Australia, Vol 32, No 6, June 1960.

6. Bradley, J. N., and A. J. Peterka, "The Hydraulic Design of Stilling Basins: Small Basins for Pipe or Open Channel Outlets," Proceedings, ASCE, Journal Hydraulics Division, Vol 83, No HY5, Paper No 1406, 1957.

7. Keim, S. R., "The Contra Costa Energy Dissipator," Proceedings, ASCE, Journal Hydraulics Division, Vol 88, No HY2, March 1962.

8. "Research Studies on Stilling Basins, Energy Dissipators, and Associated Appurtances," U.S. Bureau of Reclamation, Hydraulic Laboratory Report No Hyd-399, June 1, 1955.

9. Henderson, F. M., Open Channel Flow, The Macmillan Company, New York, 1966.

10. Davis, W. B., "Transition Phenomena in Radial Free Surface Flow," M. S. Thesis, Massachusetts Institute of Technology, 1958.

11. Saddler, C. D., and M. S. Higgins, "Radial Free Surface Flow," M. S. Thesis, Massachusetts Institute of Technology, 1963.

12. Rouse, Hunter, B. V. Bhoota, En-Yun Hsu, "Design of Channel Transitions," Proceedings, ASCE, p 1382, November 1949.

13. Moore, Walter L., and Carl W. Morgan, "The Hydraulic Jump at an Abrupt Drop," Proceedings, ASCE, Journal Hydraulics Division, No HY6, p 1449, December 1957.

14. Forster, John W., and Raymond A. Skrinde, "Control of the Hydraulic Jump by Sills," Transactions, ASCE, Vol 115, p 973, 1950.

15. Hsu, En-Yun, Discussion of "Control of the Hydraulic Jump by Sills," by John W. Forster and Raymond Skrinde, Transactions, ASCE, p 990.

16. Laushey, Louis M., Discussion of "Control of the Hydraulic Jump by Sills," by John W. Forster and Raymond Skrinde, Transactions, ASCE, p 996.

17. Moore, Walter L., and Carl W. Morgan, "The Hydraulic Jump at an Abrupt Rise," (Unpublished Report).

18. Rand, Walter, "Flow Over a Vertical Sill in an Open Channel," Proceedings, ASCE, Journal Hydraulic Division, No HY 4, p 4408, July 1965.